and 3. The one at the location 1) reflects a deeper anomalous source, and the one at the location 2) seems to be due to a deeper source at the northern edge, and an east-dipping source extended from the level of n=1 and 3. While those at the locations 3) and 4) are the extension from the depth level of n=1 and 3, and move about 100m toward the east.

2–1–3 Spectral Diagrams

Spectral analysis was made for each of the five survey lines in which SIP (Spectral Induced-Polarization) surveys were conducted. The following three diagrams were used for the analysis: Phase Spectrum (Figure II-2-19), Cole-Cole Diagram (Figure II-2-20) and Magnitude Spectrum (Figure II-2-21). Moreover, the results of comparing these spectral responses with the typical spectral responses of the whole Morro do Accampamento area and with those found in the province of the C-1 ore body are also given.

(1) Phase Spectrum (Figure II-2-19)

The phase spectra observed in this survey area show the variation enough to consider the intensity, distribution and extension of the IP anomalous zones, and the distribution of the sulfide minerals (pyrite), but it is difficult to discriminate clearly the minerals only from those.

The following three kinds of phase-spectral patterns were observed:

1) Pattern showing downward at higher frequency range (Figure II-2-24 (H)).
2) Pattern showing stable in harmonic frequency range between 0.1 Hz and 1.125 Hz (Figure II-2-24 (F)).
3) Pattern showing peaks in the lower frequency range and/or at the frequency of between 0.1 Hz and 1.125 Hz (Figure II-2-24 (I)).

Each of these three kinds of phase spectra shows a strong IP effect. And in the lower frequency range than 5 Hz, it seems to reflect pyrite, because it shows either a peak or stable at lower frequency range than 0.1 Hz. The phase spectrum showing no IP effect is shown in Figure II-2-24(J).

Patterns of the item 1) are found at the east of Lines 1405S, 1420S and 1450S, where the negative coupling effects were observed. Hence, it is thought that the geological environments, which cause negative coupling effect, are distributed at above areas. And spectral pattern of item 3) is observed partly in the lower frequency range of 0.1 Hz through 1.125 Hz of the one of item 1). Then, phase spectrum of item 1) seems to be due to mainly the negative coupling effect and partly due to the origin causing the one of item 3).

Patterns of the item 2) are caused by pyrite mainly, and are found in the IP anomalous zones observed in the distribution area of no graphite schist and of the formations not including graphite schist. Both of graphite schist and pyrite show strong IP effect, but those spectral patterns are different each other. The pattern of the former shows downward in the higher frequency range, but the latter shows a concave curve, in which the phase increases from lawer frequency to higher frequency and decreases gradually at higher frequency range.

The negative coupling effects can be observed not only in the distribution area of graphite schist but also at a strong resistivity contrast of between neighbouring formations, so that this effect is found occasionally in the province of a large-scale massive sulfide ore deposit of low resistivity. Therefore, it should be taken care to interpret the negative coupling effect which is observed in the area of no graphite schist and of the formation not including graphite schist. The negative coupling effects observed in the survey area are distributed along the resistivity discontinuities seemed to reflect the fault structures, so that those is thought to be due to resistivity contrasts.

Phase spectra of the item 2) are concentrated in the three IP anomalous zones at the northern, southeastern and southern parts of the survey area (fig. II-2-31), and this spectral pattern is thought to be a standard one in the survey area.

Each of phase spectra of the item 3) is distributed in the southeastern IP anomalous zone on Lines 1420S and 1430S, and shows a similar pattern as the one in Fig II-2-24 (A) This pattern shows partly a similar pattern as the one of the item 2), but is not due to pyrite only, because phase variation in the lower frequency range of 0.1 Hz through 1.0 Hz is different from that of the item 2). It is thought that the variation of phase in the lower frequency range is of a very important factor for the mineral discrimination, and the distribution area of phase spectra of the item 3) is a target area of the drilling survey. However, the variation in this item 3) is not clearly so that the mineral discrimination became very difficult.

(2) *Cole-Cole Diagram (Figure II-2-20)*

The Cole-Cole diagram is made in order to understand the intensity of mineralization causing the IP anomalous zone. The following three kinds of Cole-Cole diagrams are used as a standard for the interpretation, as shown in Figure II-2-22.

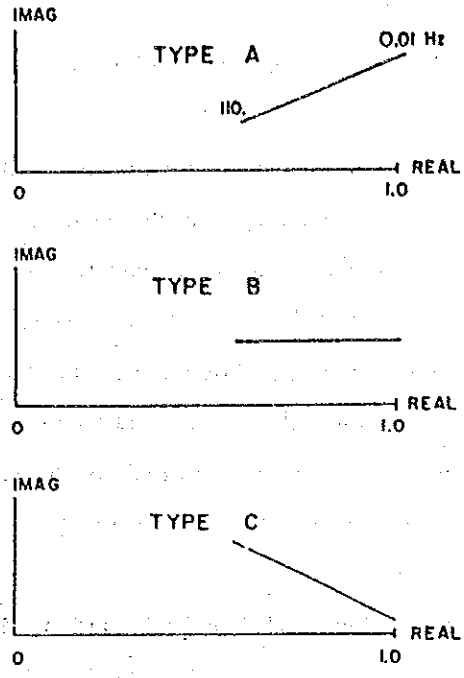

Fig. II-2-22 Cole-Cole Diagram of Three Spectral Types for Rock and Ore Samples

1). A spectral pattern shown in Figure II-2-22 (A), which reflects a strong mineralization, shows a low resistivity and a strong IP effect, and is observed in the distribution area of sulfides, graphite schist and some kind of clay.

2) A spectral pattern shown in Figure II-2-22 (B), which reflects a medium alteration and a small amount of pyrite.

3) A spectral pattern shown in Figure II-2-22 (C), which reflects alluvial formation, limestone etc. accompanying no mineralization.

A low-resistivity and strong IP anomalous zone, in which the spectral patterns of the item 1) and 2) are observed among these three spectral patterns, is thought to be a potential zone of ore deposits.

Spectral patterns of the items 1) and 2) are observed in the southeastern IP anomalous zone, but as each of those shows a intermediate pattern of between the items 1) and 2), this IP anomalous zone is thought not to be due to a strong mineralization. Those of the item 2) are predominantly distributed in the northern IP anomalous zone.

Those of the item 3) are dominated in the no IP anomalous zone.

(3) **Magnitude Spectrum**

Magnitude spectrum was made to understand the intensity of IP effect, as shown in Fig II-2-21.

When there is a strong IP effect, the magnitude decreases notably toward higher frequency. The spectral patterns showing a notable decrease in the magnitude are found in the southeastern, southern and northern parts of the survey area, which are extracted as the potential IP anpomalous zones. The most of those are distributed in the southeastern part among these three parts.

As discussed above, the spectral patterns showing a strong IP effect in three kinds of spectral diagrams, that is, phase spectrum, Cole-Cole diagram and magnitude spectrum,are mostly observed in the southeastern, southern and northern IP anomalous zones. Therefore, each of these three anomalous zones is thought to be a target of the drilling survey.

(4) **Spectral Responce Observed Near C-1 Ore Body and in Morro do Accampamento Area**

Among the typical spectral responces acquired by the SIP electrical surveys of the three-year period, ten spectral responces, in total, obtained from the property tests of the core samples and observed near the C-1 ore body, are shown in Figure II-2-24. The discussions of those spectral patterns are given as follows:

Figure (A) is a spectral pattern observed above the C-1 ore body in the first-phase. And Figures (B) and (C) are spectral patterns obtained from the property test of the core samples collected from amphibolite and from schist within the C-1 ore body, respectively. These three spectral patterns are typical ones representing the C-1 ore body, and are extracted in order to compare with those mentioned below.

Figure (D) is a spectral pattern observed on the line 310S conducted on the second phase. Figure (E) is a spectral pattern obrained from the property test of the core sample collected at the same depth of the MBP-3 hole as the one where a spectral pattern of Figure (D) was observed. This core is graphite quartz schist containing pyrrhotite and pyrite.

Figures (F) through (J) are the results of the third-phase SIP survey. Figure (F) is a spectral pattern observed in the IP anomalous zone of the line 1430S at the southern part of the survey area, which is thought to reflect pyrite. Figure (G) is the one obtained from the property test of the core sample collected at 24 m in depth of the MBP-4 hole. This core contains pyrite mainly and sphalerite, galena and chalcopyrite as a part. And this spectral pattern can be found easily in the results of the property test of the core samples collected between ground surface and 170 m and at the depth of more than 300 m of this hole. Figure (H) is the one observed in the strong IP

PHASE SPECTRUM

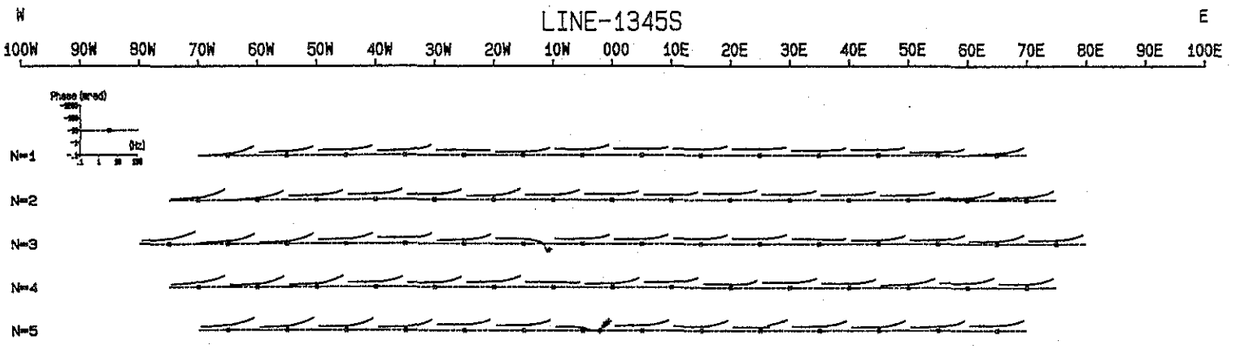

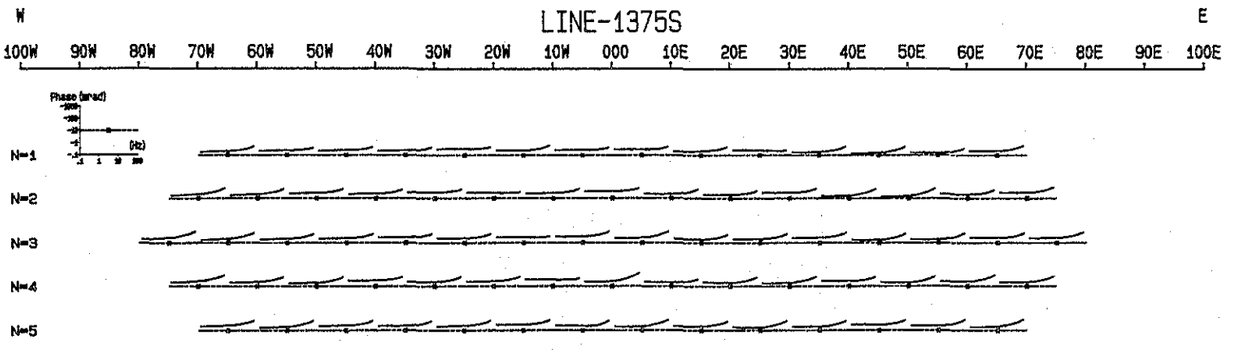

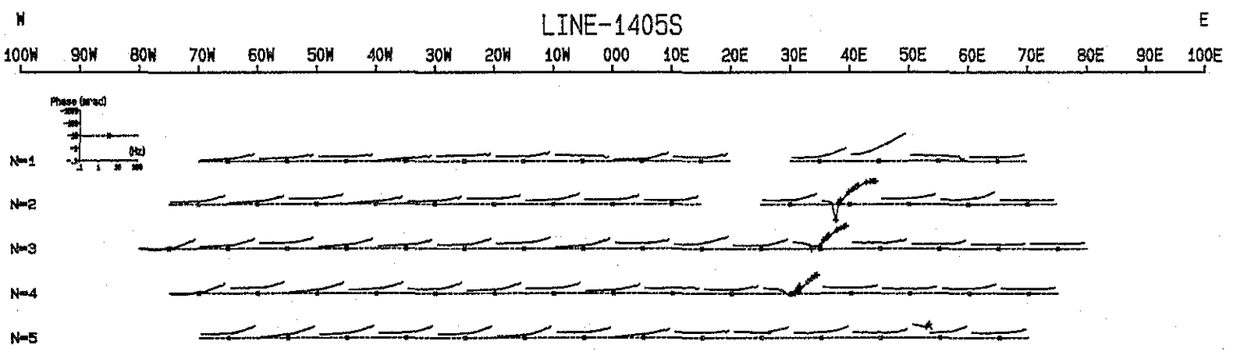

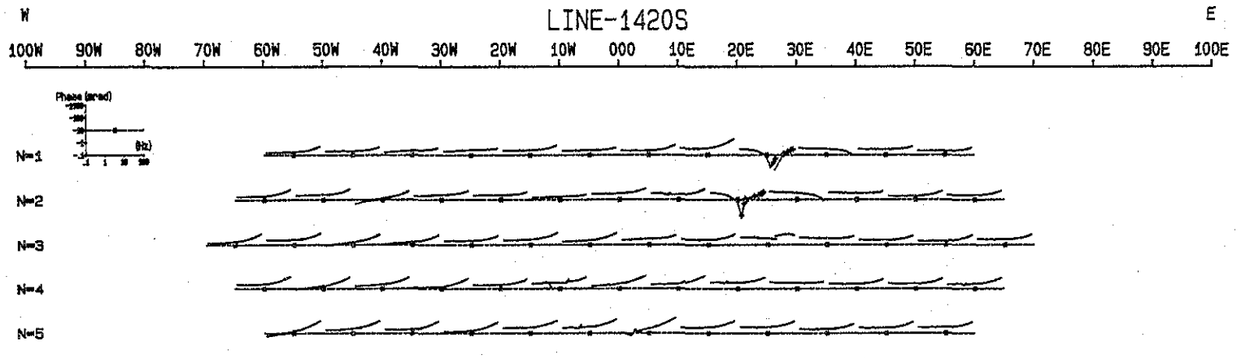

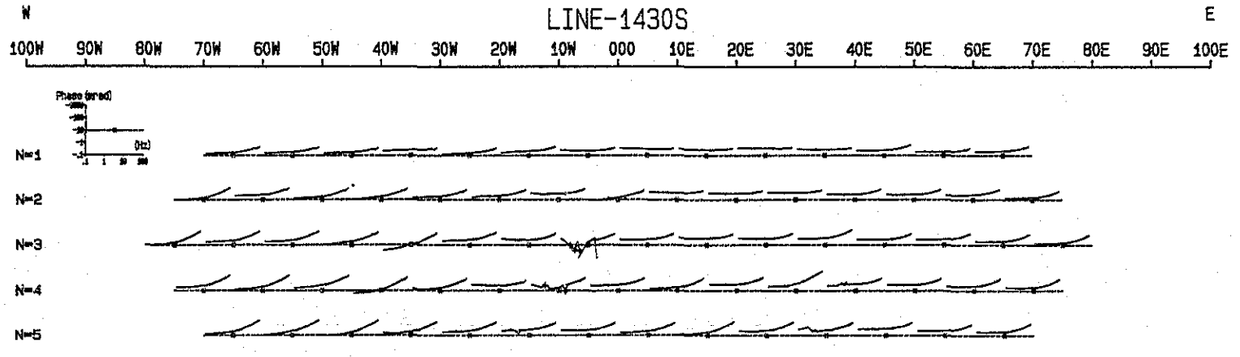

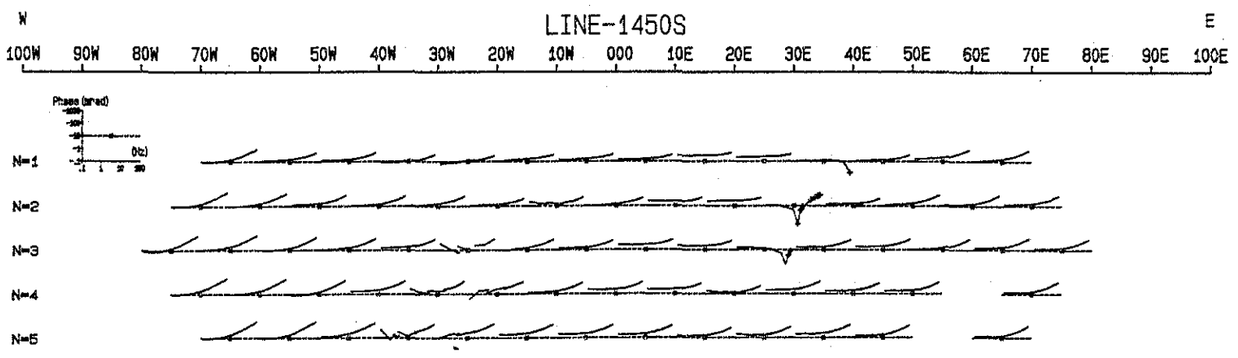

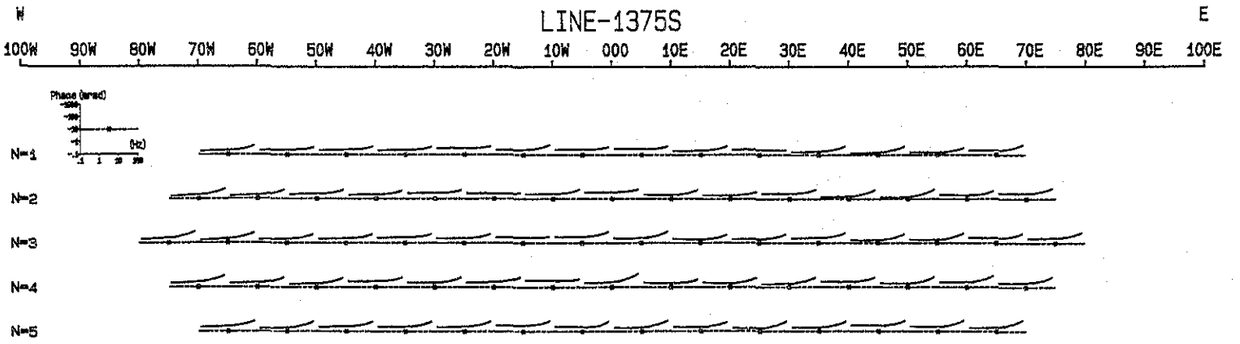

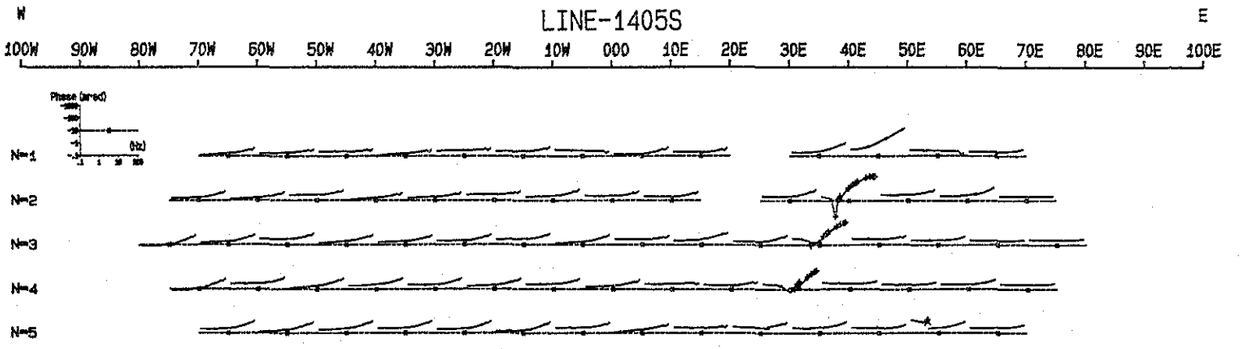

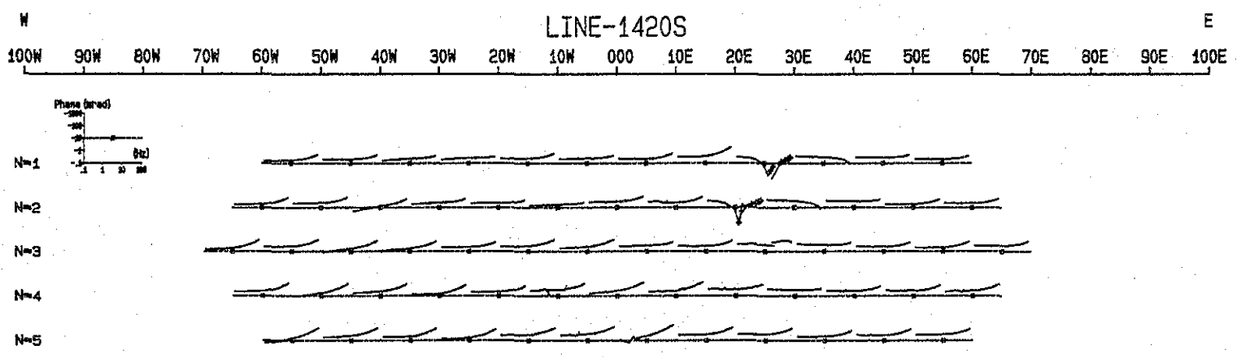

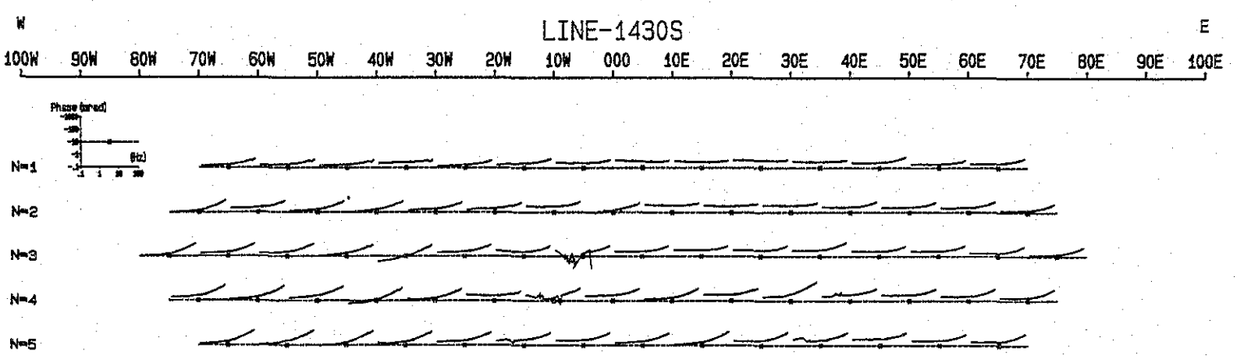

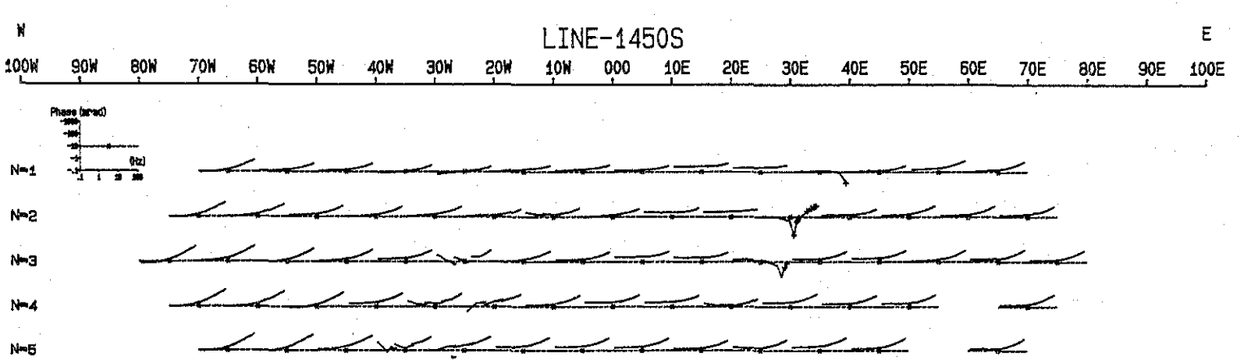

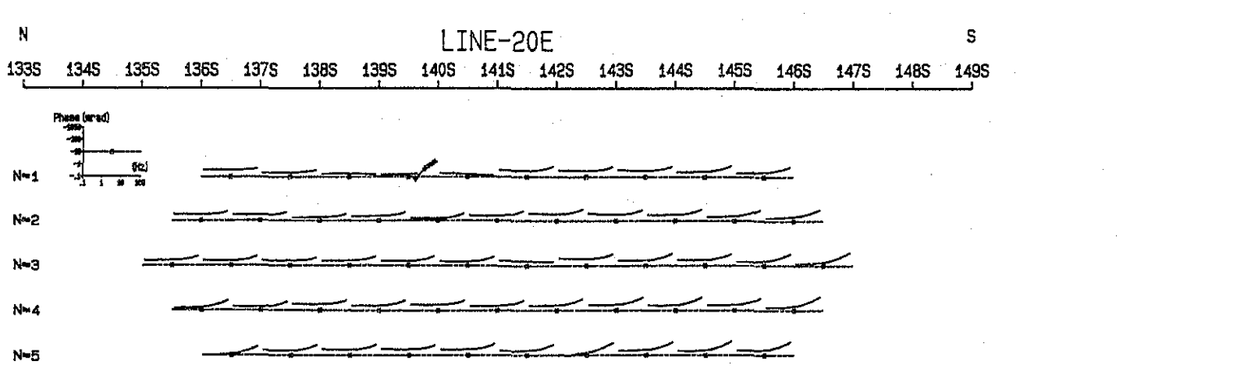

Fig. II-2-19 Phase Spectrum Diagram

Cole-Cole SPECTRUM

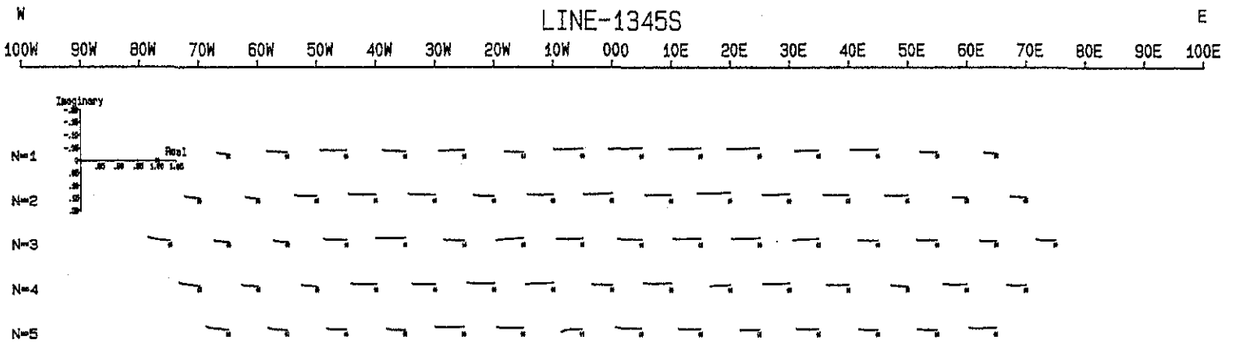

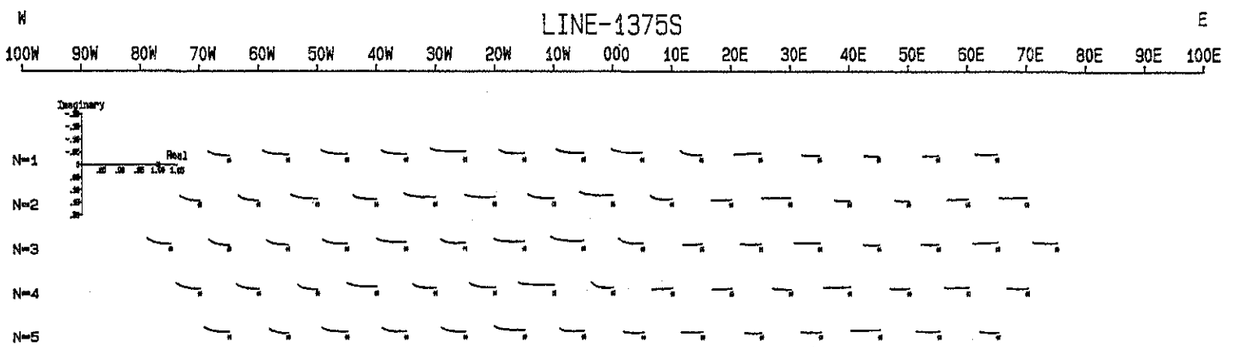

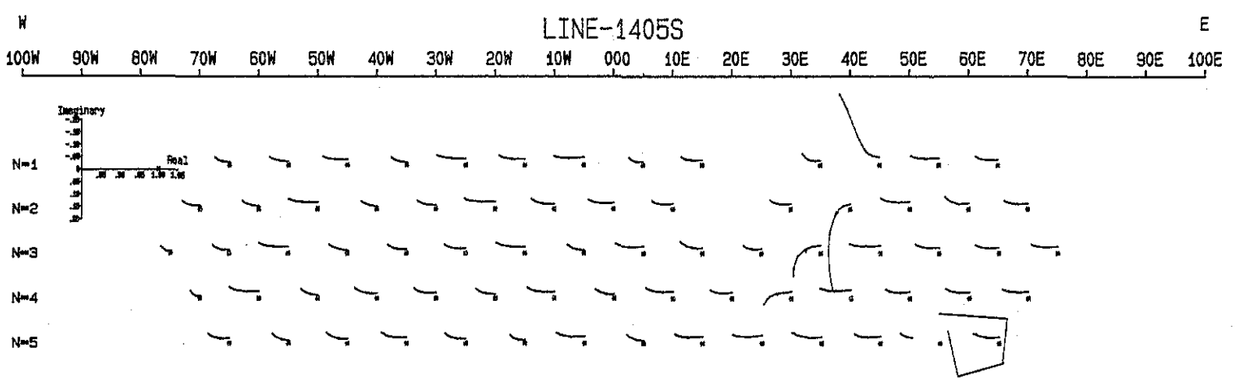

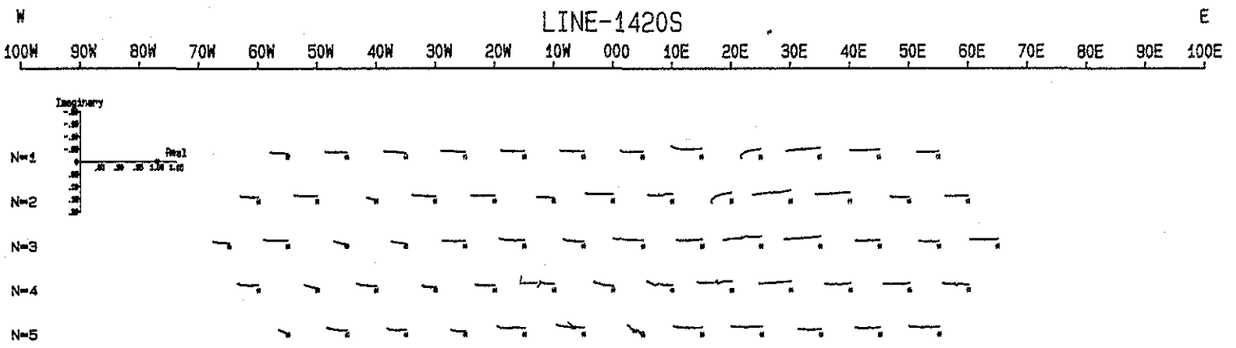

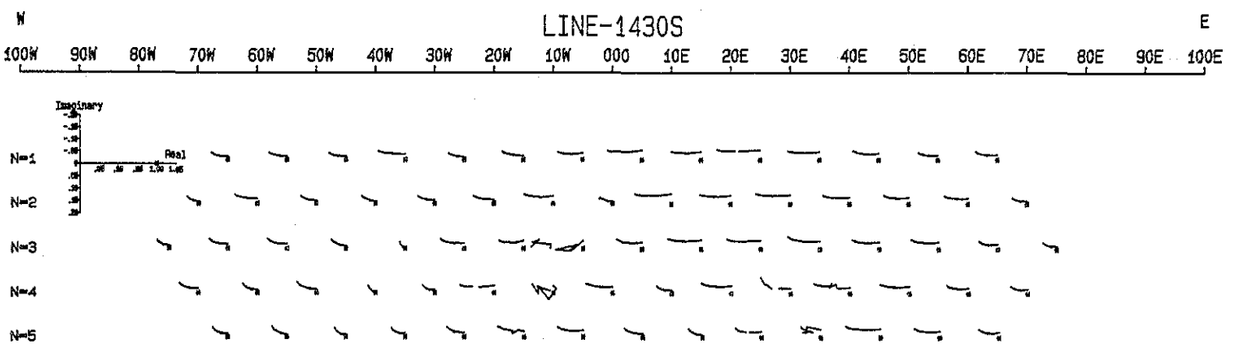

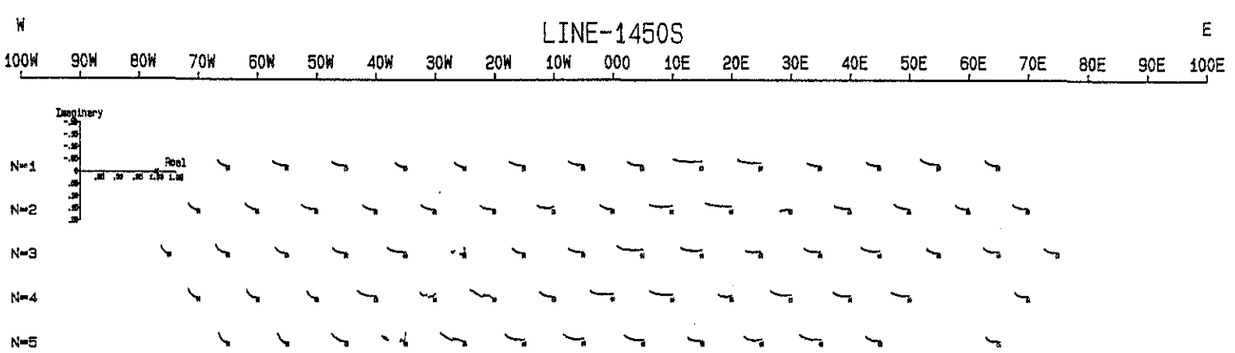

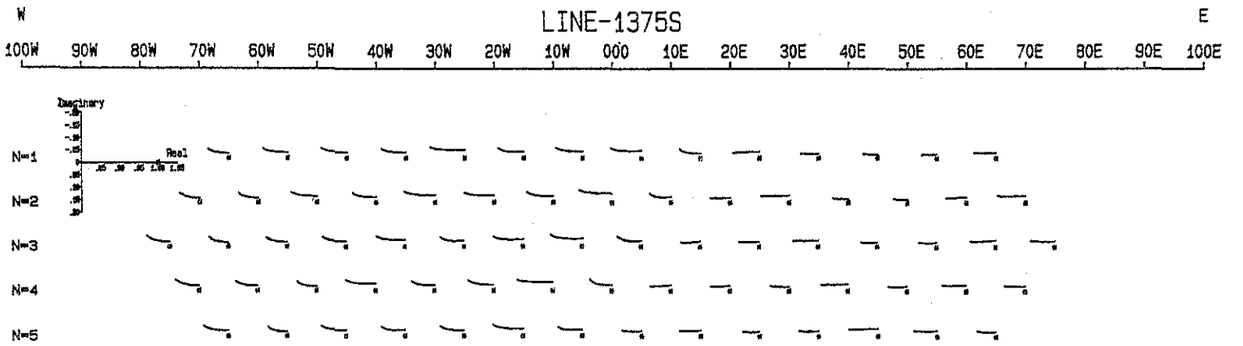

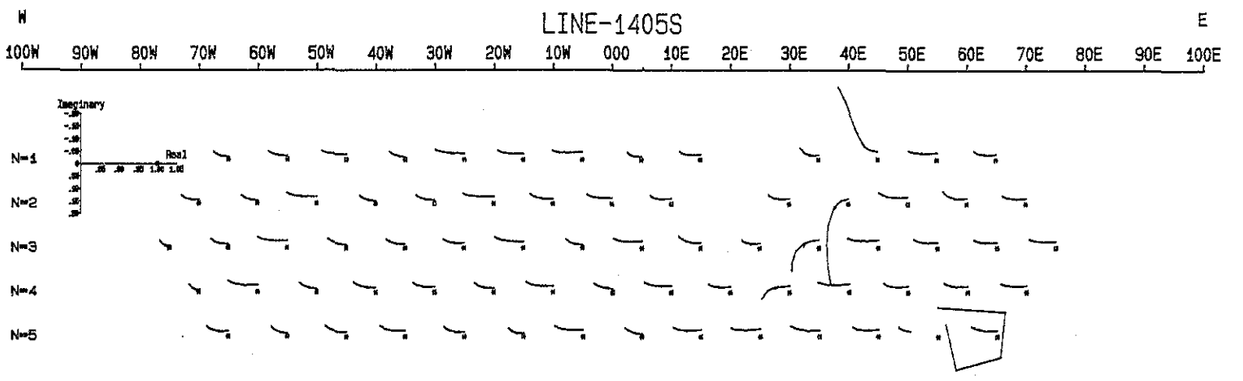

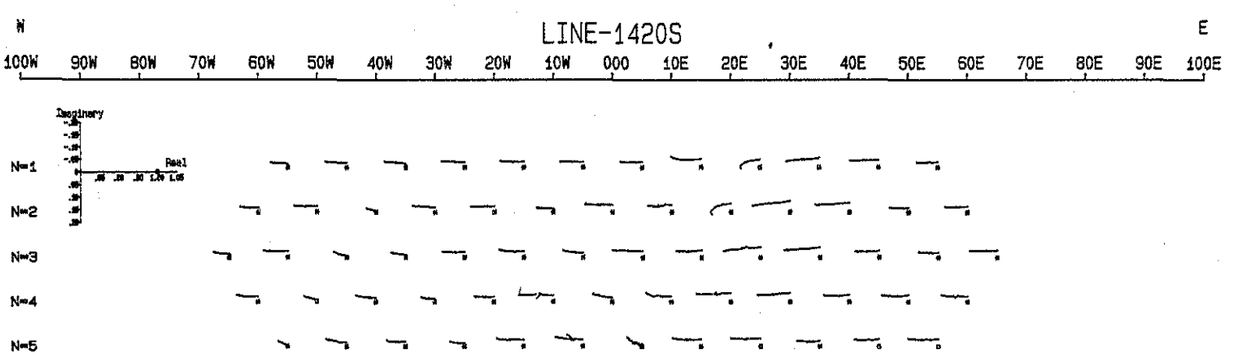

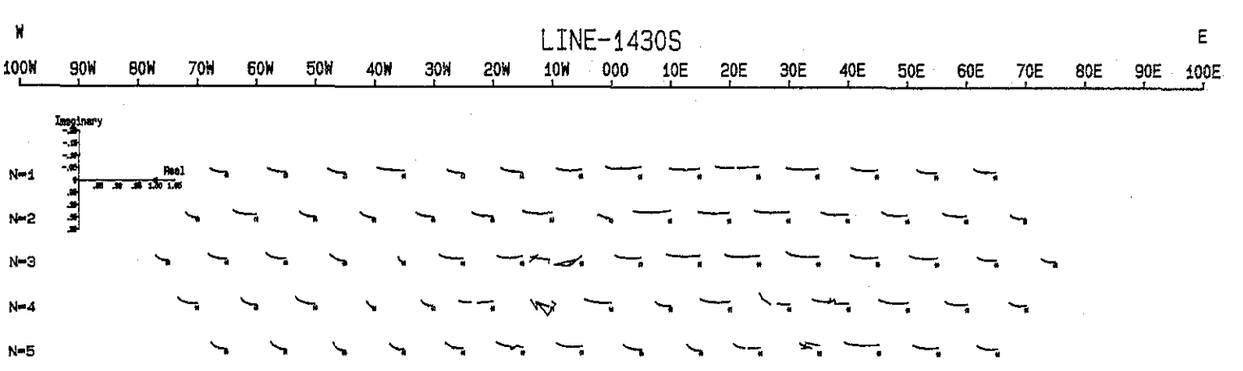

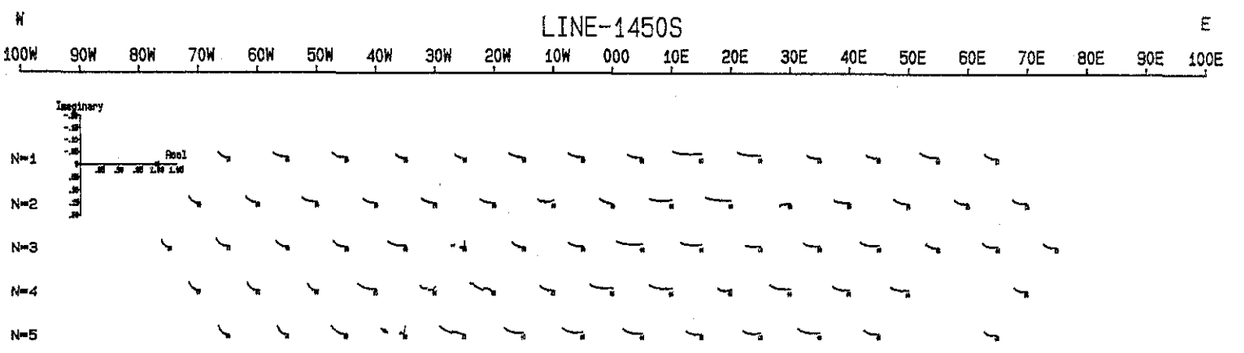

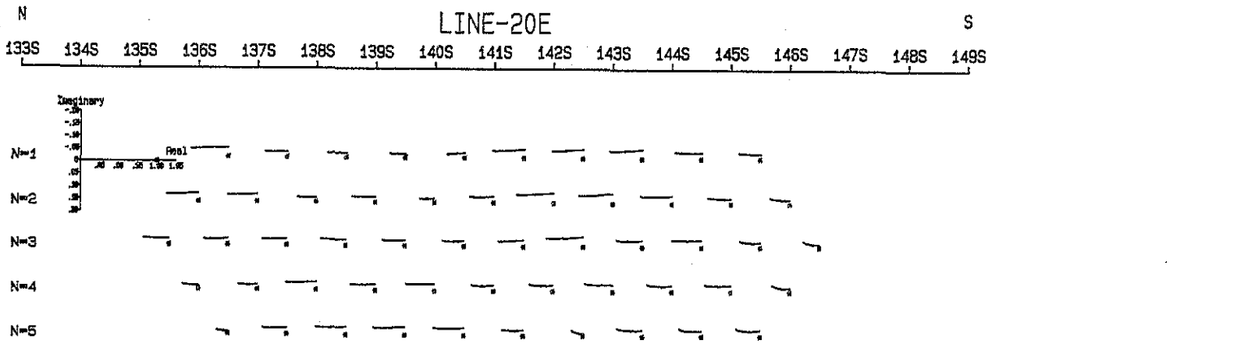

Fig. II-2-20 Cole-Cole Diagram

MAGNITUDE SPECTRUM

LINE-1345S

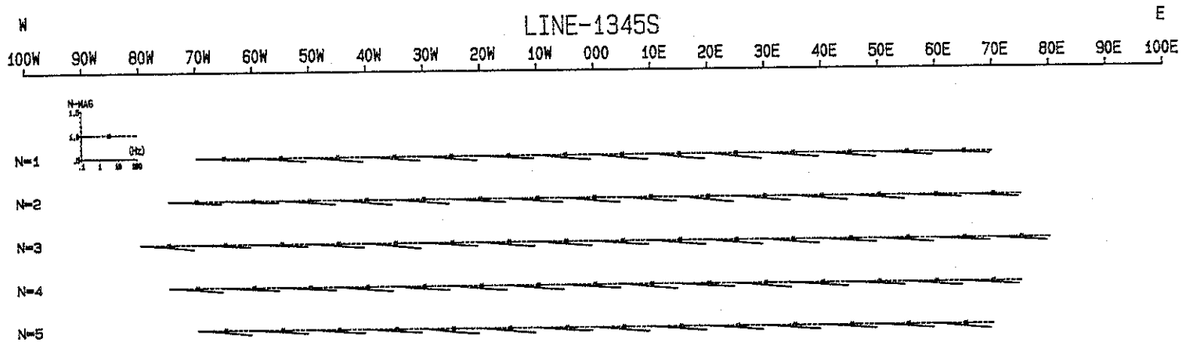

LINE-1375S

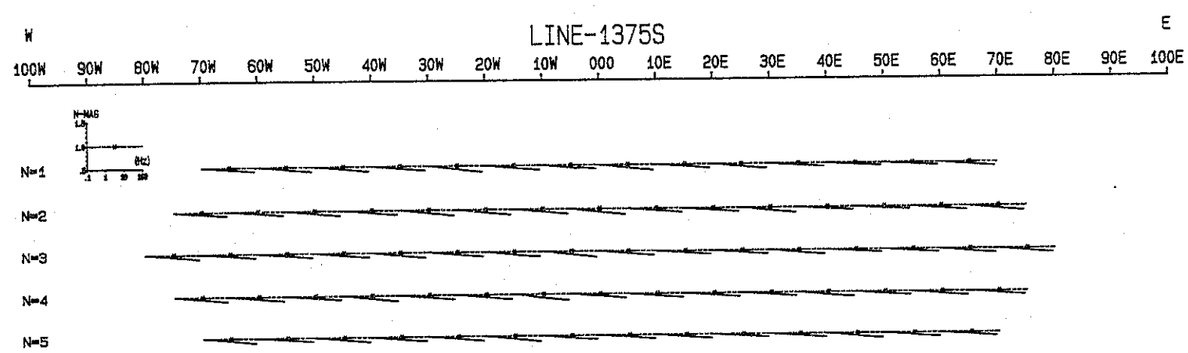

LINE-1405S

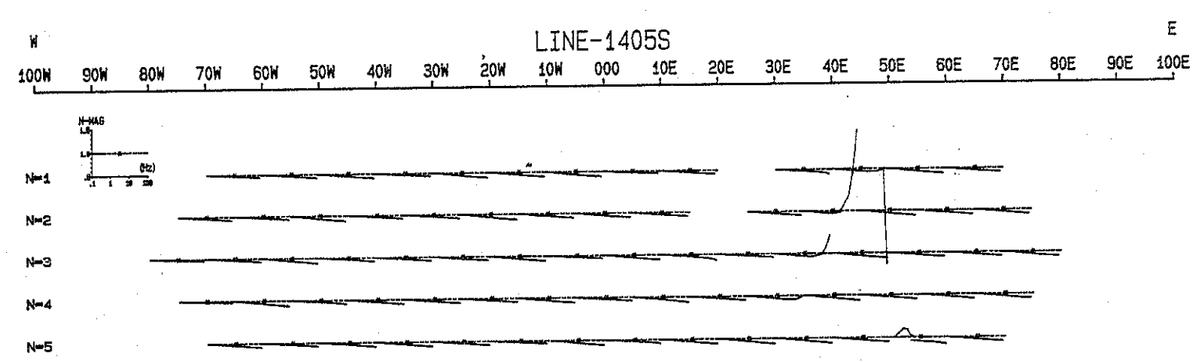

LINE-1420S

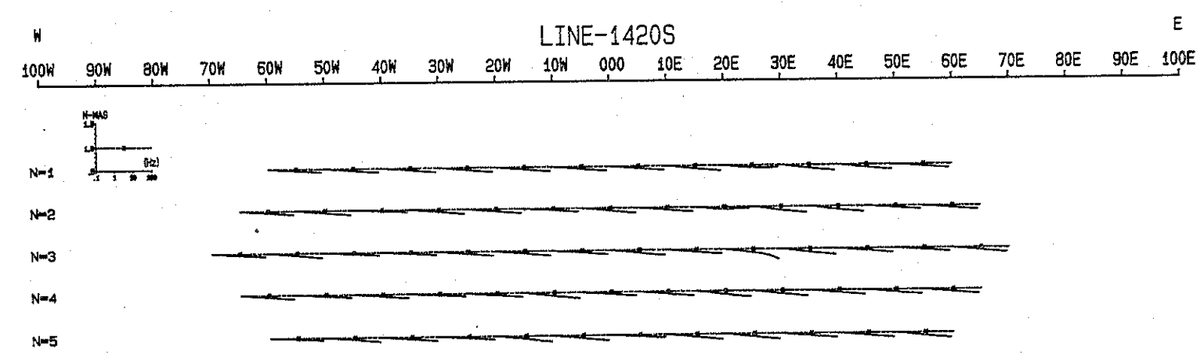

LINE-1430S

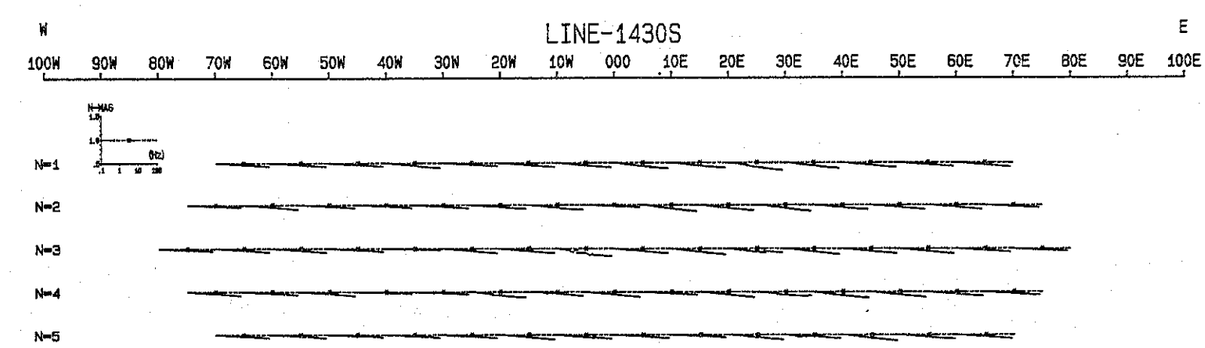

LINE-1450S

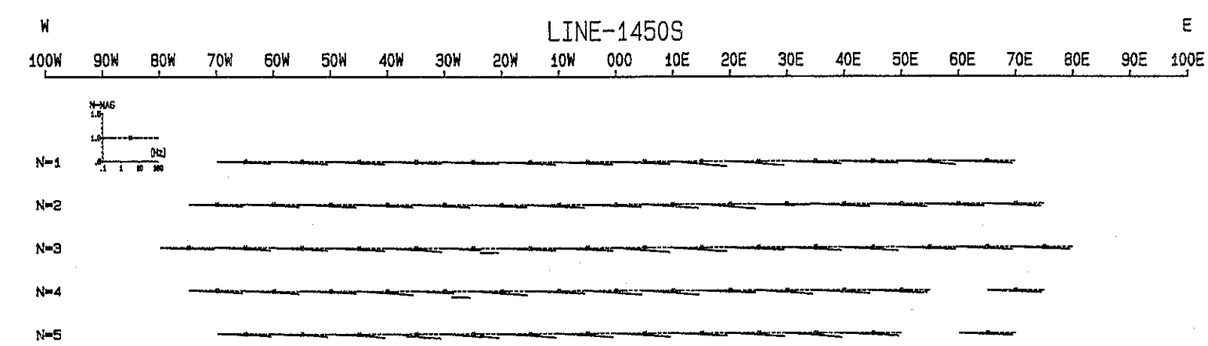

N LINE-20E S

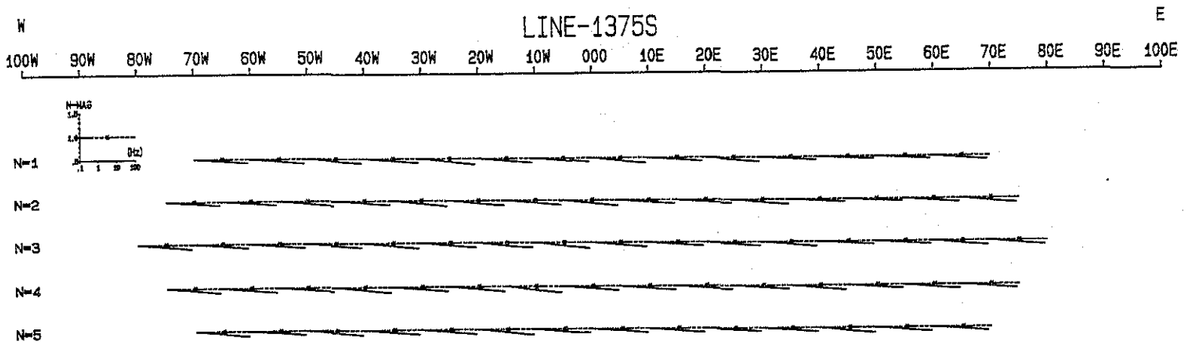

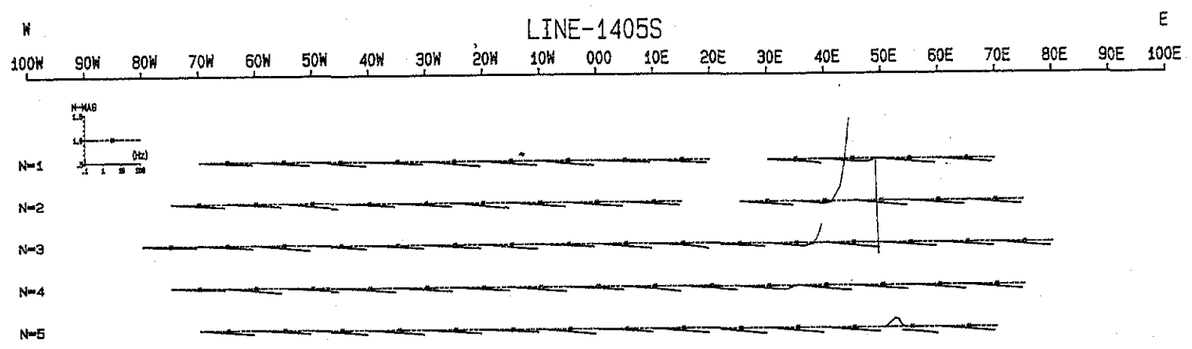

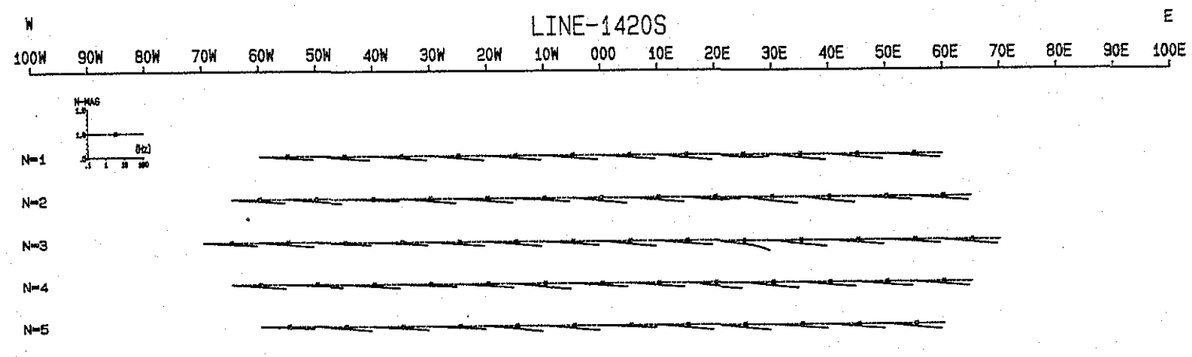

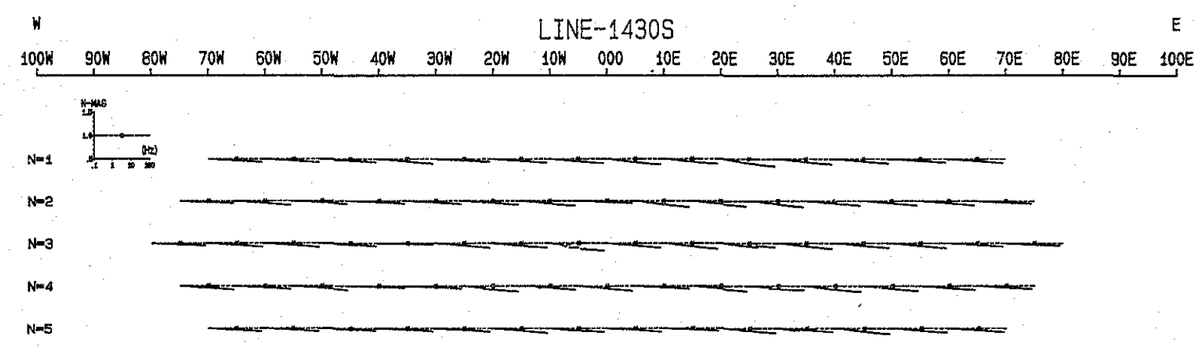

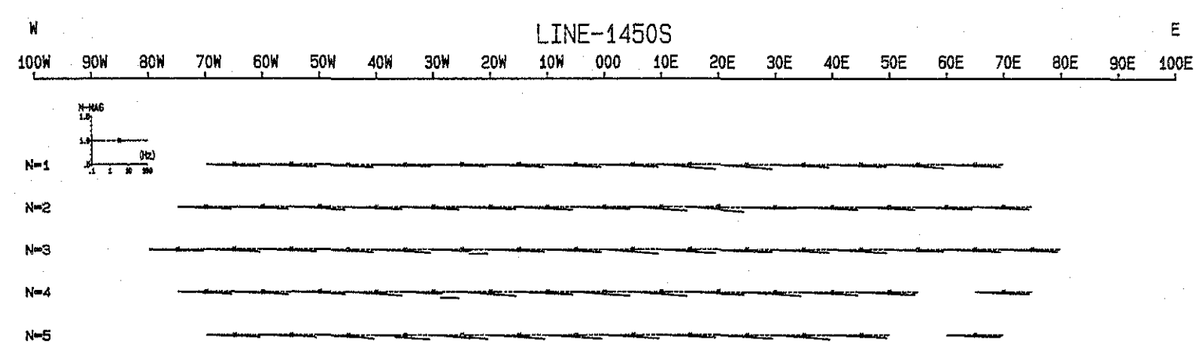

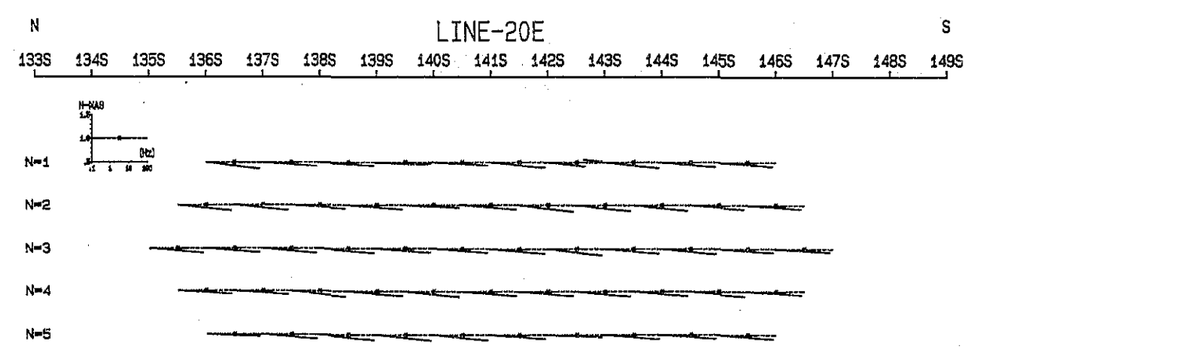

Fig. II-2-21 Magnitude Spectrum Diagram

anomalous zone of the line 1420S. Figure (I) is the typical spectral pattarn near the massive ore deposit found by PM-138-Go, drilled at measuring point 42E of the line 1430S. And Figure (J) is the one, found bloadly in the no-IP anomalous zone of the survey area.

In the Cole-Cole diagrams, nine spectral patterns except for Figure (J) among these ten patterns shows that the imaginary parts decreases towards higher frequency. The above nine patterns suggest that those are caused by the existence of the highly conductive materials such as graphite schist, by the strong mineralization and/or by sulfide minerals.

Discrimination of minerals is done usually using the phase spectrum.

In this survey, the discriminations of the anomalous sources were made as minutely as possible for the nine spectral patterns, as shown in Figures (A) through (I), being the typical patterns in this survey area. Each of the nine phase spectra shows a basic pattern due to sulfide minerals in a same manner as the one of the Cole-Cole diagram. Among these nine figures, Figures (B), (C) and (G) are the spectra reflecting strongly IP effect, which show the decrease in the phase within the higher frequency range.

It is very difficult to discriminate minerals only from the phase spectrum because the spectrum due to graphite schist and/or sulfide minerals varies with those contents, those volumes, and the environment in which those exist. However, each of the characteristic phase sprectral patterns can be observed for much pyrite/chalcopyrite and much sphalerite/galena, respectively.

A spectral pattern for much pyrite/chalcopyrite shows a gently concave curve towards the higher frequency. And the one for much sphalerite/galena shows a gently concave curve in a same manner of the above curve and also an anomalous peak between 0.1 Hz and 1.0 Hz in this curve. Each of the phase stepectra of Figures (A), (B) and (I) indicates a spectral variation (anomalous peak) due to a small amount of sphalerite/galena. It is thought that the amplitude of this anomalous peak depends on the volume percent of sphalerite, galena and pyrrhotite, and that this peak will appear notably if the ore deposit of sphalerite and/or galena is high grade.

On the other hand, a phase spectrum for much pyrite/chalcopyrite indicates a stable distribution of phases within the whole frequency range as shown in Figure (C), but the frequencies of the anomalous peak in the concave curve for pyrite and chalcopyrite are different each other. It is thought in general that the former is found in the frequency range of less than 0.125 Hz, and the latter near 1.0 Hz.

A spectral response in Figure (A) observed above the C-1 ore body shows a similar pattern as those in Figures (D), (F) and (I). Therefore, it can be said that the similar mineralized zones as the C-1 ore body may exist in the IP anomalous zone, in which similar spectral patterns as that

in Figure (A) are distributed. While, a spectral response in Figure (C) is thought to be due to pyrite.

The both spectral responses shown in Figures (A) and (C) are distributed in the southeastern IP anomalous zone, a center of which is found between Lines 1420S (measuring points 10E through 40E) and 1430S (30E through 50E), and in the southern IP anomalous zone. In detail, the former are found in the depth of the southeastern IP anomalous zone, and the latter in the shallower part from 200 m in depth between measuring points 30E and 50E of Line 1430S, and in the shallower part between measuring points 20E and 40E of Line 1420S (Fig. II-2-25 (1),(2)).

Therefore, it is thought that the anomalous source in the shallower part of the southeastern and southern IP anomalous zones are pyrite, and the anomalous source in the depth of the southeastern IP anomalous zone is pyrite and sphalerite/galena, so the latter is of a target of the drilling survey.

The spectral responses shown in Figure (C) are dominated in the northern IP anomalous zone, where no spectral response observed in Figure (A) is found. But, a small amount of sphalerite/galena and pyrrhotite were detected by the assay analysis of the core samples of the PM-77 hole, drilled in the northern IP anomalous zone. This suggests that the distribution area of such minerals is limited only in the province of the PM-77 hole, and no spectral pattern observed in Figure (A) is found in the anomalous zone. And this assumption is encountered by the drilling results of the MBP-6 hole. The reasons why the MBP-6 hole was located in this IP anomalous zone are as follows:

1) The IP effect of the northern IP anomalous zone was very strong.
2) A small amount of sphalerite/galena and pyrrhotite were detected in the PM-77 hole.
3) It was thought that although the both shallower anomalies in the southeastern and northern IP anomalous zones may be due to the same source, the deeper anomalous sources of the both IP anomalous zones are different each other.
4) As the geological structure in the northern part of the survey area was not clearly determined, it was able to clarify the geological structure and the IP anomalous source by conducting the drilling survey.

2–1–4 Model Simulation

Two-dimensional model simulation analyses were conducted for the typical IP anomalies on three survey lines, 1345S, 1420S and 1430S.

In preparing two-dimensional models, data were input in consideration of geological condi-

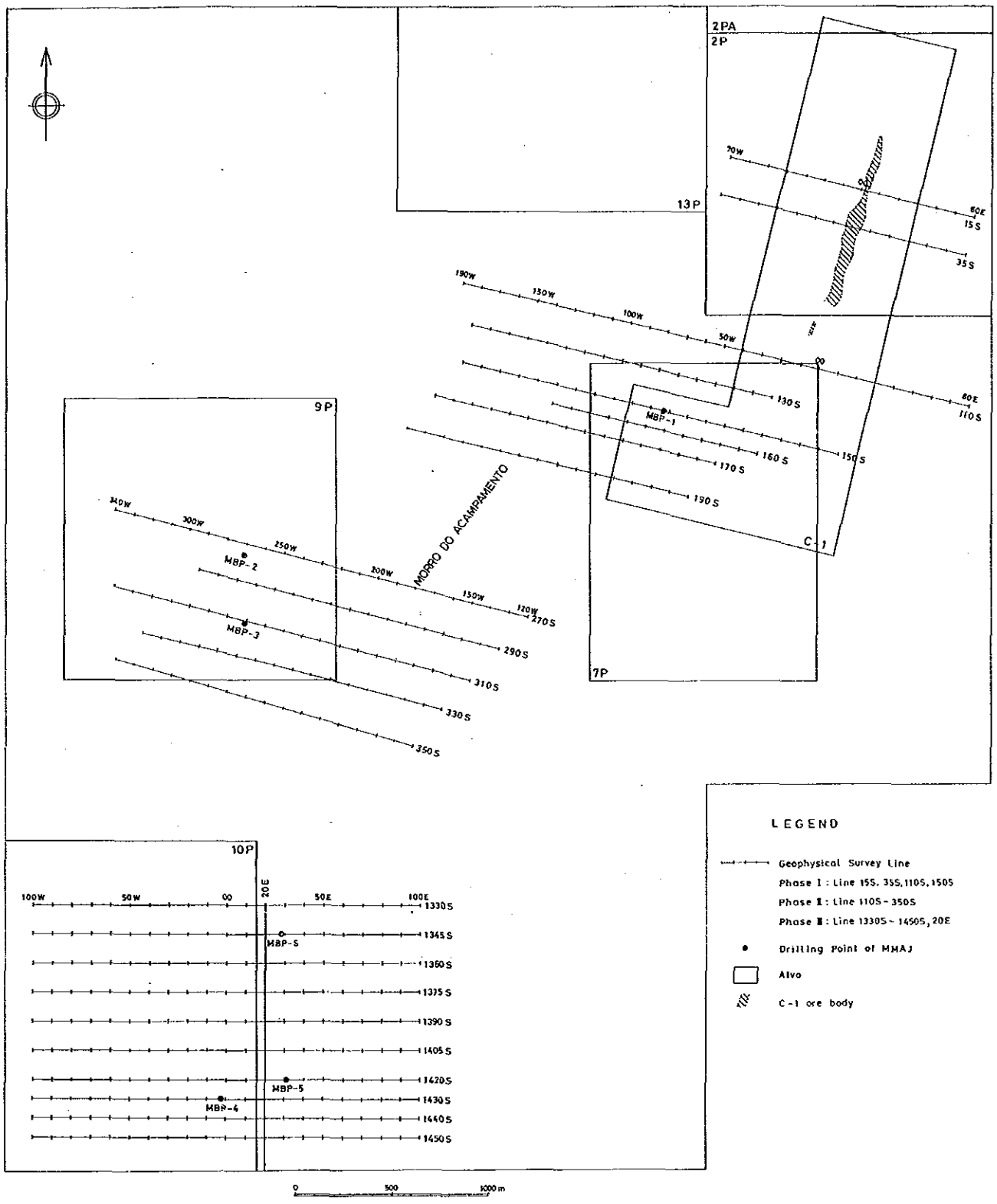

Fig. II-2-23 Location Map of SIP Survey (Phase I, II, III)

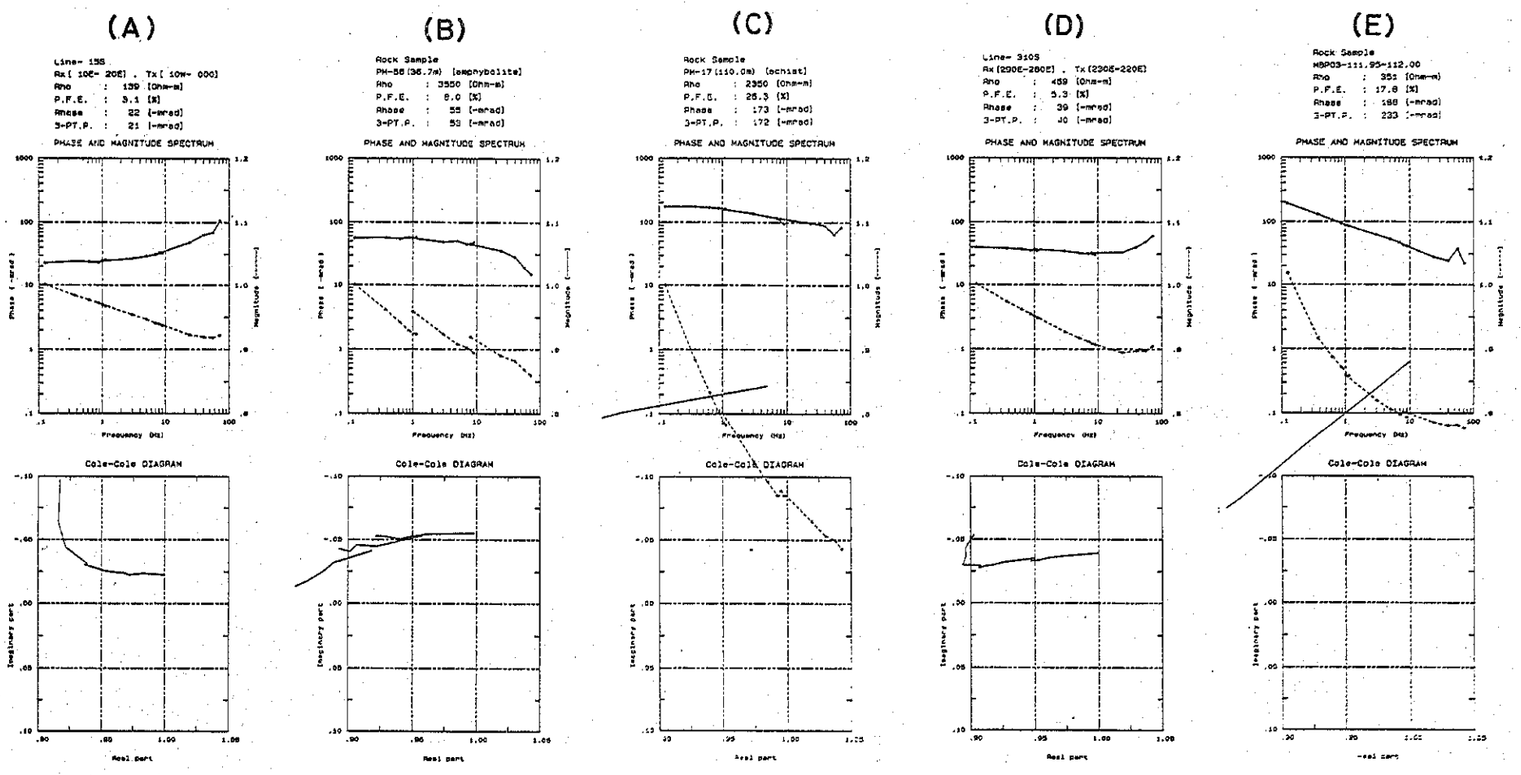

Fig. II-2-24 Typical Spectra in the Surveyed Area

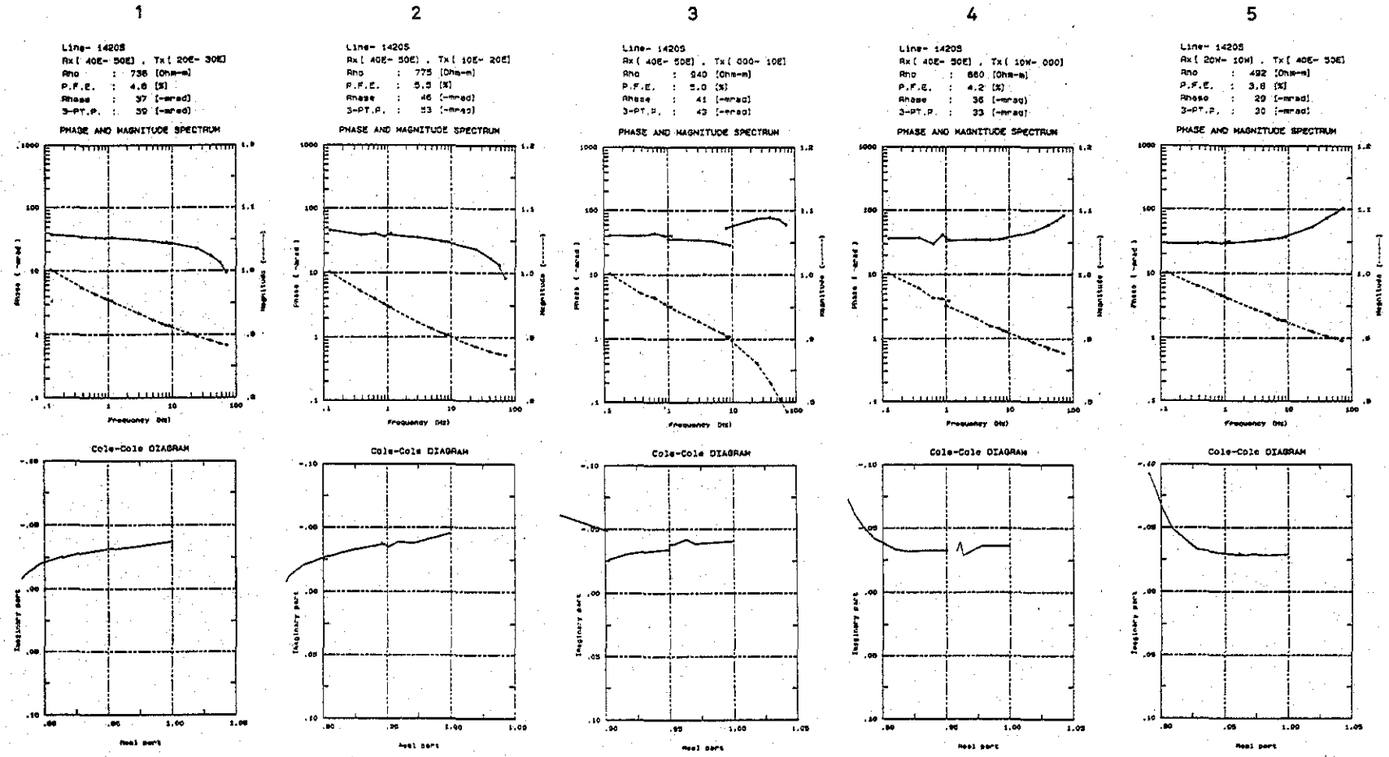

Fig. II-2-25(1) Typical SIP Spectra in Line-1420S

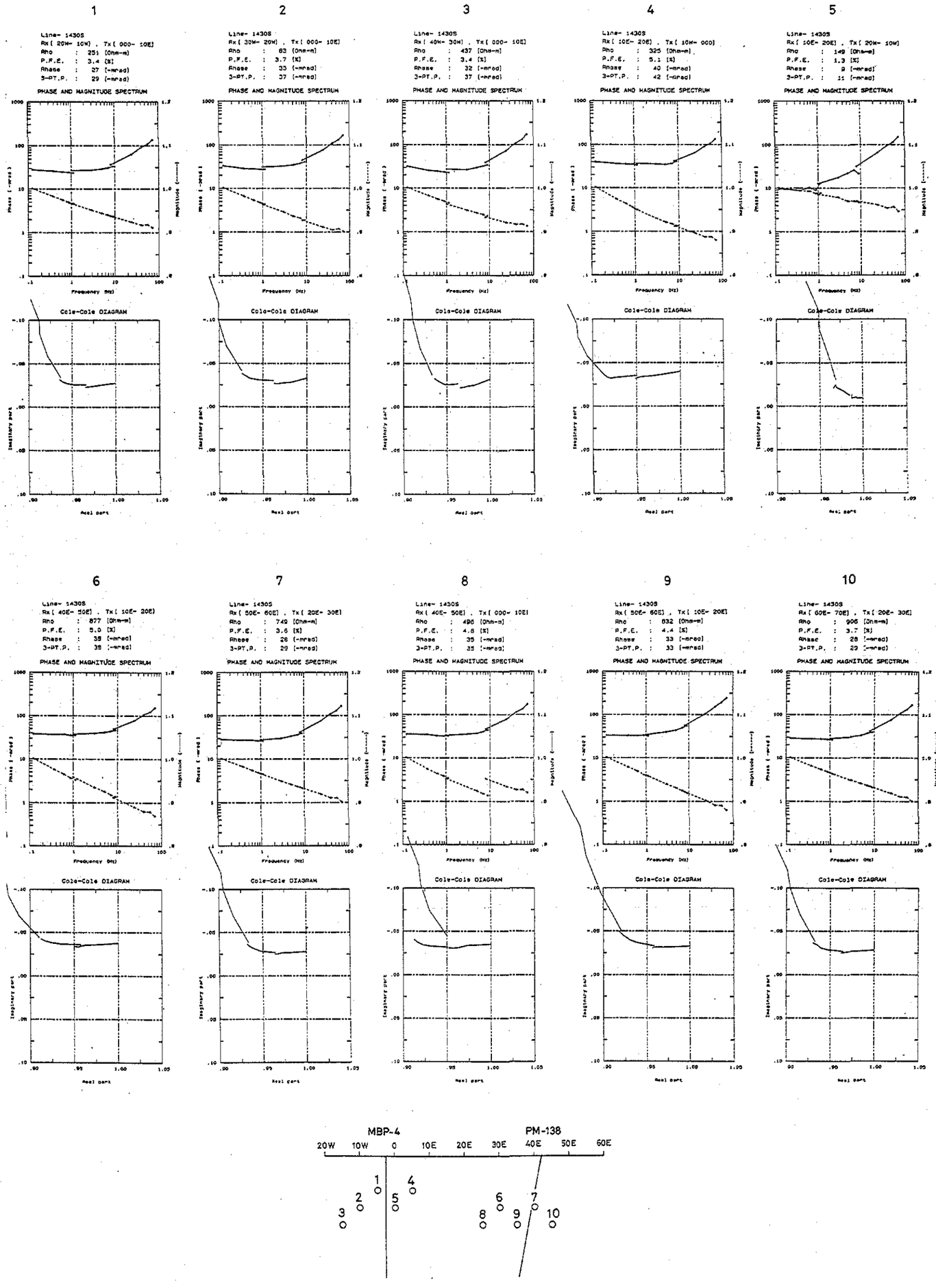

Fig. II-2-25(2) Typical SIP Spectra in Line-1430S

tions and other information acquired thus far, including the results of drilling surveys and property test of core samples. Calculation was then repeated until the values calculated approximated the values observed.

The first simulation was conducted after the field work in order to determine the locations of two drill holes. And the second simulation was conducted after the property test and mineral assays of core samples. Results of the two-dimensional model simulations are described below.

(1) **Line-1430S** (Figure II-2-28)

An IP anomaly of P.F.E. of more than 4.0 % is distributed between measuring points 10W and 40E.

P.F.E. values of more than 4.0 % are considered to indicate sulfide (pyrite) dissemination, and were therefore assigned Code 5 (500 Ω·m, -50 mrad) and Code 6 (900 Ω·m, -50 mrad). Code 1 (1,000 Ω·m, -20 mrad) and Code 3 (800 Ω·m, -20 mrad) were assigned for those considered as the background. Code 1 and Code 3 were set separately because a resistivity structure with SW-NE trend was assumed in the vicinity of measuring point 10W from the plan maps.

The drilling work of the MBP-4 hole was conducted in parallel with the geophysical survey. A sulfide dissemination zone was found at a depth of approximately 20 m through 80 m. In addition, a pyrrhotite mineralization zone was confirmed at about 287 m in depth. But this mineralization zone was not considered in the simulation model because the thickness of this zone is very thin.

Figure II-2-28 (1) shows the results of the property measurements and mineral assays of core samples. The assay result of core samples shows a phase difference of -81 mrad at a depth of 46.7 m, indicating the simulation model was proper. However, as this model did not reflect the ore body found by PM-138-GO hole. Code 9 (800 Ω·m, -100 mrad) was assigned to the ore body. The result is shown in Figure II-2-28 (2), in which no difference in phase pseudosection from Figure II-2-28 (1) is found and the effect of Code 6 set at the shallower part can be seen on the pseudosection. Taking into consideration of the continuity of geology from drilling cores, it is thought that the pyrite dissemination zone is not distributed horizontally such as in Figure II-2-28 (2), but this zone dips sharply toward the east. Since the ore body found by PM-138-GO hole is located at the edge of this dissemination zone, the new model in which each of the bodies of Codes 5, 6 and 9 shows a eastward dip. The result shown in Figure II-2-28 (3) also shows no difference from that in Figure II-2-28 (2). And the result calculated by eliminating Code 9 from Figure II-2-28 (3) is shown in Figure II-2-28 (4). But no difference is found in the phase diffe-

rence pseudosections of between Figure II-2-28 (3) and Figure II-2-28 (4), because of a large effect due to the dissemination zone (Code 6). Figure II-2-28 (5) is the result calculated by eliminating Code 6 at the west Code 9 (ore body), in which the effect of ore body (Code 9) can be found more clearly than that in Figures II-2-28 (3) and (4), indicating the simulation model is proper.

Therefore, it is understood that, since the effect of the ore body model located near the large-scale model of dissemination zone can not be recognized in the calculated phase difference pseudosection, it should be taken the geological structure into consideration in constructing a simulation model.

The highest resistivity in the model was set at 1,000 Ω·m, but the property test showed that the average resistivity value was approximately 10,000 Ω·m. This difference suggests that a lot of fracture zones may exist around the MBP-4 hole, and that the rocks are affected by such factors as the permeation of groundwater, causing a decrease in resistivity value.

(2) Line-1420S (Figure II-2-27)

An IP anomaly with the P.F.E. of more than 4.0 % is found around measuring point 30E. P.F.E. values of more than 4.0 % are considered to indicate sulfide (pyrite) dissemination, and were therefore assigned Code 2 (1,200 Ω·m, -50 mrad). As in the Line-1430S, Code 1 (1,200 Ω·m, -23 mrad) and Code 3 (800 Ω·m, -20 mrad) were assigned for those considered as the background.

The calculation result before the drilling is shown in Figure II-2-27 (1). A concentration of sulfide minerals was presumed to exist between measuring points 20E and 40E, at a depth of approximately 30 m and 150 m, in an ellipsoidal configuration, and therefore the MBP-5 hole was drilled at measuring point 30E.

The MBP-5 hole revealed that pyrite dissemination exists at a depth of approximately between 200 m and 240 m. Phase difference of -59 mrad was detected at a depth of 218 m in the property test of core samples. In the shallower part, however, the value was -30.9 mrad and no IP anomalous source as strong as the one set for simulation model before the drilling was conducted. Figure II-2-27 (2) shows a 2-D model constructed by taking the drilling results into consideration. Code 2 was set at a depth of more than 150 m, dipping toward the east. The calculation result indicates that the simulation model is proper.

2-D MODEL CALCULATION

LINE-1345S JOB:035 (0.125Hz)

CODE :	1	2	3	4	5	6	7
RESIS(Ωm):	1200	4000	500	1200	450	1000	1200
PHA(mrad):	20.0	20.0	10.0	50.0	25.0	25.0	35.0

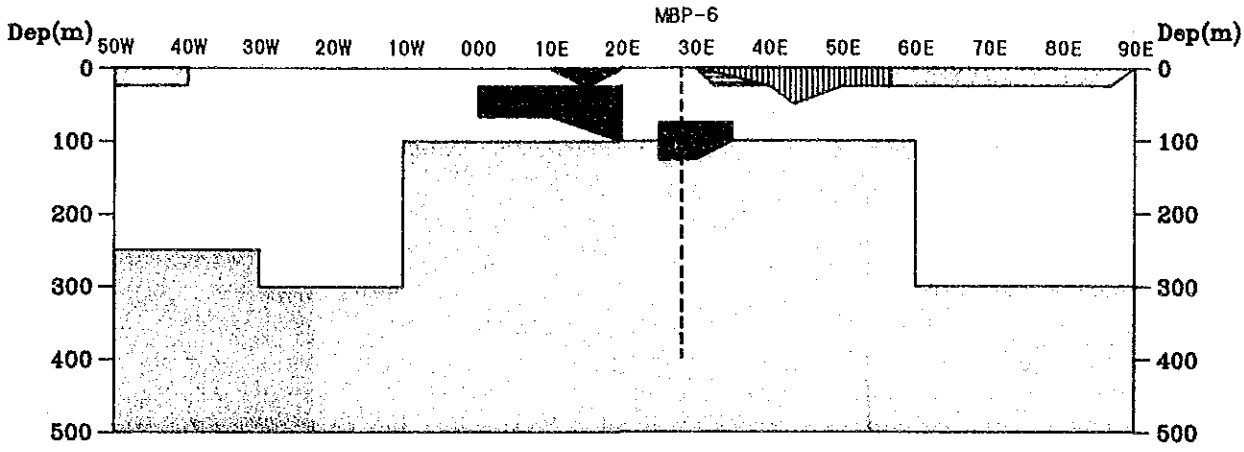

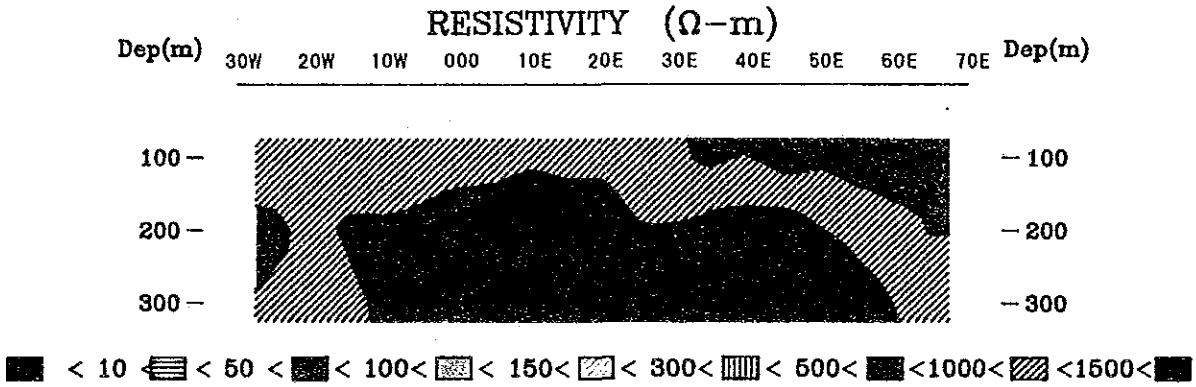

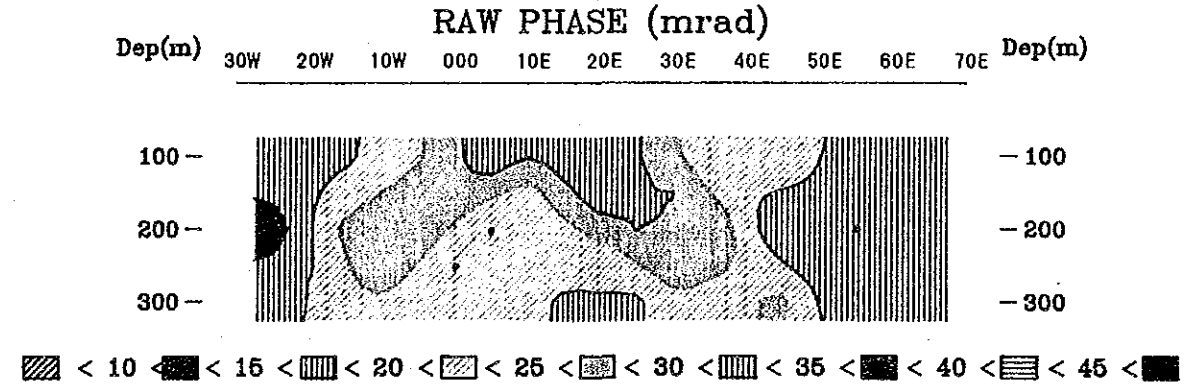

Fig. II-2-26 (1) 2-D Model Calculation (Line-1345S)

(before the drilling)

2-D MODEL CALCULATION

LINE-1345S JOB:066 (0.125Hz)

CODE :	1	2	3	4	5	6	7	8	9
RESIS(Ωm):	1200	4000	500	1200	450	1200	4000	1200	500
PHA(mrad):	20.0	25.0	20.0	35.0	25.0	30.0	20.0	50.0	10.0

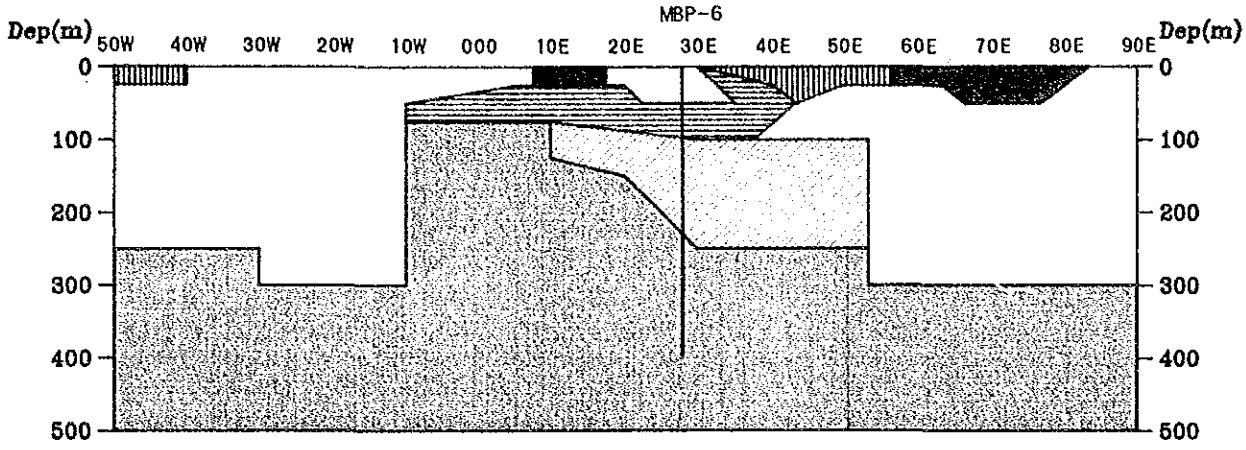

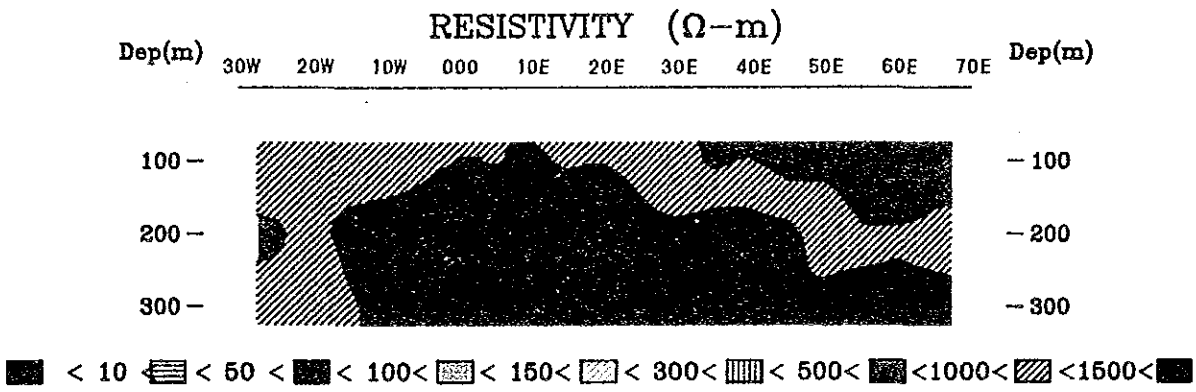

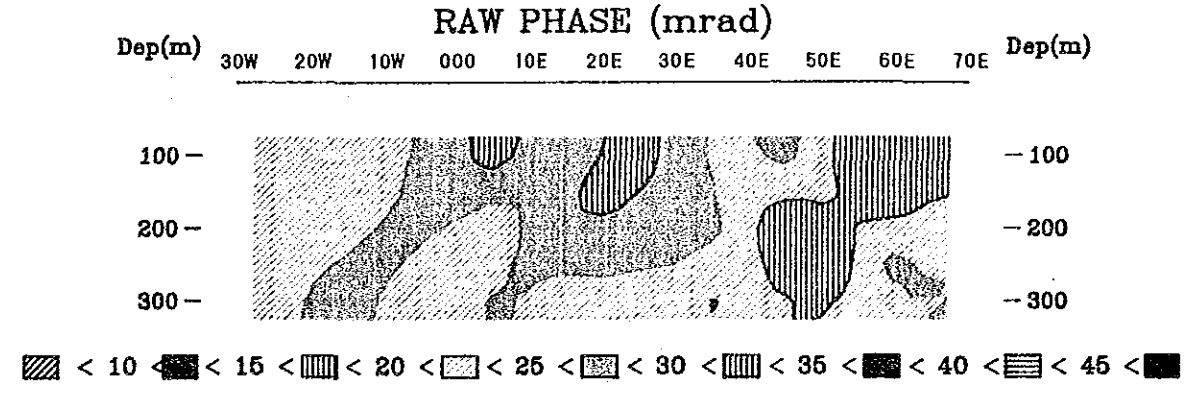

Fig. II-2-26 (2) 2-D Model Calculation (Line-1345S)
(included the drilling results)

2-D MODEL CALCULATION

LINE-1420S JOB:032 (0.125Hz)

CODE :	1	2	3	4	5	6	7	8	9	10
RESIS(Ωm):	1200	1200	800	600	1200	500	300	150	700	1200
PHA(mrad):	23.0	50.0	20.0	35.0	15.0	35.0	37.0	15.0	23.0	35.0

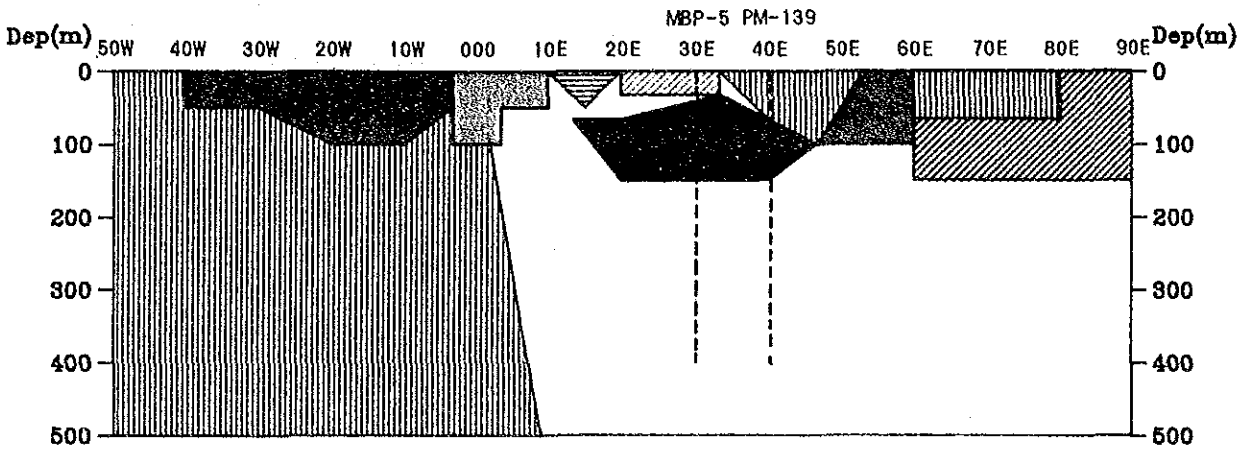

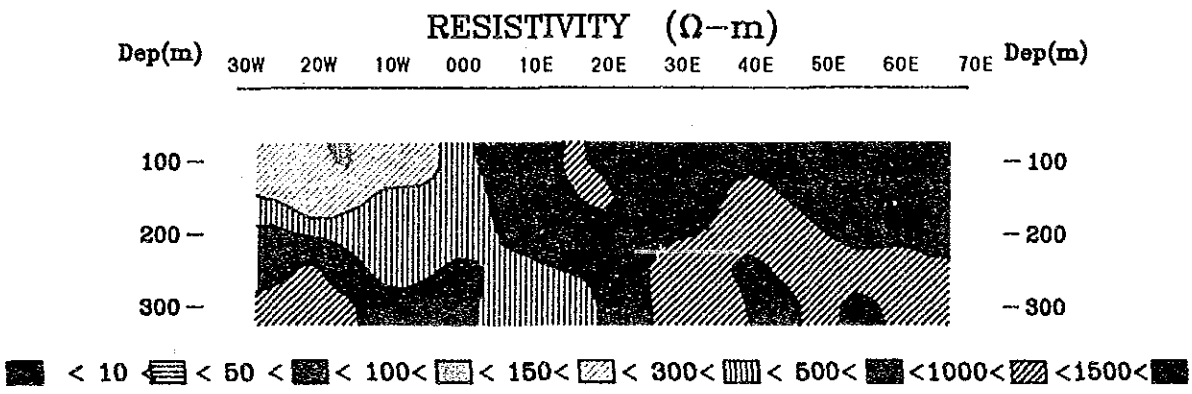

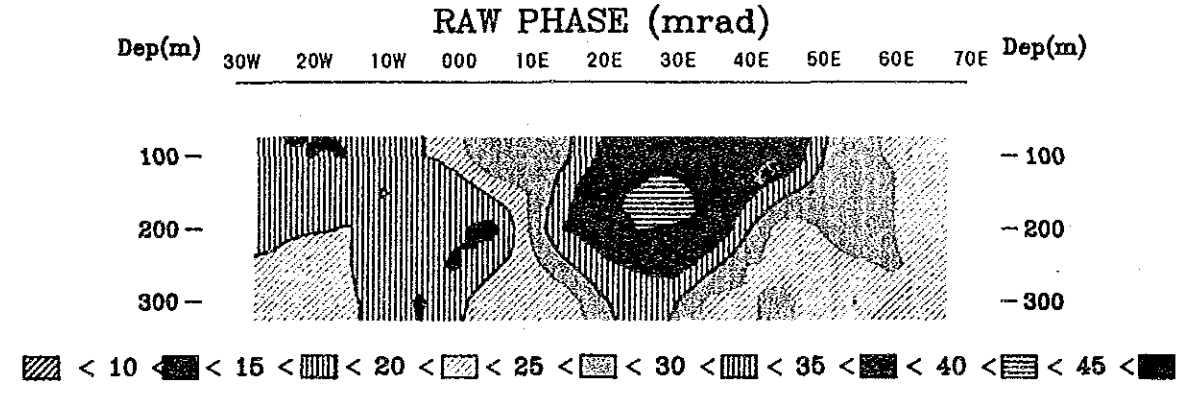

Fig. II-2-27 (1) 2-D Model Calculation (Line-1420S)

(before the drilling)

2-D MODEL CALCULATION

LINE-1420S JOB:045 (0.125Hz)

CODE :	1				5	6	7	8	9	10
RESIS(Ωm):	1200	1200	800	600	1200	800	300	150	700	1200
PHA(mrad):	23.0	60.0	20.0	35.0	15.0	30.0	30.0	20.0	23.0	35.0

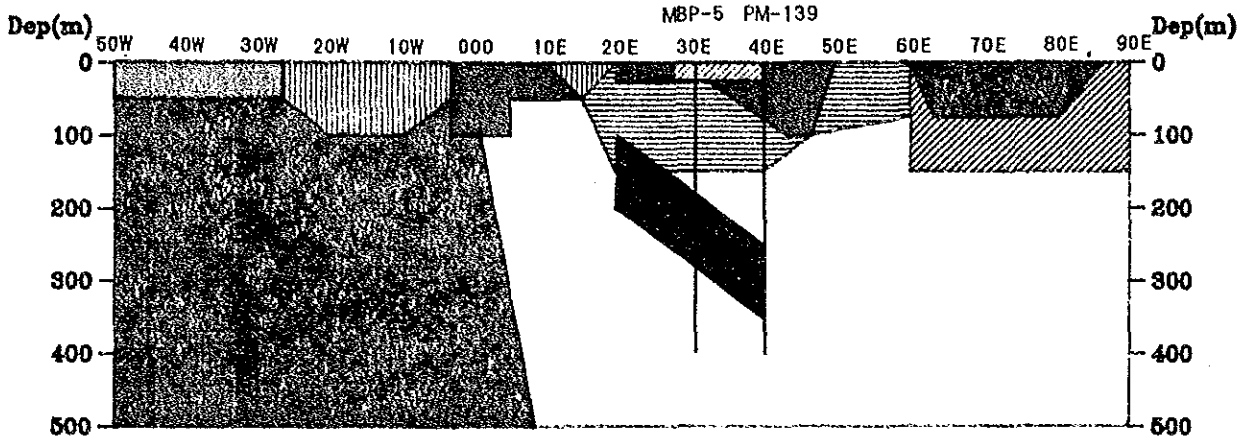

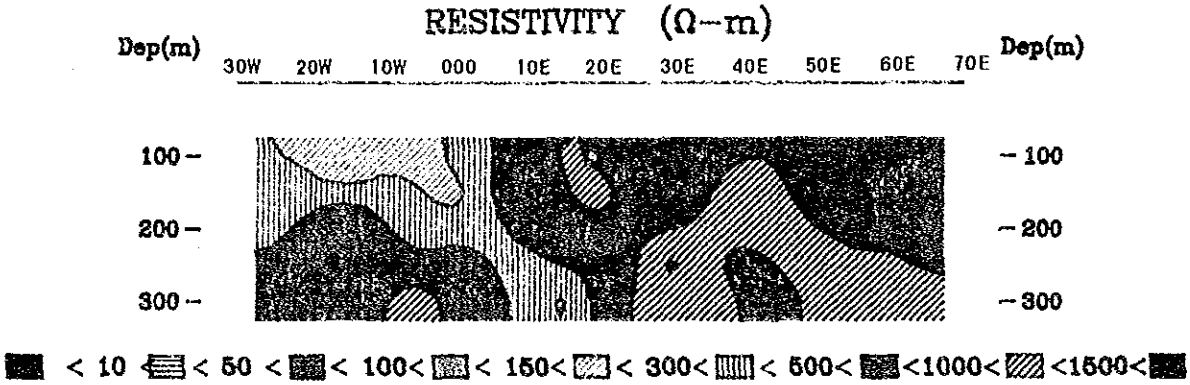

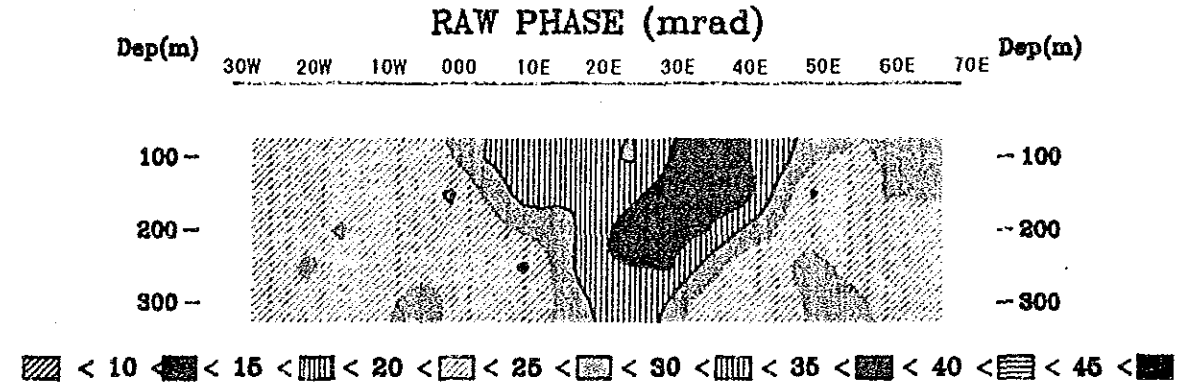

Fig. II-2-27 (2) 2-D Model Calculation (Line-1420S)
(included the drilling results)

2-D MODEL CALCULATION

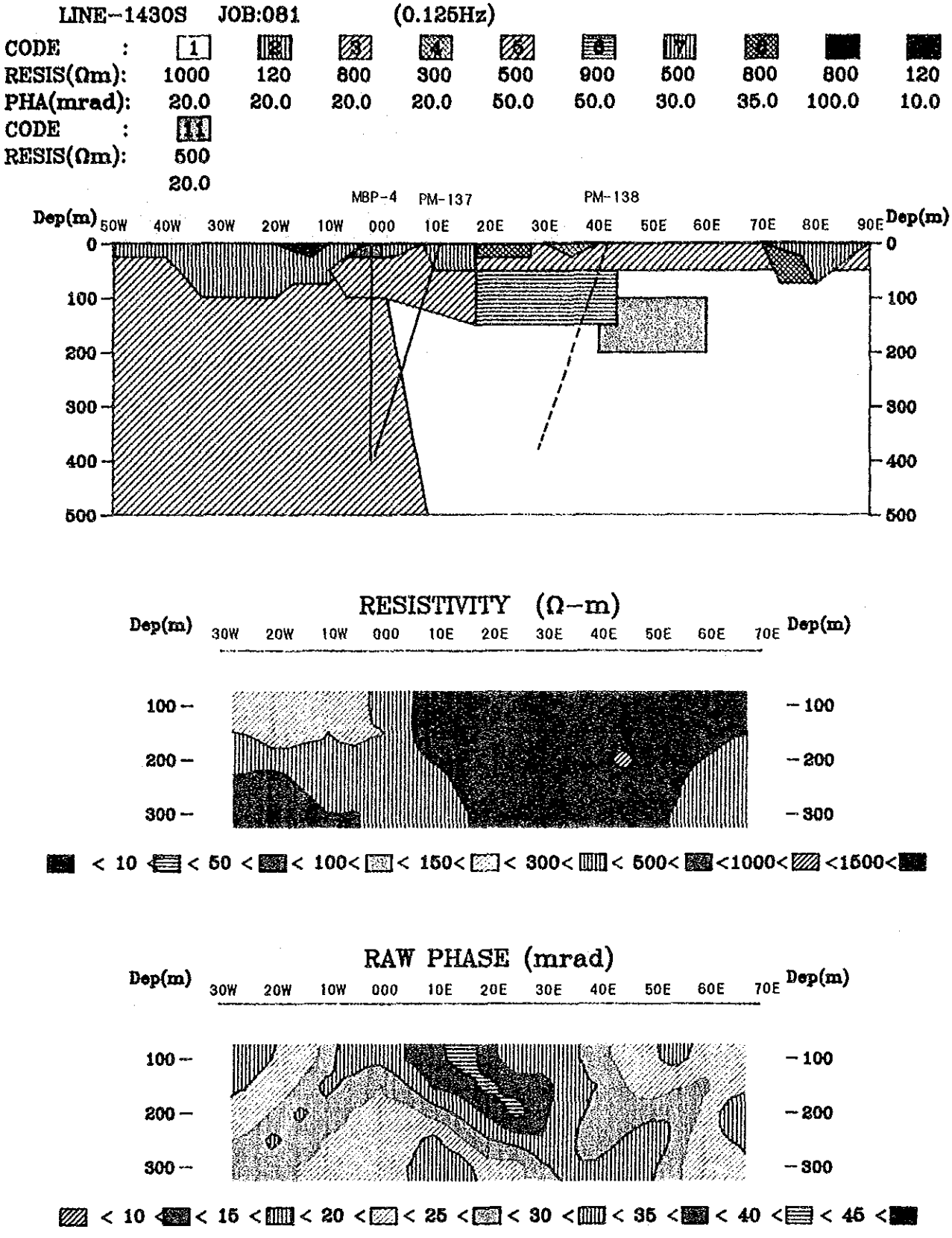

Fig. II-2-28 (1) 2-D Model Calculation (Line-1430S)

(first model including the drilling results)

2-D MODEL CALCULATION

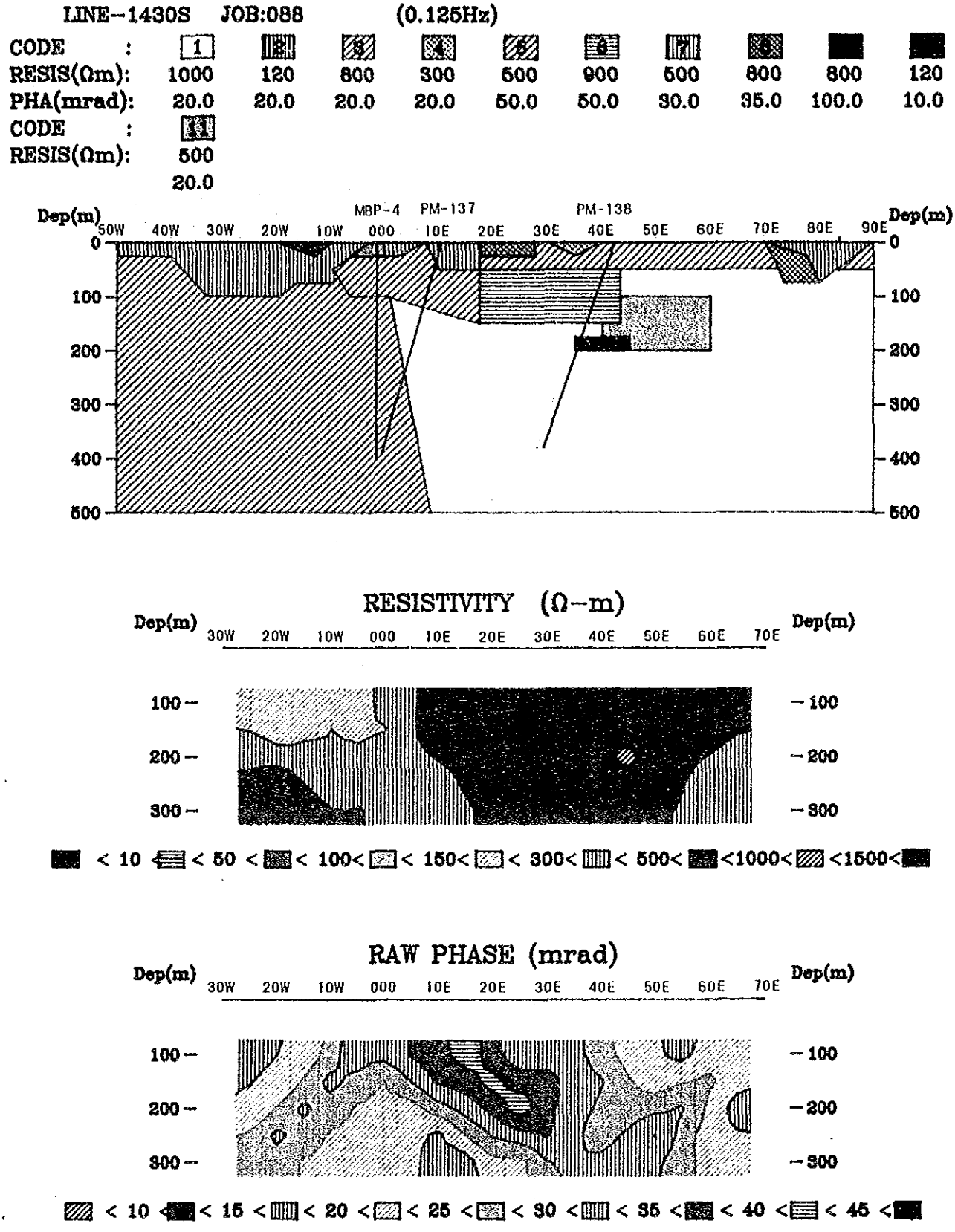

Fig. II-2-28(2) 2-D Model Calculation (Line-1430S)

(included Code 9, the ore body found by PM-138-GO)

2-D MODEL CALCULATION

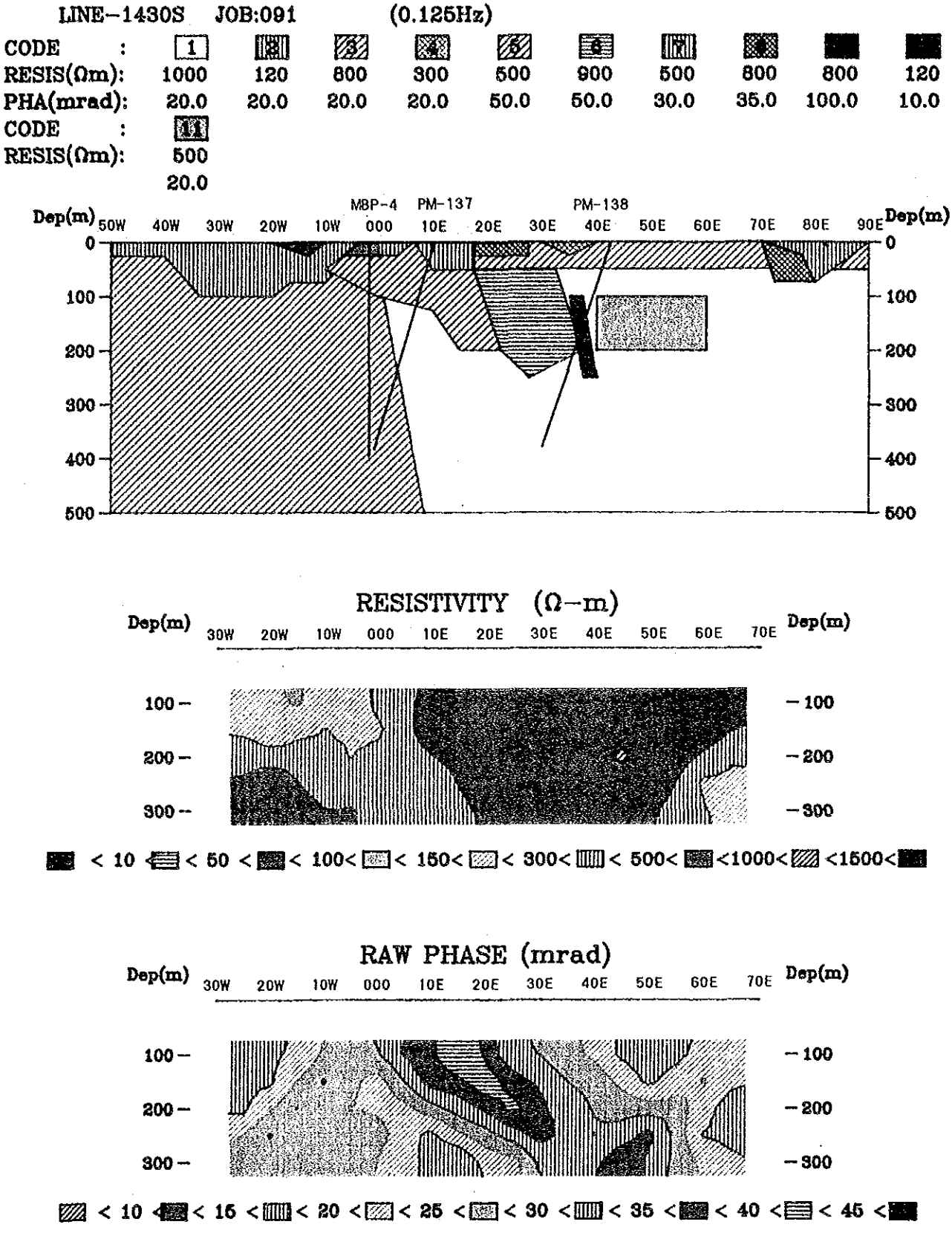

Fig. II-2-28 (3) 2-D Model Calculation (Line-1430S)

(inclined the Code 5, 6 and 9 toward the east)

2-D MODEL CALCULATION

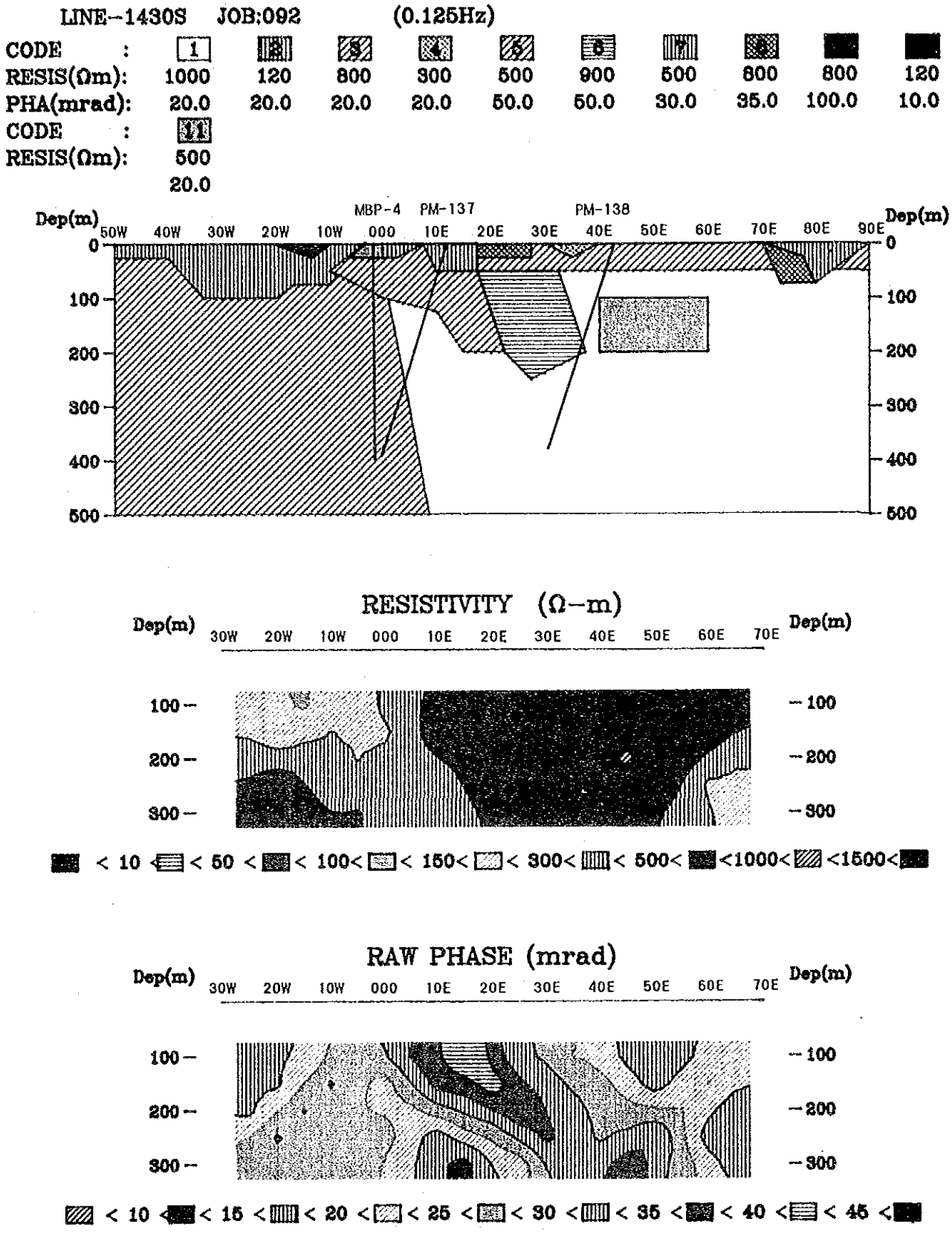

Fig. II-2-28 (4) 2-D Model Calculation (Line-1430S)

(eliminated the Code 9 from Fig. II-2-28(3))

2-D MODEL CALCULATION

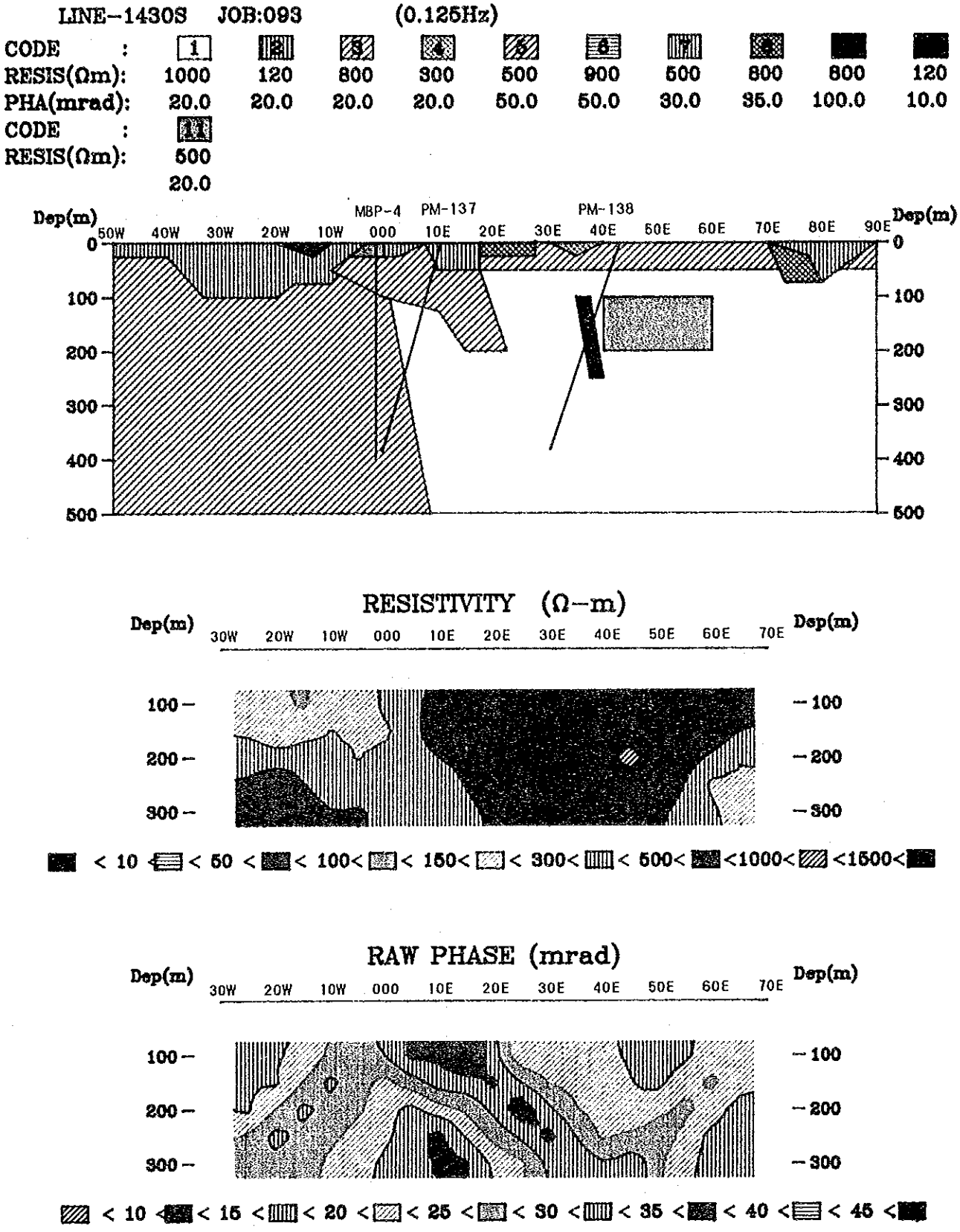

Fig. II-2-28(5) 2-D Model Calculation (Line-1430S)
(eliminated the Code 6 from Fig. II-2-28(3))

(3) Line 1345S (Figure II-2-26)

An IP anomaly with P.F.E. of more than 4 % is found between measuring points 10W and 35E. P.F.E. values of more than 4 % are considered to indicate sulfide (pyrite) dissemination, and were therefore assigned Code 4 (1,200 Ω·m, -50 mrad). Code 1 (1,200 Ω·m, -20 mrad) and Code 2 (4,000 Ω·m, -20 mrad) were assigned for the background. Since compact schist including much quartz is seemed on the plan maps to be widely distributed in the northern part of the survey area in which the Line 1435S was located, resistivities of the background were set high.

The calculation result before the drilling was shown in Figure II-2-26 (1). Code 4 was divided into two blocks in view of the distribution pattern of an IP anomaly. The western block was assumed, based on the results of the previous drilling, to represent pyrite dissemination zone and, therefore the MBP-6 hole was drill in the eastern block.

The drilling of MBP-6 hole confirmed the existence of pyrite dissemination zones at the depth of between 210 m and 220 m, and at the depth of between 370 m and 390 m. However, the amount of sulfide minerals contained in the core samples was considerably less than those in the samples from the other two holes, and only a small amount of sulfide minerals was found at depth of between 75 m and 125 m for which Code 4 was assigned. In the property test of the core samples, however, phase differences of between -35 mrad and -45 mrad were detected in the shallower part and at a depth of more than 250 m. Figure II-2-26 (2) shows a 2-D model constructed by taking the drilling results into consideration. Although phase difference of -35 mrad set for Code 4 was smaller than those of the other two lines, the distribution pattern of phase difference close to the one actually observed was obtained by changing phase difference of the background to -25 mrad. Therefore, it is thought that the IP anomaly observed in this line does not represent the sulfide dissemination locally distributed, but is orginated from the weak dissemination within schist widely distributed.

2–2 Drilling Surveys

In the drilling surveys, one hole was drilled in parallel with the geophysical survey and two other holes were drilled based upon the analysis of the geophysical survey. Drilling was performed by Geologia e Sondagens, Ltda. a Brasilian exploration company (GEOSOL) employing one drilling machine.

The instruments used for each hole are shown in Table II-2-1, and the drilling results, articles of consumption, the number of diamond bits consumed are shown in Table II-2–2.

Table II-2-1 Drilling Equipments

Drilling Machine	SONDEQ Model SS-51		
	Capacity	550m (by BW rods)	
	Dimensions	1,130 × 2,600 × 1,700 (㎜)	
	Hoisting Capacity	4,500kg	
	Spindle speed	80-230-310-600-1000	
	Engine	Perkins Model 42031	
Water Supply Pump	SONDEQ Model SB-1		
	Capacity	4,500 liters/hour	
	Engine	Agrale Model M-BS	
Drilling Pump	SONDEQ Model SB-140		
	Cylinder bore diameter	$2 \cdot \frac{3}{4}$ inches	
	Capacity	5,700 liters/hour	
	Engine	Agrale Model M-790	
Mud Mixer	not used		
Generater	not used		
Drilling Tools	Drilling rod	BW 3.05m	179 pcs
	Casing pipe	HX 3.00m	7 pcs
		NX 3.00m	80 pcs
Derrick	Made in Geosol	12m High	

(1) Location of Drill holes

One of the holes, MBP-4, was located to detect the continuity of known mineralisation based upon the data from the former CPRM exploration program and to search for the possible mineralized horizon below the known mineralization. Two other holes, MBP-5 and MBP-6, were located to detect continued and/or new mineralization based upon the results of the geophysical survey done in 1988.

The locations of these three holes are shown in Fig. II-1-1.

(2) Readjustment of the Land and Drilling Equipment and Supplies Transportation

Both the cutting of the roads for transportation and the readjustment of the land were not

Table II-2-2 Drilling Results and Consumed Articles

	MBP-4	MBP-5	MBP-6
Location(coodinates)	E792.62 N8548.36	E792.95 N8548.46	E792.93 N8549.215
Inclination	-90 degree	-90 degree	-90 degree
Drilling Depth	400.00 m	400.45 m	401.32 m
Core Length	399.65 m	400.45 m	401.32 m
Core Recovery	99.9 %	100 %	100 %
Casing	30.05 m	37.00 m	24.80 m
Drilling Period	June 7 ~ July 1	Aug. 8~Aug. 24	Aug. 25~Sep. 7
Actual working days	22 days	14 days	12 days
Working time(drilling time)	180 hours	148 hours	143 hours
Working time(others)	121 hours	98 hours	85 hours
Trouble recovery	6 hours	5 hours	
Mounting & Dismounting	18 hours	26 hours	33 hours
Disel Oil (l)	1000	905	965
Lubrif (l)	14	5	7
Graxa Haste (kg)	90	139	215
Bentonite (kg)	400	625	150
Soluvel (l)	115	143	190
Sement (kg)	100	0	0
Metal Crown HX	1	1	1
Diamond Bit HX	2	2	1
Diamond Bit NX	14	6	4

required because the sites of three holes were flat. Drilling equipment was transported directly into and out of the drilling sites using large-sized trucks.

(3) Water for Diamond Drilling

Water for diamond drilling was supplied from the stream and pond in the vicinity of each site using water pumps and hoses. The distance and the relative height from the source of water to the MBP-4 site are about 350 meters and 30 meters respectively; the MBP-5 site, about 250 meters and 23 meters respectively; the MBP-6 site, about 150 meters and 15 meters respectively.

(4) Drilling

Soil was penetrated in each hole by conventional drilling methods using HX metal crown. After encounting bed rock, drilling was also performed by conventional method using HX and NX type diamond bits.

Progress of three holes are as follows:

MBP–4 (Figure II-2-29 (1))

* 0 ~ 14.50m

Surface soil was cut by a conventional method uing HX Metal crown.

* 14.50 ~ 30.05m

Strongly weatherd mica schist was cut by the conventional method using HX diamond bit. Casing pipes of NX size were inserted from the surfaces down to 30.05m.

* 30.05 ~ 400.00m

Muscovite-biotite schists, garnet-muscovite-biotite schists, amphibolites and some other rocks were cut by the conventional method using NX diamond bits. Those rock facie were stable until the drilling depth reached about 208m where the hole collopsed. The hole was cemented with concrete between 118.80m and 208m. The hole were reamed near the bottom when the depth reached to 345m. The drilling was completed at the planned depth of 400m midnight, July 1st. The equipment was moved to the MBP-5 site on August 8.

MBP–5 (Figure II-2-29 (2))

* 0 ~ 21.90m

Surface soil and strongly weathered and argillized rocks were cut by conventioal methods using HX metal crown.

* 21.90 ~ 31.00m

Strongly weathered mica-schist was cut by conventional methods using HX diamond bit. Casing pipes of NX size were inserted from the surface down to 31.00m.

* 31.00 ~ 400.45m

Muscovite-biotite schist, amphibole-biotite schist, amphibolite and other types of rocks were cut by conventional methds using NX diamond bits. Drilling was continual because of the stable rock facies and diamond bit consumption was low. When the hole reached the depth of 56.45m, drilling water escaped at a depth of 37m and above shallower than 37m. The hole between 31.00 ms and 37.00m were reamed, then casing pipes of NX size were inserted. When the reaming was completed, the drilling rod broke in the lower part of the hole. Four and a half hours were spent during the recovery of those drilling rods and hole cleaning.

MBP–6 (Figure II-2-29 (3))

* 0 ~ 19.10m

Surface soil was cut by conventional methods using HX metal crown.

* 19.10 ~ 24.80m

Strongly weathered mica-schists were cut by conventional methods using HX diamond bit.

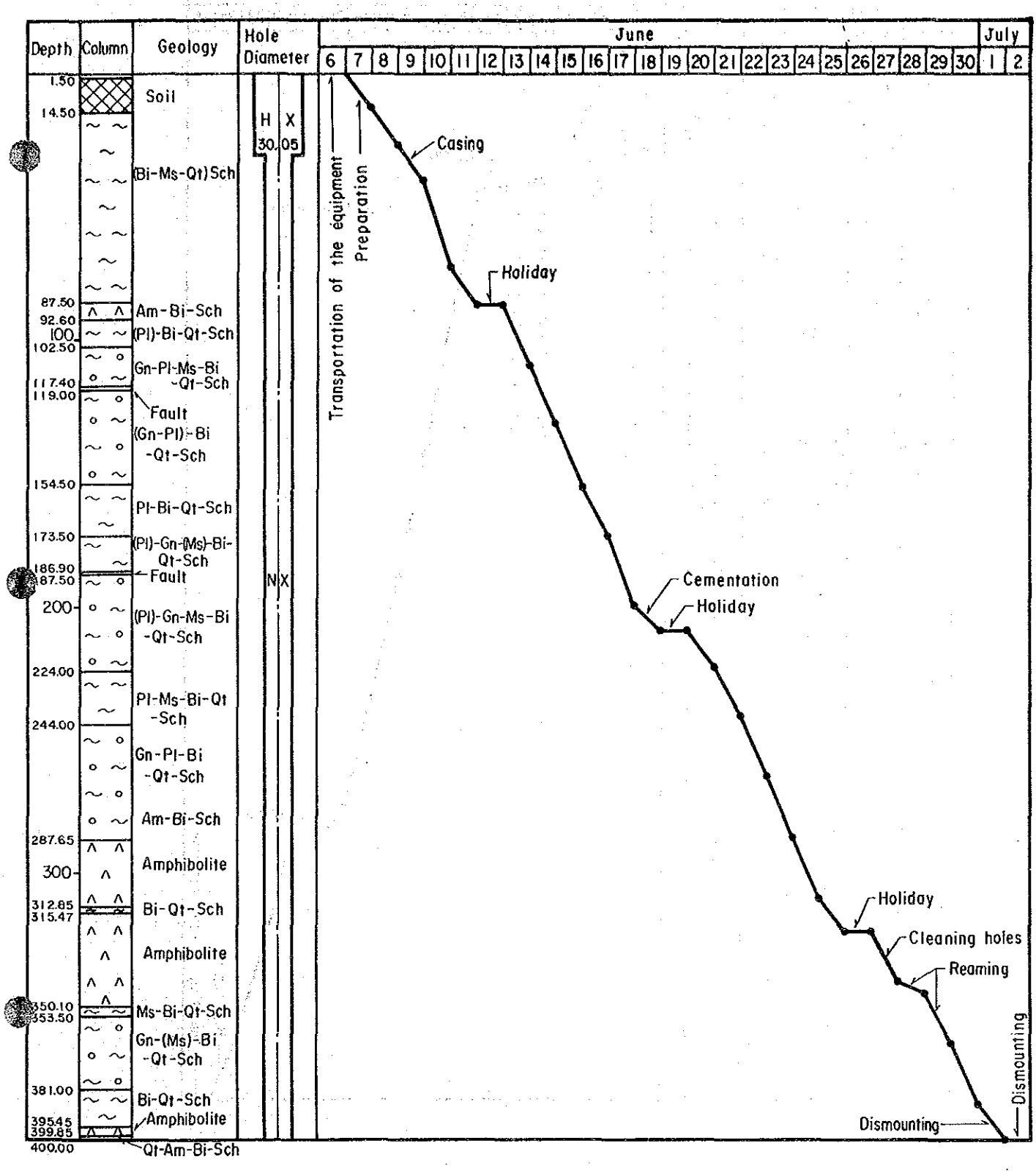

Fig. II-2-29(1) Progress Record of MBP-4

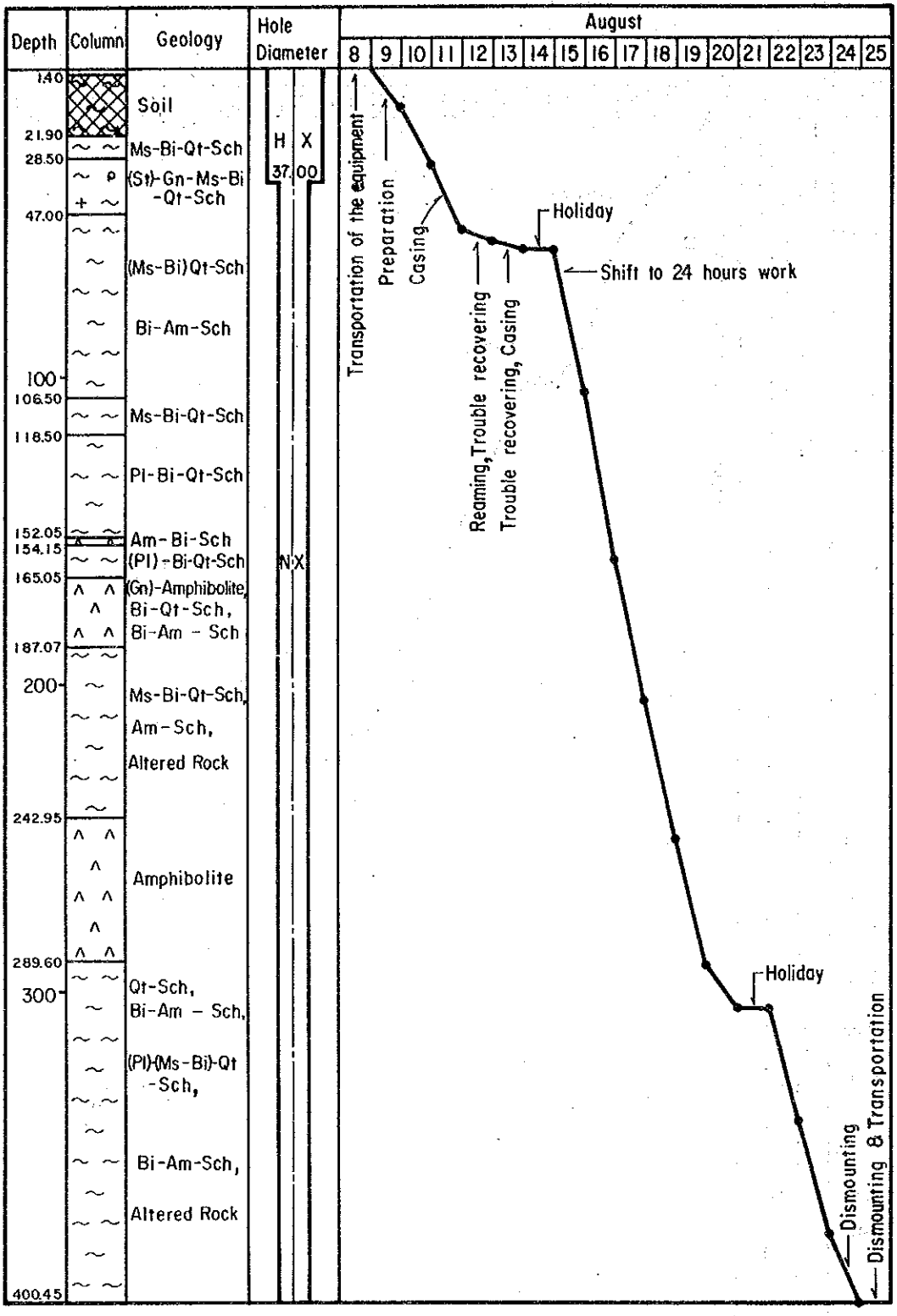

Fig. II-2-29(2) Progress Record of MBP-5

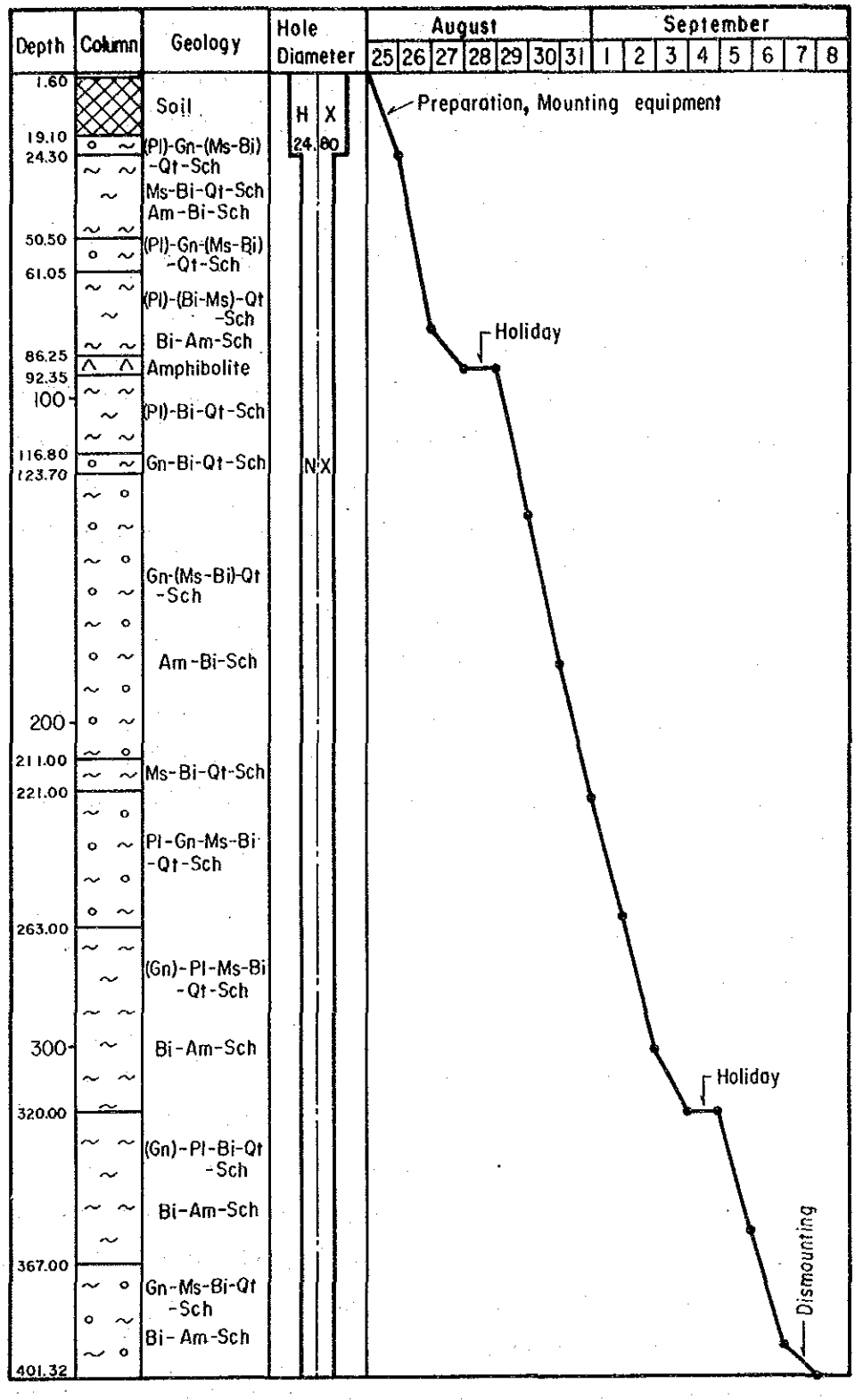

Fig. II-2-29(3) Progress Record of MBP-6

Casing pipes of NX size were inserted from the surface down to 24.80m.

* 24.80 ~ 401.32m

Mica schist, biotite-amphibole schist, amphibolite, and other types of rocks were cut by conventional methods using NX diamond bits. Drilling was continued because of the stable rock facies. Diamond bit and bentonite cosumption was lowest in this local.

(5) Drill Hole Deviation

A survey of the deviation of drill holles was not carried out in any hole.

2–2–1 Geology and Mineralization of Hole MBP-4

Geology columns of each hole were made at a scale of 1:200 (Figure A-3). They were then compiled in bending line graphs showing the increase and decrease of principal rock forming minerals and ore minerals in the rock. Figure A-3 indicates the changes in amount of each mineral with the change in depth, but it does not indicate the relative amount among those minerals. At the same depth of Figure A-3 and Figure II-2-30, the rock name is offen different. It is because the rock names of Figure II-2-30 were compiled for conveneince while the scale of Figure II-2-30 was made by enlarging the scale of Figure A-3.

In the column "Plagioclase" under "Principal Constituent" of Figure A-3, no discriptions were intentionally made with the naked eye. That is not because plagioclase does not exist, but because it was difficult to identify with the naked eye. Labolatory experiments, number of samples, and results are shown in Table II-1-5, Table II-2-3, respectively.

(1) Surface geology of the Surroundings

The C-1 ore body is found about 5 km northeast of Alvo 10P, the main part of the survey area in this year. Amphibolite from the Pip_3 formation is distributed around the C-1 ore body and goes under the schists of the Pip_4 formation south-east of the ore body and ore surfaces in the Alvo-10P, according to our survey carried out in 1987 and CPRM(1982), Pip_4 formation between above mentioned two locations is divided into three members north to south, namely felspathic biotite-quartz schist ($Pip_4 vxt_1$), plagioclace-microcline-biotite-quartz schist ($Pip_4 vxt_2$) and sericite-microcline-quartz schist ($Pip_4 vxt_3$) in ascending order. At the nearest area to the Alvo-10P, $Pip_4 vxt_2$ reappears. These formations are generally distributed in an elliptical shape with the longer axis trending north-northeast.

Between C-1 ore body and Alvo-10P, there are some north-northeast trending structures,

they are a syncline trending north northeast from C-1 ore body and an anticline trending north northeast to the north apart from the syncline by about 500m, both of them are overturned to northwest. These folds do not reach to the Alvo-10P, according to the former survey. Two large faults trending north northeast, passing Alvo-10P are also presumed. One runs south southwestward from the area in the north of C-1 ore body by 700 ~ 1000 meters and the other runs from the area in the southwest of C-1 ore body by about 2km.

In this year's survey area, amphibolite of Pip_3 formation is distributed in the westernmost and southwest parts, in the rest of the area Pip_4 formation is distributed. Pip_4 formation is not known in detail due to its poor outcrops and strong weathering. However, it is thought to consist of the alternation of muscovite-quartz schist (Ms-Qt-Sch), biotite-quartz schist (Bi-Qt-Sch), biotite-muscovite-quartz schist (Bi-Ms-Qt-Sch), garnet-muscovite-biotite-quartz schist (Gn-Ms-Bi-Qt-Sch), amphibole schist (Am-Sch), amphibolite among others.

Amphibolite in the alternation typically crops out trending north northwest in the central west of the survey area. Due to flat topography, laterite and "Canga" limonitized is often present on the surface. Canga covers a relatively large area in the eastern half of the survey area.

Two main northeast trending faults divide the survey area into three parts. These faults were formerly inferred by airphoto interpretation and from the geological discontinuity checked by this years surface geological survey. These inferred faults might be a discontinuous zone caused by folds for a reason mentioned later.

Between these faults, smaller north northwest trending faults are presumed to be present. Some faults trending northwest to north northwest are also inferred by the geophysical survey. Strikes of the plane schistosity (in this area, the plane of schistosity is not very different from the bedding plane) trend north to northwest in the vicinity of amphibolite (Pip_3) in the west of the survey area and change to northeast to east northeast in the areas of east section. Almost all the planes of schistosity dip a east to southeast. That is, the trend of the geological structure excells in north northwestern direction in the western part of the survey area corresponding to the geogical distribution. The trend changes to northeast in the east to northeastern part.

(2) Geology of the Hole (Fig. A-3)

0.00 ~ 1.50m

Dark brown to pale brown soil.

1.50 ~ 14.50m

Brown to pale brown soil. Rock forming minerals are scarcely left undeformed; only micas

are discriminated. However, at 7.90-8.05m, 9.30-9.75m, 10.65-11.00m and 12.25-12.38m, rocks are slightly weathered and rock forming minerals are mostly left undeformed. They are originally Ms-Qt-Sch.

14.50 ~ 20.00m

Pale grey Ms-Qt-Sch are limonitized along schistosities. Biotite is hardly observed. There are massive white quartz at 14.50-14.70m and at 17.50-17.62m. The core intersects distinct schistosity by 70 to 80.

20.00 ~ 28.80m

Grey Ms-Bi-Qt-Sch. Generally, there is much more biotite than muscovite. At 25.73-26.43m and at 26.50-26.55m, the rock is composed primarily of biotite. At the bottom of this section, there is less muscovite and biotite. 28.10-28.20m is massive quartz. The section from the top down to 22.70m is limonitized along schistosities. The ore crosses distinct schistosity by about 70° at 20-26m and by 80°-40° at 26-28m.

28.80 ~ 73.50m

Bi-Ms-Qt-Sch. 28.80-65.60m is grey and 65.60-73.50m is pale grey. At 28.50-54.00m, the amount of muscovite is more than that of biotite, below 54.00m the amount of biotite and muscovite are about equal. Microscopic observation of thin sections show: biotite, muscovite, quartz as the principal rock forming minerals; sphene and apatite as minor minerals included at 30.00m; biotite, muscovite and quartz as principal mineralzation accompanied with large quantities of sphene and very small quantity of potash feldspar, plagioclase, zircon and apatito (Table A-3). 30.50-30.60m is massive quartz and 39.20-39.25m is mostly composed of biotite. At 51.00-52.00 m, 74.00-75.00m there are many small, irregular shaped massive quartz fragments less than 10cm.

Below about 27.00m fine grained pyrites are included as disseminations and partly as stringers; 43-49m is particularly rich in pyrite. The dissemination zone is observed down to 90m and also includes sphalerite and galena. At 33-37m, 43-49m the rock is particularly rich in pyrites. Both of galena and sphalerite occur as network stringers in 29.25-30.05m, as dissemination at 43.40-44.80m, as both of network stringers and disseminations at 65.10-66.10m, 66.30-66.60m and 67.60-67.80m, as stringers at intervals subparallel to the schistosities and as stratabound at 78.25-78.30m. In each occurrence, the relative amount of the above minerals is pyrite, sphalerite, galena in descending order. Galena occurs sporadically aid there is very little of it. Sphalerite, chalcopyrite, galena and fractured pyrite in irregular shaped veinlets at 43.65m were observed by microscope on a polished section. (Table A-3).

Schistosity is well developed from the top down to 63m and intersects the core by 70° to

80°. Below 63m the schistosity is not distinctly observed although microfolds (drag folds) are.

73.50 ~ 76.30m

Bi-Qt-Sch. 73.50-75.20m is grey and 75.20-76.30m is pale greenish grey. Muscovite is rarely found. 75.20-76.30m is rich in biotite and at 75.20-75.25m and 75.55-75.65m, amphibole is included. Little chlorite is found at 75.20-76.30m.

Schistosity is well developed. In the upper half of the section, microfolds (drag folds) are developed, and in the lower half, the schistosities cross the core by 80°.

76.30 ~ 80.40m

This section is pale grey to grey and includes a lot of chlorite as the products of hydrothermal alteration. Muscovite and biotire are not likely to be found.

At 78.25-78.30m, pyrite, sphalerite, galena are included in a stratabound state and their relative amount is in that order.

Schistosity crosses the core by 40°.

80.40 ~ 86.00m

Grey Pl-Bi-Qt-Sch. There is little biotite. The upper part of the core is chloritized and the lower part is likely silicified. Chlorite occurs also as the product of hydrothermal alteration and often occurs at 80.90-81.25m and 81.70-82.20m. Plagioclase porphyroblasts are found throughout.

Schistosity crosses the core by 80° to 85° and is distinct everywhere except in the middle of the core.

86.00 ~ 87.50m

Bi-Qt-Sch. has a fine dark banded structure. There is more biotite here than in the above horizon. Secondary chlorite is also observed.

Schistosity is well developed and microfolds (drag folds) are observed.

87.50 ~ 92.60m

Dark greenish grey Amphibole-biotite schist. Beds with more biotite and beds with more amphibole have associated fine alternation of a few millimeters to one centimeter of thickness. Some aggregations of amphibolite make a convex lenticular shape in biotite mass. The amphibolite may be boundine. In the upper half of the section, plagioclase porphyloblasts are observed. In the lower half, chllrites occur as stringers.

A small quantity of pyrite occurs along schistlsity as disseminations and also as films in fine cracks, increasing from the upper to the lower part. Lenticuler massive quartz occurs in two parts. They may be boundins.

Schistosity is well developed and crosses the core by 80°, except 65° to 70° at the bottom.

92.60 ~ 102.50m

(Plagioclase)-biotite-quartz-schst. 94.00-94.60m is grey. 94.87-100.70m has bands of pale and dark grey. 100.70-102.50m is pale greenish grey with faint bands. A large amount of biotite is included. Chlorite occur as stringers in the upper half with very little calcite is stringers in the lower half. Plagioclase porphyroblasts occur sporadically. Massive quartz with pyrite occurs at 92.50-92.60m, 94.60-94.87m. They may be segregations. They core generally crosses the clear schistosity by 70° ~ 85°. Microfoldings are also partially observed.

Two fractures with slickenside are observed. The fractures cross the core by 50° and 60°, respectively, and the rakes of striation on the fracture planes are 60° to 65°. The fractures are interpreted to have occurred as the result of normal faulting.

102.50 ~ 117.40m

(Garnet)-plagiclase-biotite-quartz-schist. Very pale greenish grey and having faint banded structures. Garnets occur sporadically as porphyroblasts. Plagioclase porphyroblasts are more than that of garnet. Chlorite occures as stringers along schistosities, with halos of weak chloritization.

Calcites also occur as stringers crossing a schistsity. Massive quartz with pyrite occurs at 103.75-103.95m, possibly as a segregation. Massive quartz and k-feldspar occur at 112.40-112.47 m. 113.90-114.00m is slightly silicified and includes little biotite. A very small amount of pyrite occurs as films in fissures and as dissemination from the top down to about 106m.

Schistosity is well developed and crosses the core by 70° to 85°.

117.40 ~ 119.00m

Fracture zone. The upper contact plane crosses the core by 35° and the rake of the striation on the plane is 70°. The lower contact plane crosses the core by 40° and the rake of the striation on the plane is 35°. The fractured zone is chloritized with a network of calcite and limonites stringers with the fractures. This section is thought to be a fault zone.

119.00 ~ 154.50m

(Plagioclase)-garnet-biotire-quaetz-schist. Intercalated by thin beds of amphibole-biotite-schists. The core is: grey and faintly banded from the top down to 130.25m: greenish grey from 130.25m to 130.80m: pale and-dark-grey banded from 130.80m to 133.00m: pale grey from 133.00m to 133.70m: pale grey and faintly banded from 133.70 to 143.80m; and faintly grey banded from 143.80m to 154.50m. Amphibole-biotite schist beds are at 130.25-130.45m, and 130.60-130.80m. This section, except at 130.25-130.80m, is grey to pale grey with banded struc-

tures. 130.25-130.80m is greenish grey. The sections of 119.00-130.25m and 151.50-154.54m are siliceous. At 152.95-153.00m, stratified quartz with biotite and pyrite is surrounded by amphiboles. The quartz may be a boundin. At 153.25-153.35m, a small amount of amphibole is evident. Chlorite occurs very thinly along schistosities. Calcite occurs sporadicaly as stringers crossing schistosities. Garnet porphyroblast occurs equally throughout this section. Plagioclase porphyroblast occurs sporadically.

Schisosity is distinct, crossing the core by 80° to 90° except for the section with local microfolds.

154.50 ~ 173.50m

Pale grey banded plagioclase-biotite-quartz-schist. Plagioclase porphyroblast occurs. Chlorite occurs as stringers and along schistosities. At 155.35-160.00m limonite occurs in fractures and like dissemination as a result of weathering, 156.95-157.10m is more siliceous. Many irregular shaped massive quartz are found at 160.30-160.80m. They may be segregations. Quartz fragments with k-feldspar and chlorite as altered products occur at 167.00-168.00m.

Schistosity is well developed, crossing the core by 80° to 85°, with the exception of partial microfoldings.

173.50 ~ 177.50m

Pale grey banded plagioclase-garnet-biotite-quartz-schist. Garnet and plagioclase occur as porphyroblast. Secondary chlorite occurs as hydrothermal alteration products. Calcite stringers cross schistosity.

Well-developed schistosity crosses the core by 75° to 85°.

177.50 ~ 224.00m

(Plagioclase)-garnet-muscovite-biotire-quartz-schist. A very faint banded structure is observed with a repetition of grey and pale grey. Garnet porphyroblasts are rish at 182-190m and plagioclase porphyroblasts are found in the lower half of the section. The entire section is rich in biotite but muscovite. Chlorite as hydrothermal alteration occurs at 177.50-183.00m. Calcite stringers also occur. At 186.90-187.50m, the core is fractured and includes calcite. The section 200.79-201.05m is composed mostly of biotite and includes pyrite in fractures. The section at 201.80-202.00m is amphibole-biotire-schist. A large quantity of biotite is found in the sections at 209.10-109.20m and 209.35-209.50m. White irregularly-shaped massive quartz fragments with a maximum diameter of 25cm are included sporadicaly throughout the section. These may be the parts of the segregation veins.

Schistosity is well developed and crosses the core by 50° to 80°, with the exception of 205-

212m where microfolds are observed.

224.00 ~ 244.00m

Plagioclase-muscovite-biotite-quartz-schist. It is grey and partly pale grey with faint banded structures. Plagioclase porphyroblasts occur and calcite stringers are entirely included. Chloritization like hydrothermal alteration is strong at 232.50-232.60m and 236.40-237.70m.

Schistosity is well developed and crosses the core by 70° to 80°, except for local microfolds.

244.00 ~ 286.60m

Garnet-Plagioclase-muscovite-biotite-quartz-schist. It is grey and intercalated with thin beds of dark greenish grey biotite-amphibole-schist. The principal schist contains porphyroblasts of plagioclase and garnet. Chlorite occurs along schistosity throughout the section and hydothermal chloritization is observed at 261.30-261.70m, calcite stringers also occur in the upper part of the entire section. Biotite-amphiobole-schist beds are at 262.90-263.65m, 265.20-265.55m, 268.70-269.15m and 272.70-273.00m. A large amount of biotite is found at 279.40-279.55m and at 286.45-286.53m. Small irregular shaped white massive quartz gragments are included throughout the section. Quartz, biotite, muscovite and plagioclase are identified as principal minerals while very small quantities of potash-feldspar, sphene, zircon, apatite and fine grained muscovite are identified as minor minerals through microscopic observation at 282.85m. (Table A-1).

Schstosity is not distinct in some parts. Where it is distinct, it crosses the core by 60° to 80°.

Very small amounts of pyrrhotite and pyrite are disseminated throughout the section.

286.60 ~ 287.65m

Grey silicified zone accompanied by pyrrhotite. (Original rock is thought to be the same as upper horizon). Pyrrhotite is at 286.70-287.65m. It is partly massive and partly banded at 286.85-287.20m. In the banded zone, much chlorite and garnet are found. Very small amounts of pyrite are also found throughout the mineralized zone. In the silicious zone some calcite stringers are found. Laminated pyrrhotite, chalcopyrite and very small quantities of sphalerite at 287.10m are observed by microscope on a polished section. (Table A-2).

A banded mineralized zone crosses the core by 65° to 70° and the angle matches that at the contact between the mineralized zone and the upper and lower lithology.

287.65 ~ 312.85m

Green amphybolite. At the lowermost and uppermost parts, biotite is included accompanied by calcite stringers. Hornblend, quartz and plagioclase as principal minerals and very small quantities of biotire and leucoxene are identified in the texture of schistosity at 290.55m by microscopic observation of thin sections. (Table A-2).

The entire section is disseminated by very fine-grained pyrrhotite, and at the bottom, the pyrrhotite develops a little more along schistosities and in stringers.

Schistosity is distinct where biotite is included. The schistosity crosses the core by 45° to 60° in the uppermost part and by 65° to 70° at the bottom.

312.85 ~ 315.47m

Grey biotite-quartz-schist with a faint banded structure. The entire section is silicified. Many quartz beds are less than a few centimeters thick are along schistosity. They may be the parts of the segregation veins as the products of folding. At 314.40-314.70m, a small amount of amphibole (chlorite?) is included.

Schistosity crosses the core by 65° to 70°.

315.47 ~ 350.10m

Grey amphybolite. In the upper part, 315.47-321.50m, and at the bottom, biotite is found. In the lower half of the section, chlorite stringers are found. Calcite stringers, partly along schistosity, occur throughout the section. At 324.90-325.30m spotted calcites about one millimeter in diameter are found. Segregations of quartz are scattered throughout the section, sometimes having very small amounts of pyrrhotite and chalcopyrite. At 328.50-329.30m, 333.70-335.30m, 338.10-339.00m, 349.40-350.10m, a fine banded structure with few millimeters of each band can be observed. The bands are composed of quartz-dominant zone and amphybole-dominant zone. At 341.60-345.10m, rhythmic alteration of green and dark green zones, each five centimeters thick, can also be observed. Varying colors indicate different chemical compositions.

Very small amounts of pyrrhotite, pyrite and chalcopyrite are found throughout the section.

Schistosity is not distinct in many parts, except where it crosses the core by 60° to 80°. From one part with distinct schistosity to the other the angle of schistosity crossing the core changes rapidly from 40° to 90°, indicating a fold.

350.10 ~ 353.50m

Muscovite-biotite-quartz-schist. It is pale grey with a "salt and pepper" banded structure. (Hereafter salt and pepper is used to identify black minerals like biotites in grey to light grey minerals). The bands composed of biotite are very short accompanies by small amounts of secondary chlorite.

Schistosity is distinct, crossing the core by 70° to 75°.

353.50 ~ 367.80m

Pale grey banded garnet-muscovite-biotite-quartz-schist like "salt and pepper". Garent por-

phyroblasts abound in the upper half of the section. Plagioclase porphyroblasts occur locally. Some secondary chlorite occurs, especially at 360.60-360.95m. Below 360m, very small quantities of pyrrhotite are accompanied by quartz segregation 363.65-364.50m, 366.85-367.30m are more siliceous.

Schistisity is distinct and cross the core by 45° to 70°.

367.80 ~ 369.15m

Dark green biotite-amphybole-schist. It is accompanied by very small amounts of pyrrhotite and chalcopyrites with segregations of quartz.

The contact of the schist with upper formation is clear and crosses the core by 60°. Schistosity is distinct.

369.15 ~ 381.00m

Grey to pale grey, "salt and pepper" banded (garnet)-biotite-quartz-schist. Plagioclase porphyroblasts abound at 370.40-371.00m where their maximum diameter is five millimeters. Secondary chlorite occurs along schistosity at 373.00-374.70m and 379.65-379.80m. A small amount of coarse grained amphyboles occurs at 377.90-378.60m and 379.25-379.50m. A very small amount of pyrite occurs in fractures throughout the section. Sphalerite occurs in segregation of quartz at 373.40m.

Schistosity is partly indistinct. Where they are distinct, they cross the core by 60° to 90°.

381.00 ~ 394.70m

Grey, "salt and pepper" banded biotite-quartz-schist. Small, irregular shaped massive quartz fragments occur pressed perpendicular to the schistosity. They are thought to be the parts of segregation veins. Hydrothermal chlorite is abundant at 381.90-382.20m and 387.50-389.40m. The former section is a little siliceous and is accompanied by pyrite stringers. Very little pyrite occurs in this section, particularly with calcite in fractures.

Very small quantities of pyrrhotite are also scattered.

Schistosity is generally distinct, crossing the core by 69° to 70° in the upper part and by 85° to 90° in the lower part.

394.70 ~ 395.45m

Dark green biotite-amphibole-schist. The section about ten centimeters from the top is mostly composed of biotite with some quartz fragments and pyrrhotite.

Distinct schistosity crosses the core by 60° to 70°.

395.45 ~ 399.85m

Green and fine grained amphibolite. Segregations of calcite occur very thinly among amphi-

boles and vein-like segregations of calcite occur at 395.90-396.00m.

Fine grained pyrrhotite is scattered in the section of 0.5 centimeters at 395.65m.

Schistosity is distinct only at the uppermost part and crossies the core by 50°.

399.85～400.00m

Pale greenish-grey biotite-amphibole-quartz-schist. Biotite and amphibole are not abundant. Pyrrhotite occurs along the schistosity.

(3) Geological structure

Schistosity generally crosses the core by 70° to 80° . As schistosity in this hole is generally parallel to the bedding plane, the plane of schistosity is regarded as representating the bedding plane. In the geological structure observed in the core, microfolding (When the wave length of folds is less than about 20cm, and the enveloping surface of the fold extends parallel to the long axis of the core, they are called as this in this report.) are partly seen parallelling partly crossing obliquely the schistosity. Microfoldings abound at 67-75m and are observed sporadically in the parts. The folds are thought to be parasitic or drag folds, judging from the shape and the scales. Two fracture zones, 117.40-119.00m, 186.90-187.50m, interpreted as faults are present. Both sections are finely fractured, and include calcite. The upper fracture has a slickenside at the contact plane between two litholongies. They were clearly formed after the metamorphism. They are not correlated to any faults observed on the surface, nor to any faults observed in other drill holes at present.

(4) Mineralization

Mineralizations in this hole are classified into two types. One type is dissemination of pyrite, with irregular-shaped thin veinlets of sphalerite, galena, and chalcopyrite at 28-80m in biotite-muscovite-quartz-schist and biotite-quartz-schist. Sphlerite, galena, chalcopyrite are scattered in small quantities in the spread pyrite dissemination. Mineralizations cross and/or parallel schistosities. The amount of the ore minerals are pyrite, sphalerite, galena and chalcopyrite in descending order. Gold and silver were detected in very small quantities. Assay results are shown in Table II-2-3. The value of copper, lead and zinc are high in 43.4044.80m, 65.10-66.60m and 70.45-72.40m, but low in the others. The highest value of zinc and lead are 1.2% and 4294ppm respectively in 66.10-66.60m and the highest value of copper is 1608 ppm in 43.40-44.20m.

The second type is pyrrhotite mineralization in the section of 286.70-287.65m represented

by banded ore and massive ore in 286.85-287.20m. Banded ore are accompanied by chlorite, garnet and small quantities of pyrite. The mineralization occurs at the contact between the upper garnet-biotite-quartz schist and the lower amphibolite. Small amount of pyrrhotite are also present in the lower amphibolite, but the upper schist. Therefore the occurrence of pyrrhotite is thought to be relted to the presence of amphibolite.

2–2–2 Geology and Mineralization of Hole MBP-5

(1) Surface Geology of the Surroundings

For the surface geology around the MBP-5, see 2–2–1, (1).

(2) Geology of the Hole

0.00 ~ 1.40m

Brown soil. A zone.

1.40 ~ 21.90m

Reddish brown and yellowish brown soil. Only quartz and mica can be discriminated. Few minerals remain after weathering. Lithology is possibly biotite-muscovite–quartz schist.

21.90 ~ 28.50m

Muscovite-biotite-quartz-schist with black and white bands a few millimeters thick. At 26.85 -27.20m many massive quartz fragments at a scale of 1cm by few cms having lenticular shape parallel to schistosity. They may be the parts of segregations.

Limonite occurs along schistosity.

Schistosity crosses the core by 60° to 70° accompanied by microfolding in the lower half section.

28.50 ~ 47.00m

(Staurolite)-garnet-muscovite-biotite-quartz-schist with a black and white banded structure. Staurolite porphyroblasts are included at 35.00-40.50m. Their longer axes are 1 to 1.5mm and shorter axes are less than 1mm. Garnet porphyroblasts are included thoughout the section at a diameter less than 2mm. Many small massive quartz fragments are included along schistosity at 37.00-38.00m.

There are many microfoldings throughout the section and they are parallel to the schistosity. Where there are no foldings, schistosity crosses the core by 50° to 70°.

47.00 ~ 106.50m

Grey and light grey (muscovite-biotite)-quartz-schist. The quantity of two micas is not the same throughout the section. A black and white banded structure is developed 47.00-67.70m and below that are "salt and pepper" bands. Amphibole-biotite-schists are intercalated at 91.40-91.65 m, 97.25-97.55m and 101.70-102.05m. Thin amphibole layers are observed along schistosty at 68.70-68.80m and the complex of amphibole and lenticular shaped quartz grains is observed at 73.38-73.40m.

The section is weakly disseminated by pyrite with the most intense dissemination occuring at 46.90-49.70m. At 67.05-67.15m and 67.70-68.55m, the dissemination is accompanied by silicification. Very small quantities of sphalerite, and galena are found at 61.65-61.73m.

The angles of schistosity crossing the core are very unstable due to many microfoldings. Microfoldings continue throughout the section, specially above a 70m depth.

106.50 ~ 118.50m

Grey muscovite-biotite-quartz-schist with some muscovite. Lithofacies are very stable. Schistosity is developed and crosses the core by 70° to 80°.

118.50 ~ 152.05m

Grey plagioclase-biotire-quartz-schist with a little biotite and some plagioclase porphyroblasts. A white layer with more quartz and a grey layer with less quartz of a few milimeters to 2 cm from a fine alternation.

The section is very weakly disseminated by pyrite.

Schistosity is developed and crosses the core by 70° to 80°.

152.05 ~ 154.15m

Dark green amphibole-biotite-schist accompanied by calcite and quartz stringers.

Schistosity is distinct where biotite is included and it crosses the core by 70°.

154.15 ~ 165.05m

Grey (plagioclase)-biotire-quartz-schist. This section exhibits the same fine alternation as that of the section of 118.50-152.05m. Biotite-amphibole-schists beds are intercalated. The section 154.70-154.95m is rich in biotite and also has amphibolite. The section 158.55-158.70m is amphibolite-biotite-schist and small amphibolites form lenticular shape in biotites. The amphibolite may be boudin. Biotite-quartz-amphibole complex 2cm thick is included at 158.80m. The section 3cm thick is rich in biotite and accompanied by chlorite at 159.50m. In 154.10-154.35m spherical amphibole-biotite-schists are taken in. They are 7 by 15cm and 5 by 2cm. At 160.10m stringers of secondary chlorite cross the schistosity. The section 163.85-163.95m is coarse-grain-

ed biotite-amphibole-schist as is section 164.02-164.05m, also. The section 164.75-165.05m is biotite-amphibole-quartz-schist. In this section, amphibole gradually increases toward the lower contact. This section is thought to be a mixture of overlying biotite-quartz-schist and underlying amphibolite when this section has been formed.

Pyrite is very poorly disseminated throughout the section and along schistosity with biotite.

Microfolding are formed in the upper half and schistosity crosses the core by 60° to 70° in the lower half.

165.05 ~ 176.00m

Green (garnet)-amphibolite. Biotite and garnet less than 1 millimeter in diameter are included in the lower half. Very small quantities of pyrrhotite and pyrite disseminate this section.

The both planes of upper and lower contacts are sharp. The contact plane with lower formation crosses the core by 40°. Schistosity is distinct only in the uppermost part, crossing the core by 60°.

176.00 ~ 187.70m

Alteration of grey biotite-quartz-schist and dark green biotite-amphibole-schist. Each schist layer is approximately a few tens of centimeters thick with a maximum thickness of 1.6 meters and minimum thickness of few centimeters in 184.60-187.70m.

There is very little pyrite pyrrhotite in this section.

Microfolds are widely formed. In the upper section schistosity cross the core by 70° to 85°.

187.70 ~ 223.15m

Grey muscovite-biotite-quartz-schist with muscovite in very small quantities. The section 188.00-188.20m is amphibole-biotite-schist. In 191.30-192.10m small quantity of biotite and amphibole are included.

Some kind of alteration is observed. The section at 190.15-190.30m is bleached and accompanied by chlorite. At 192.95-193.05m, chlorite and epidote are filled in fractures. The section at 205.00-205.58m is silicified and above 205.00m it is chloritized. The sections at 203.25-203.35m and at 204.15-204.25m are weakly chloritized. The section at 204.25-205.00m is bleached and includes calcite stringers. Quartz, biotite and muscovite are the principal minerals and very small quantities of potash-feldspar, plagioclase, zircon, apatite, chlorite, leucoxene and fine grained muscovite are identified at 218.00m by microscopic observation of thin section (Table A-1). This section is disseminated by pyrite more strongly than upper section and accompanied by very poor sphalerite at 205.45-224.50m. Sphalerite, chalcopyrite and very small quantities of pyrite and cubanite in irregular shaped veinlets at 210.30m are identified by microscopic observation of

polished section. (Table A-2).

Schistosity is very much disturbed and microfoldings are formed throughout the section.

223.15 ~ 242.95m

Pale, orange-grey altered rock. Original lithology is probably mica schist. Amphibolite with minute amounts of biotite occurs in the section at 225.93-226.65m and at 239.10-240.85m. The upper boundary at 223.15m is sharp while the lower boundary at 242.95m is gradual. The alteration is silicification and that of forming k-feldspar, accompanied by pyrite dissemination and calcite stringers. Quartz, muscovite and chlorite as principal minerals and very small quantity of potash-feldspar, sphene and fine grained muscovite are identified at 227.95m by microscopic observation of thin section. (Table A-1). A cemented fracture zone is observed at 230.95-231.70m. The degree of cementation is the same as that of the surrounding parts. The fracture zone is thought to be as old one. Schistosity is not distinct in the section, except in the lower part of the section where it, crosses the core by 70° to 85°.

242.95 ~ 289.60m

Green and coarse-to-very coarse grained amphibolite. A little biotite is found throughout, but is especially rich at 258-269m. A bed of biotite-amphibole-quartz-schist is intercalated at 276.85-277.60m, and a bed of amphibole-chlorite-biotite-quartz-schist is intercalated at 280.43-281.33m. The section at 288.70-289.60m is amphibole schist. Hornblend, plagioclase and small quantity of epidote are observed at 249.55m by microscopic observation of thin section. (Table A-1).

Little pyrite is disseminated.

Schistosity is distinct in the upper half and crosses the core by 60° to 70°.

289.60 ~ 292.90m

Alteration of quartz-schist and biotite-amphibole-schist. The section at 289.60-291.05m is silicified including k-feldspar, chlorite and biotite, and is disseminated by pyrite.

Schistosity is distinct, crossing the core by 50° to 60°.

292.90 ~ 333.90m

Alteration of (plagioclase)-(muscovite-biotite)-quartz-schist and biotite-amphibole-schist. The former schist is grey and latter dark green. The latter schist beds at 303.20-304.30m, 306.70-307.80m, 309.00-310.30m and 310.60-310.95m are usually thinner than the former. There is less biotite than amphibole in them. The quantities of muscovite and biotite in the former schist are unstable throughout the section. K-feldspar is included as an alteration product at 292.30m and 293.60-295.80m, chlorite and pyrrhotite accompany schistosity. Secondary

chlorite is also observed at 300.60-301.50m, 305.90-306.00m, 311.15-311.40m, 320.70-320.95m and 321.50-321.70m. The section at 306.40-306.70m is white massive quartz. The entire section is disseminated by pyrrhotite and pyrite.

Schistosity is distinct and crosses the core by 60° to 80° in the upper part and by 70° to 85° in the lower part. Microfolds are developed in the mid-section.

333.90 ~ 337.95m

Pale orange grey altered rock. Silicification, chlorite and k-feldspar as alteration products are observed. The section has many irregular shaped fractures and is partly fractured a few millimeters is diameter. These fractures are filled with light grey clay minerals and limonite. Fractured and argillized parts 2cm wide occur at 334.50m and 335.30m. The slickenside in them cross the core by 50°. Almost all of these parts are thought to be older fracture zone.

No mineralization was observed.

Schistosity is indistinct.

337.95 ~ 400.45m

Generally grey (plagioclase)-(muscovite-biotite)-quartz-schist with black and white banded structures a few millimeters wide below 389.50m. Mica occurs in small amounts. The section at 338.18-338.64m is biotite-amphibole-schist, and the section at 355.05-355.60m is amphibolite-biotite-schist. The section at 339.85-341.65m is silicified and chloritized. The section at 340.00-352.18m is chloritized at intervals. The section at 345.45-346.40m is silicified, chloritized with pyrite. Chloritization is also observed at 361.45-362.10m, 367.70-368.00m, 387.20-387.25m, 387.85-389.90m.

The entire section is very slightly disseminated by pyrite.

Schistosity is distinct except for a few parts. Some microfolds are observed in the upper and lower parts. In the middle part, schistosity crosses the core by 70° to 85°.

(3) Geological Structure

Schistosity is generaly well developed. As bedding planes are generally parallel to schistosity, the core mostly crosses the bedding plane by 60° to 80°. Microfolds are observed, sometimes parallel to schistosity, sometimes not, their enveloping surfaces extend sub-parallel to the long axis of the core. The axial planes of the microfolds are mostly inclined toward the bottom. They abound in the section shallover than 70m in 180-220m and 303-316m. From the surface geology, geological discontinuous zone was assumed near the location of the hole MBP-5.

(4) Mineralization

Almost the entire section has a slight continuous dissemination of pyrite, concentrated at 200-240m. Sphalerite and galena are scattered in small amounts at 205-225m sections. Sphalerite and galena are also scatteredat 61.65-61.73m. Sphalerite and galena occur in muscovite-biotite-quartz schist. Lead and zinc occur small amounts. The maximum value of lead and zinc are 444ppm and 3340ppm respectively in 222.00m-223.00m. The maximum value of copper is 409ppm in 221.00-222.00m. Gold and silver are scarcely observed. Assay of core in the section of 61.50-62.00m and 205.00-205.90m is shown in Table II-2-3. The host rock and occurrences of this mineralization are similar to that of MBP-5 in 27.00-80.00m. The sections at 165-173m, 185-188m, 293-298m, and 313-334m are very slightly disseminated by pyrrhotite. The distribution of pyrrhotite in the upper two sections nearly coincides with that of the amphibolite and biotite-amphibole schist. Pyrrhotite in the lower two sections occur in plagioclase-muscovite-biotite-quartz schist and muscovite-biotite schist.

2–2–3 Geology and Mineralization of Hole MBP-6

(1) Surface Geology of the Surroundings

For the surface geology around the MBP-6, see 2–2–1, (1).

(2) Geology of the Hole

0.00 ~ 1.60m

Brown soil.

1.60 ~ 19.10m

Argilized soil. It is reddish brown, dark brownish grey, yellowish dark grey yellowish brown. In the lower part, only mica can be discriminated, and original textures remain. Limonitization and argillisation is more prevelant among muscovite, biotite and quartz, and can be seen with the naked eye. The same texture as the lower bed rock is found in 18.00-19.10m.

19.10 ~ 24.30m

Black and white banded (plagioclase)-garnet-muscovite-biotite-quartz-schist. Pink garnet porphyroblasts have a diameter less than 1 mm. Limonite occurs along schistosity throughout the section. Microfolds are developed throughout the section and mostly parallel the schistosity.

24.30 ~ 50.50m

Muscovite-biotite-quaetz-schist in a stronger black and white banded structure. Beds of

amphibole-biotite-schist are intercalated at 40.85-42.20m and 43.00-43.25m. In the latter section, small amphibolite masses occur in spherical shapes in the biotite mass. At 24.30-27.50m, limonite occurs along schistosity. Section 29.00-29.10m is strongly limonitized and argillized and slickensides are observed at the upper and lower contacts.

There is very little pyrite in this section. Silicification is at 39.25-40.85m.

Schistosity is well developed and parallel to the banded structures, crossing the core by 60° to 80°. Microfolds are partly observed.

50.50 ~ 61.05m

Grey (plagioclase)-garnet-(muscovite-biotite)-quartz-schist with some micas. Pink garnet porphyroblasts have a maximum diameter of 3mm. At 50.50-52.50m, a banded structure is distinct, below there that is no banded structure. The entire section is a little more siliceous.

The core crosses schistosity at the uppermost part by 55° to 70°.

61.05 ~ 61.90m

Greenish-grey biotite-amphibole-quartz-achist. The upper half is mostly composed of biotite and quartz in a very disturbed structure.

Schistosity is also very disturbed.

61.90 ~ 86.25m

Grey (plagioclase)-(muscovite-biotite)-quartz-schist, intercalated in the middle with thin beds of biotite-amphibole-schist. Irregular-shaped massive quartz fragments are scattered throughout this section.

Section at 70.00-79.00m is very slightly disseminated by pyrrhotite and pyrite.

The structures of this section are very much disturbed. Schistosity, where no microfolds are present, cross the core by 70° to 90°.

86.25 ~ 92.35m

Amphibolite. It is green and very coarse grained at the top and bottom with the maximum diameter of 5mm. Little biotites occur at the top and in the middle. White massive quartz intercalates at 87.60-87.85m.

The entire section is very slightly disseminated by pyrite and pyrrhotite.

Schistosity at the bottom crosses the core by 90°.

92.35 ~ 116.80m

Grey (plagioclase)-biotite–quartz-schist. It is more siliceous and has small quantities of biotite throughout, except at the bottom. Intense chloritization occurs frequently at 121.10-121.45m.

Distinct schistosity crosses the core by 80° to 90°. Microfolds are few.

116.80 ∿ 123.70m

Grey garnet-biotite-quartz-schist. Pink garnets have a diameter less than 1mm. Silicification and chloritization are observed at 118.65-120.00m and 121.10-121.45m. Section at 123.20-123.50m is rich in biotite.

Distinct schistosity crosses the core by 70° to 80° in the upper half and follows microfolds in the lower half.

123.70 ∿ 125.05m

White massive quartz which may be meta-chert.

The upper contact is flat and crosses the core by 25°. The lower contact has an irregular, undulated shape.

125.05 ∿ 211.00m

Grey garnet-(muscovite-biotite)-quartz-schist, intercalated by thin beds of amphibole-biotite -schist. In the former schist, the amounts of muscovite and biotite vary, although, the amount of biotite is generally larger. The beds of amphibole-biotite-schist are found at 168.30-168.45m, 170.60-170.85m, 173.92-174.00m, 174.55-175.85m and 180.25-180.50m. Pink garnet porphyroblasts have a diameter of 0.5 to 5mm. Strong silicification and chloritization occur at intervals.

Microfolds are found throughout the long axis of the core except at 160-170m, and are generally oblique with the extention of micas.

Mineralization is scarcely observed except for very small amounts of pyrite.

211.00 ∿ 221.00m

Grey muscovite-biotite-quartz-schist with few micas.

Very slight pyrite dissemination is observed, especially at 215-225m.

Microfolds are observed throughout the section.

221.00 ∿ 263.00m

Grey plagioclase-garnet-muscovite-biotite-quartz-schist with few micas. Garnet porphyroblasts have a maximum diameter of 5mm. Plagioclase also occurs as porphyroblast. A very faint banded structure is also observed.

Very slight pyrite dissemination is observed, especially above 224m. Quartz, chlorite, potash-feldspar, muscovite, chlorite and very small quantities of plagioclase apatite and leucoxene are observed by microscope at 220.00m (Table A-2). And therefore, the rock name is chlorite-potash-feldspar-muscovite-quartz schist.

Microfolds envelope the surface parallel to the long axis of core.

263.00 ∿ 320.00m

Grey (garnet)-plagioclase-muscovite-biotite-quartz-schist intercalated with thin beds of dark green biotite-amphibole-schist. Biotite in this section occurs more than that in the above horizon. PLagioclase porphyroblasts are more plentifol in the lower half, and pink garnets less than 1mm in diameter occur sporadically. Biotite-amphibole-schist occur at 288.70-289.25m, 291.40-291.50m, 308.52-308.60m and 310.00-311.74m. The lowest section is rich in biotite in the top 10cm.

There is slight pyrite dissemination throughout the entire section and pyrrhotite is also observed at 281-284m and around 291m as disseminations.

Microfolds are also developed throughout the section.

320.00 ∿ 367.00m

Grey (garnet)-plagioclase-biotite-quartz-scist intercalated with thin beds of biotite-amphibole-biotite-quartz-schist and amphibole-schists. Biotite-quartz-schist locally include small quantities of muscovite, and porphyroblasts of plagioclase and garnet. Biotite-amphibole-quartz-schist occur at 322.50-322.75m; biotite-amphibole-schist at 324.25-324.35m and 325.50-325.65m. Amphibole-biotite-quartz-schist including pink (and plae green?) garnets are found at 327.63-328.50m. Beds of amphibole-biotite-schist are at 328.75-328.80m, 331.00-331.05m and 334.80-335.10m. Pink garnets in the middle bed are found. An amphibole-schist bed is found at 362.52-362.77m. Chloritization occurs as stringers and as hydrothermal alteration at intervals, with special strength at 360-366m.

The entire section is very slightly disseminated by pyrite.

Microfolds which envelope the surface are parallel to the long core axis occur continuouly from the upper section down to 332m. Below this point, distinct schistosity crosses the core by 70° to 85°.

367.00 ∿ 401.32m

Garnet-muscovite-biotite-quartz-schist. It is grey and is intercalated with biotite-amphiobole-schist of 393.25-393.52m. Pink garnets are observed in both schists. In the former schists, they have a diameter less than 3mm. Chloritization continues from the top down to 293m. Quartz, muscovite, biotite, chlorite are the principal minerals and very small quantities of potash-feldspar, plagioclase, zircon, apatite, calcite and leucoxene are observed at 370.75m by microscope. Quartz, biotite, muscovite, garnet are the principal minerals and very small quantities of zircon, apatite, chlorite and fine muscovite are identified at 395.75m by microscopic observation on thin section (Table A-2).

The section is very slightly disseminated by pyrite with more pyrite at 385-391m. Very small amounts of pyrrhotite are also observed at intervals. Very small amounts of sphalerite are observed at 370.40m, 380.80m and 395.80m.

Schistosity crosses the entire core by 75° to 85°. Sphalerite, chalcopyrite and small quantities of galena and pyrrhotite in fine veinlets are identified at 370.40m by microscopic observation of polished section. (Table A-2).

(3) Structure of the Hole MBP-6

Microfolds, with wave lengths less than agout 20cm and enveloping surfaces extend along the long axis of the core, occur continuously at 120-160m and 170-332m. They are paracitic or drag folds. Folded layers are generally oblique to schistosity or extention of micas. Below 332m, schistosity approximately parallel to the bedding plane crosses the core by 75° to 85° ie., the bedding plane gently dips.

(4) Mineralization of the Hole MBP-6

The core has and minor disseminated pyrite at intervals. At 216-224m and 384-391m, little more pyrite is included. Pyrrhotite is also locally observed as dissemination, especially at 70-79m. At 370.40m, 380.80m and 395.80m very small amounts of sphalerite are observed in spots. Sampling locations and assay data are shown in Table II-2-3. Copper, lead and zinc all have low values. Maximum values of copper, lead and zinc are 218ppm, 17ppm and 948ppm respectively. Gold and silver are scarcely deteated. The pyrite dissemination zone is accompanied by small amounts of copper, lead and zinc sulfides similar to that of MBP-4 in 27.00-80.00m. However, the order of the relative concetration of the elements is sphalerite, lead and copper in MBP-4, and sphalerite, copper and lead in MBP-6, both in descending order. Chloritization at 330-393m is observed but the relationship with the mineralization is not clear.

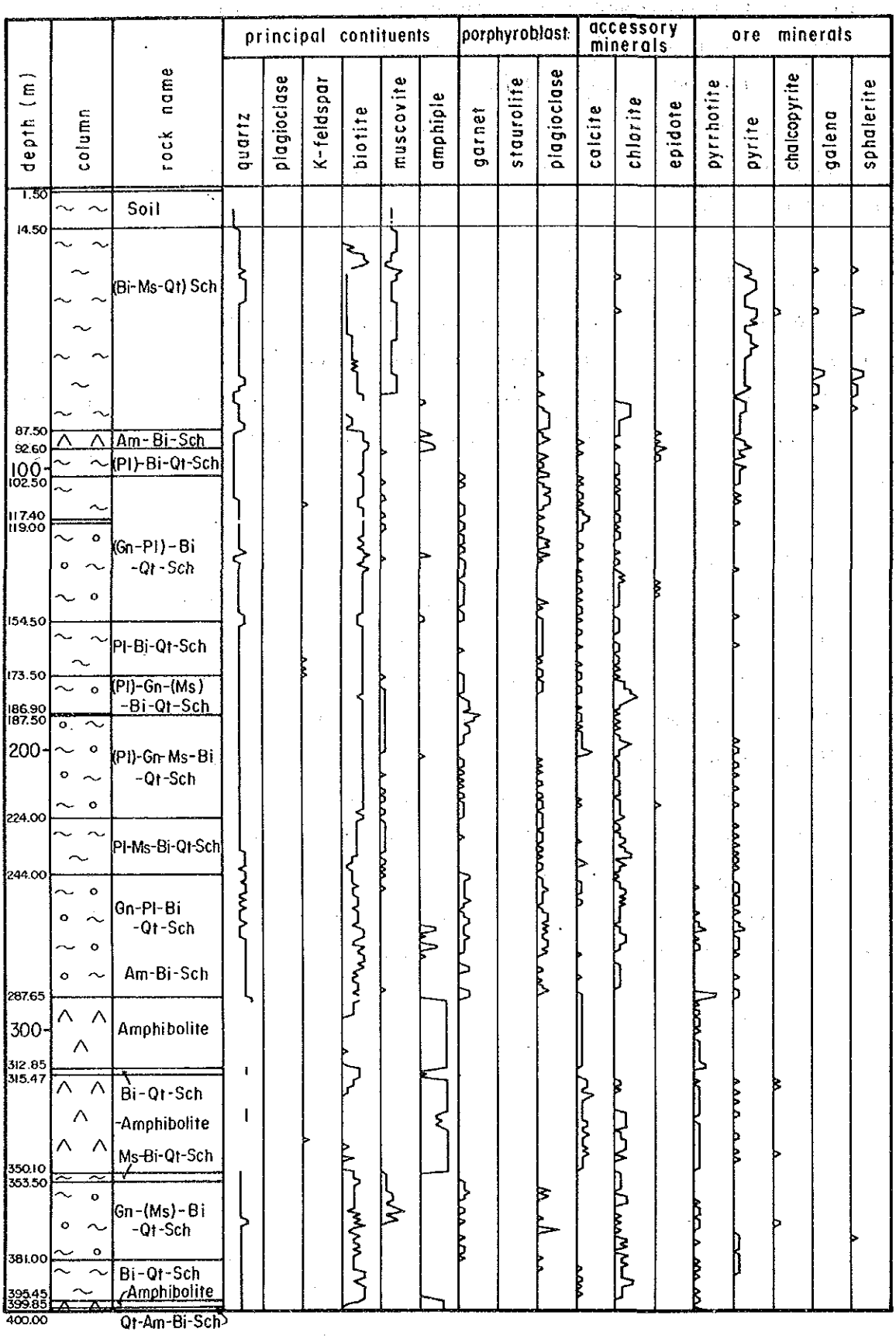

Fig. II-2-30(1) Generalized Lithologic Log of MBP-4

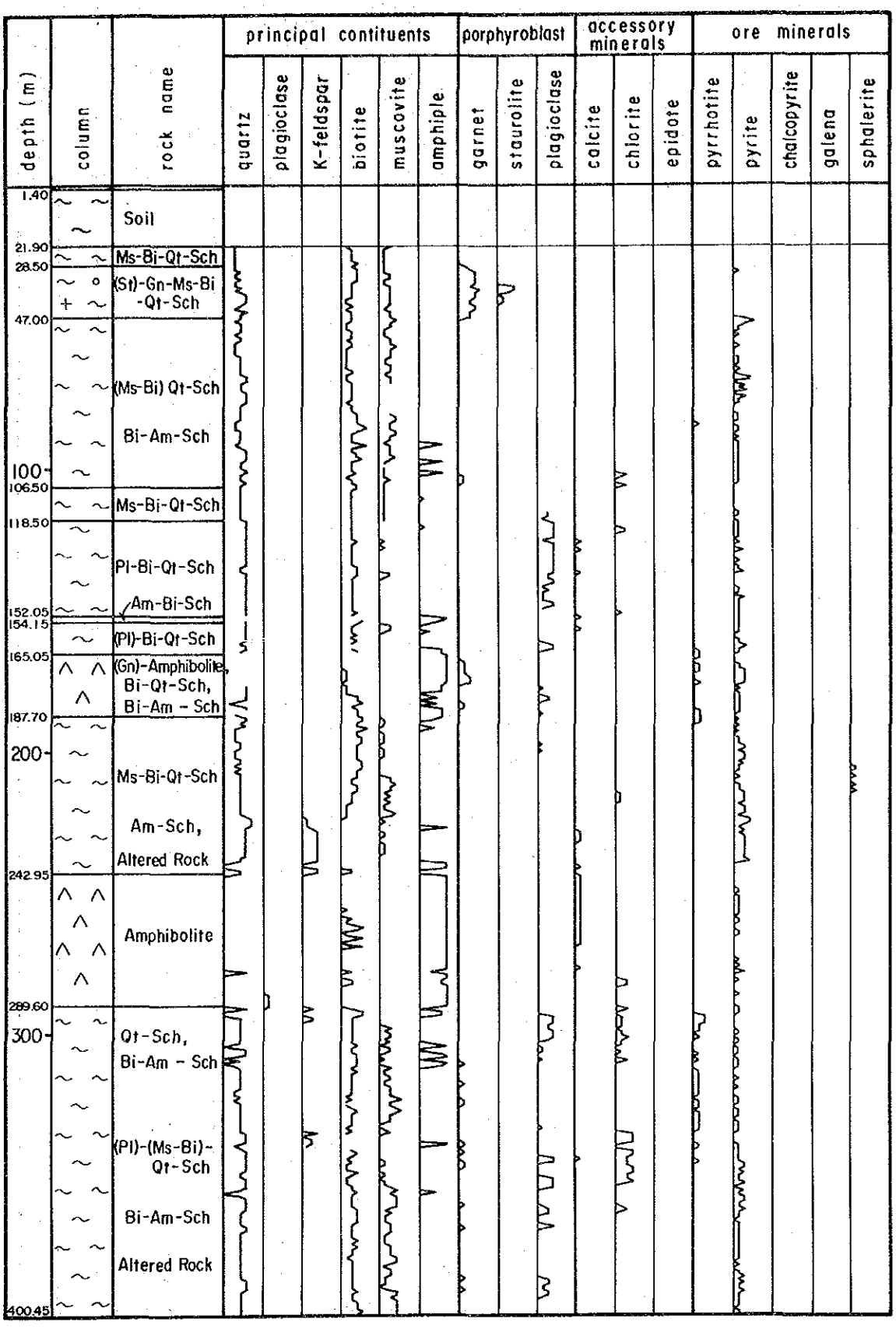

Fig. II-2-30(2) Generalized Lithologic Log of MBP-5

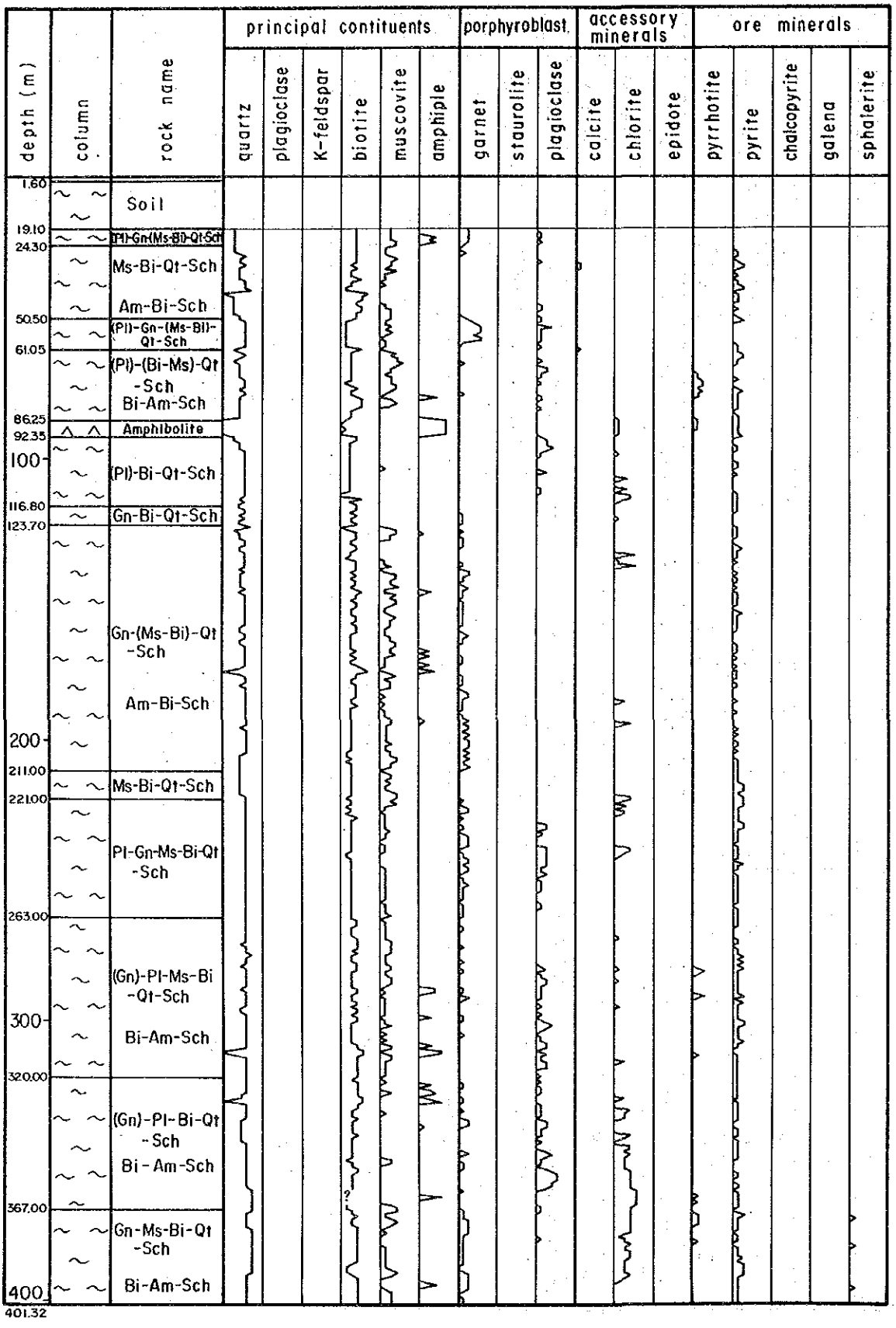

Fig. II-2-30(3) Generalized Lithologic Log of MBP-6

Table II-2-3 Chemical Assay Data of Drilling Cores

Sample No.	Depth of Hole	Core Length cm	Au ppm	Ag ppm	Cu ppm	Pb ppm	Zn ppm	S %
MBP4 – 1	28,50 – 29,25	75	<0,05	<2	150	470	572	2,0
" 2	29,25 – 30,05	80	<0,05	3	142	1486	0,54%	2,2
" 3	30,05 – 31,05	100	<0,05	10	248	668	1928	1,8
" 4	43,40 – 44,20	80	<0,05	8	1608	3700	1,2%	2,7
" 5	44,20 – 44,80	60	0,05	9	212	3872	1,1%	2,3
" 6	44,80 – 45,25	45	<0,05	<2	34	152	160	1,6
" 7	65,10 – 66,10	100	<0,05	4	142	1592	3960	1,0
" 8	66,10 – 66,60	50	<0,05	18	267	4294	0,69%	1,7
" 9	66,60 – 67,35	75	<0,05	<2	37	120	184	0,60
" 10	67,35 – 67,80	45	<0,05	<2	56	492	1078	0,86
" 11	67,80 – 68,65	85	<0,05	<2	42	228	550	0,84
" 12	68,65 – 69,55	90	<0,05	<2	88	380	784	1,2
" 13	69,55 – 70,45	90	0,10	<2	47	170	272	1,5
" 14	70,45 – 71,35	90	<0,05	7	92	3320	4140	1,9
" 15	71,35 – 72,40	105	<0,05	6	117	2470	4800	2,2
" 16	72,40 – 73,65	125	<0,05	3	86	986	2480	1,1
" 17	73,65 – 74,65	100	<0,05	<2	48	40	106	0,22
" 18	77,95 – 78,35	40	<0,05	2	192	492	1116	0,68
" 19	286,60 – 286,85	25	<0,05	<2	98	25	12	3,0
" 20	286,85 – 287,20	35	<0,05	<2	42	30	32	1,0
" 21	287,20 – 287,65	45	<0,05	<2	550	46	39	7,2
MBP5 – 1	61,50 – 62,00	50	<0,05	<2	52	274	1934	0,74
" 2	205,00 – 206,00	100	<0,05	<2	232	28	1511	0,35
" 3	206,00 – 207,00	100	<0,05	<2	126	31	348	0,25
" 4	207,00 – 208,00	100	<0,05	<2	118	20	320	0,12
" 5	208,00 – 209,00	100	<0,05	<2	176	22	1239	0,27
" 6	209,00 – 210,00	100	<0,05	<2	130	20	604	0,17
" 7	210,00 – 211,00	100	<0,05	<2	184	17	748	0,17
" 8	211,00 – 212,00	100	<0,05	2	120	33	626	0,47
" 9	212,00 – 213,00	100	<0,05	<2	57	37	544	0,12
" 10	213,00 – 214,00	100	<0,05	<2	78	47	374	0,27
" 11	214,00 – 215,00	100	<0,05	<2	35	90	320	0,65
" 12	215,00 – 216,00	100	<0,05	<2	41	32	234	0,65
" 13	216,00 – 217,00	100	<0,05	<2	60	102	328	0,49
" 14	217,00 – 217,95	95	<0,05	<2	30	63	194	0,53
" 15	218,00 – 219,00	100	<0,05	<2	27	42	230	0,34
" 16	219,00 – 220,00	100	<0,05	<2	126	9	662	0,54

Sample No.	Depth of Hole	Core Length	Au ppm	Ag ppm	Cu ppm	Pb ppm	Zn ppm	S %
MBP5 – 17	220,00 – 221,00	100	<0,05	<2	218	27	350	0,64
" 18	221,00 – 222,00	100	<0,05	<2	409	60	1012	0,57
" 19	222,00 – 223,00	100	<0,05	11	200	444	3540	0,42
" 20	223,00 – 224,00	100	<0,05	2	47	284	960	0,80
" 21	224,00 – 225,00	100	0,05	<2	57	290	1406	1,1
" 22	225,00 – 225,90	90	<0,05	<2	32	69	100	0,37
MBP6 – 1	72,00 – 72,95	95	<0,05	<2	16	13	83	0,52
" 2	73,00 – 74,00	100	<0,05	<2	17	18	84	0,82
" 3	216,00 – 217,00	100	<0,05	<2	14	11	56	0,24
" 4	217,00 – 218,00	100	<0,05	<2	11	7	65	0,11
" 5	218,00 – 218,95	95	<0,05	<2	14	9	60	0,11
" 6	220,00 – 221,00	100	<0,05	<2	9	10	80	0,10
" 7	221,00 – 222,00	100	<0,05	<2	13	12	58	0,25
" 8	222,00 – 223,00	100	<0,05	<2	14	8	68	0,24
" 9	223,00 – 224,00	100	<0,05	<2	16	6	52	0,25
" 10	369,50 – 370,50	100	<0,05	<2	104	14	948	0,36
" 11	370,50 – 371,50	100	<0,05	<2	34	15	228	0,41
" 12	371,50 – 372,50	100	<0,05	<2	218	17	228	0,11
" 13	387,50 – 388,50	100	<0,05	<2	25	11	134	0,31
" 14	388,50 – 389,50	100	<0,05	<2	21	9	262	0,31
" 15	389,50 – 390,50	100	<0,05	<2	20	8	232	0,28
" 16	394,00 – 395,00	100	<0,05	<2	14	9	182	0,10
" 17	395,00 – 396,00	100	<0,05	<2	25	10	356	0,087

Assayed by GEOLAB : Rua Aimorés, 200, Belo Horizonte, MG
Ag, Cu, Pb, Zn : Atomic absorption
Au : Fire assay
S : X-ray fluorescence

2–3 Discussion

2–3–1 Discussion on the Results of Geophysical Survey

In the survey area, zones of high apparent resistivity are widely distributed. In the south, however, are distributed zones of low resistivity, which continue for about 150 meters below the ground and turn to high resistivity zones thereafter. In comparing the values of low resistivity of schist and amphibolite distributed in this area, the resistivity value of the latter appears small. However, the low resistivities may reflect, on the one hand, the weathered zone and the influence of water in the shallow part of the ground, and, on the other hand, the fissures or fissure zone due to fault and the argillization zone previsouly discussed. Therefore, it is presumed that they do not directly represent amphibolite. The low resistivity zones associated with the fissures or fissure zone break into the high resistivity zones, and this tendency is stronger in a deeper part. The low resistivity zones extend in the directions of NE-SW and NW-SE, the latter cutting the former at right angles. A cross sectional view of the NE-SW zone indicates that this zone is dipping eastward. The high resistivity zones, on the other hand, exhibit a block structure in which a stratum is divided by several faults. They, however, correspond to the distribution of the schist of the Pip_4 formation. The resistivity variation within the high resistivity zones is considered to reflect the chert, amphibolite or amphibole-schist intercalated in the Pip_4 formation.

Broadly classified, IP anomalies are distributed in the following three areas which are considered to belong to the same anomaly source (Figure II-2-31).

(1) the southern part of the survey area, MBP–4 was drilled

(2) the southeastern part of the survey area, MBP–5 was drilled

(3) the northern part of the survey area, MBP–6 was drilled

The anomaly zone of the above area (1) is distributed inside the low to medium resistivity distribution zone presumably associated with a fracture zone. The anomaly distribution pattern, according to a cross sectional view of this anomaly zone, is considered to reflect the anomaly source of the dissemination distributed in the shallow part of the ground. The spectral pattern of this anomaly source is typically of the one found in the mineralization zones of pyrite.

The anomaly zone of the above area (2) is distributed in the zones with a little resistivity variation, and is continuing to the anomalous zone of the above-mentioned area (1). This indicates that the anomalous zones of the areas (1) and (2) are most likely to belong to the same

anomaly source, although their spectral characteristics are different. In the former area, the spectral pattern of the anomaly source exhibits the characteristics of that of pyrite mineralization. In the latter area, the spectral pattern resembles that from pyrite, it seems the possibility of existing another sulfides. The two-dimensional model simulation of the anomalous zone of the latter area indicates that the form of the anomaly source is angular ellipsoidal and, therefore, it is assumed that a sulfide mineralization in a more or less ellipsoidal form might exist below this particular anomaly zone. It was thus proposed that a drilling be conducted in this anomaly zone, assuming that the location from which the strongest anomaly was detected would be the center of the mineralization.

The anomaly zone of the above area (3) is distributed in the high resistivity zone, and its cross sectional view indicates that the zone consists of three anomaly sources. According to the model simulation, it can be assumed that two of the three anomaly sources are respectively located in the dissemination zone distributed in the shallow part of the ground (30m-60m), and in the zone in which sulfide is concentrated at a depth of approximately between 60 meters to 150 meters below the ground surface. The third anamaly source is presumably a weak dissemination of pyrite which covers the above two anomaly sources. The spectral patterns of these anomaly sources are similar to those of the anomaly zones in the said afore areas (1) and (2). Also, since the two-dimensional distribution of the IP anomaly zones generally coincides with the high Cu-Pb-Zn anomaly distribution zone detected in the geochemical survey, it was considered that the probability of mineralization in this particular zone was very high.

Therefore, it was proposed that a drilling be conducted in this anomaly zone, assuming that the location from which the strongest anomaly was detected would be the center of the mineralization.

The drillings were conducted respectively for the MBP–4 hole in the southern part of the survey area or the above mentioned area (1), for the MBP–5 hole in the southeastern part of the survey area or the above mentioned area (2), and for the MBP–6 hole in the northern part of the survey area or the above mentioned area (3). Results of the drillings and their relationship with the geophysical analyses are as follows:

(1) MBP–4 Hole and IP Anomaly

a) IP anomalies are distributed in the area from the ground surface down to an approximate depth of 200 meters. The spectral pattern of the anomaly source is associated with sulfide minerals.

b) The source of the IP anomalies is sulfide minerals, mainly consisted of disseminated pyrite.

c) Although the drilling results indicated the existence of a mineralization zone at an approximate depth of 286 meters, IP anomalies were not detected at this depth. This is probably due to the fact that the scale of this mineralization zone is rather small.

d) Resistivities detected in this drilling hole are at the minimum level within the entire survey area, and constitute a low resistivity zone. The major factor which accounts for this low resistivity zone is presumably the argillization associated with the fracture zone.

(2) MBP–5 Hole and IP Anomaly

a) The distribution pattern of IP anomalies suggested the existence of an anomaly source with a plate to massive configuration at the depth of between 30 meters to 150 meters below the ground surface. The drilling results indicated that this anomaly source was a mineralization zone of pyrite containing a small amount each of Cu, Pb and Zn, distributed at the depth of between 200 meters and 240 meters below the ground surface. This may account for the peculiar spectral pattern detected at this drilling hole.

b) The distribution pattern of resistivities in the vicinity of this drilling hole indicated a stable geological structure with no sign of geological deformation caused by faulting and other factors. The drilling of this hole revealed that this resistivity zone was a high resistivity zone influenced by the schistous rocks under silicification.

(3) MBP–6 Hole and IP Anomaly

a) The MBP–6 hole was drilled since a small-scale mineralization had already been detected by the Brazilian counterpart in the drilling of the PM-77-GO hole which was in the vicinity of the MBP–6 hole, and since the IP anomaly zone corresponded to the anomalous zone detected in the geochemical survey. It was found that the anomaly source was a dissemination zone of sulfide, as in the MBP–4 and MBP–5 holes.

b) The spectral pattern was predominantly influenced by pyrite, and no other minerals could be differentiated.

c) It is, therefore, presumed that the MBP–6 hole represents dissemination of a small amount of pyrite distributed widely from the ground surface to the depth.

As stated above, all the IP anomalies are closely correlated to the pyrite dissemination zone as the source of anomaly. This anomaly source, as revealed in the drilling survey, extends vertically, but contained only a small amount of sulfide minerals such as Cu, Pb and Zn. In the current survey, no massive ore body has been detected.

In the survey area, a folding structure with an NE-SW axis is most apparent, and it is presumed that the strata may be overturned or have a steep dip, with many faults crossing across the entire structure, which together constitute a very complicated geological structure. Any exploratory attempt for ore deposits in such an area, particularly when they are distributed only on a small scale, is inevitably difficult. Although the results of the geophysical exploration made clear the two-dimensional distribution of the pyrite dissemination zone, it was not possible to grasp a three-dimensional distirubtion of this dissemination zone. Furthermore, the survey area was predominated by pyrite and the spectral pattern showed no trace of minerals other than pyrite. Therefore, it was not possible to detect the existence of any significant ore deposits.

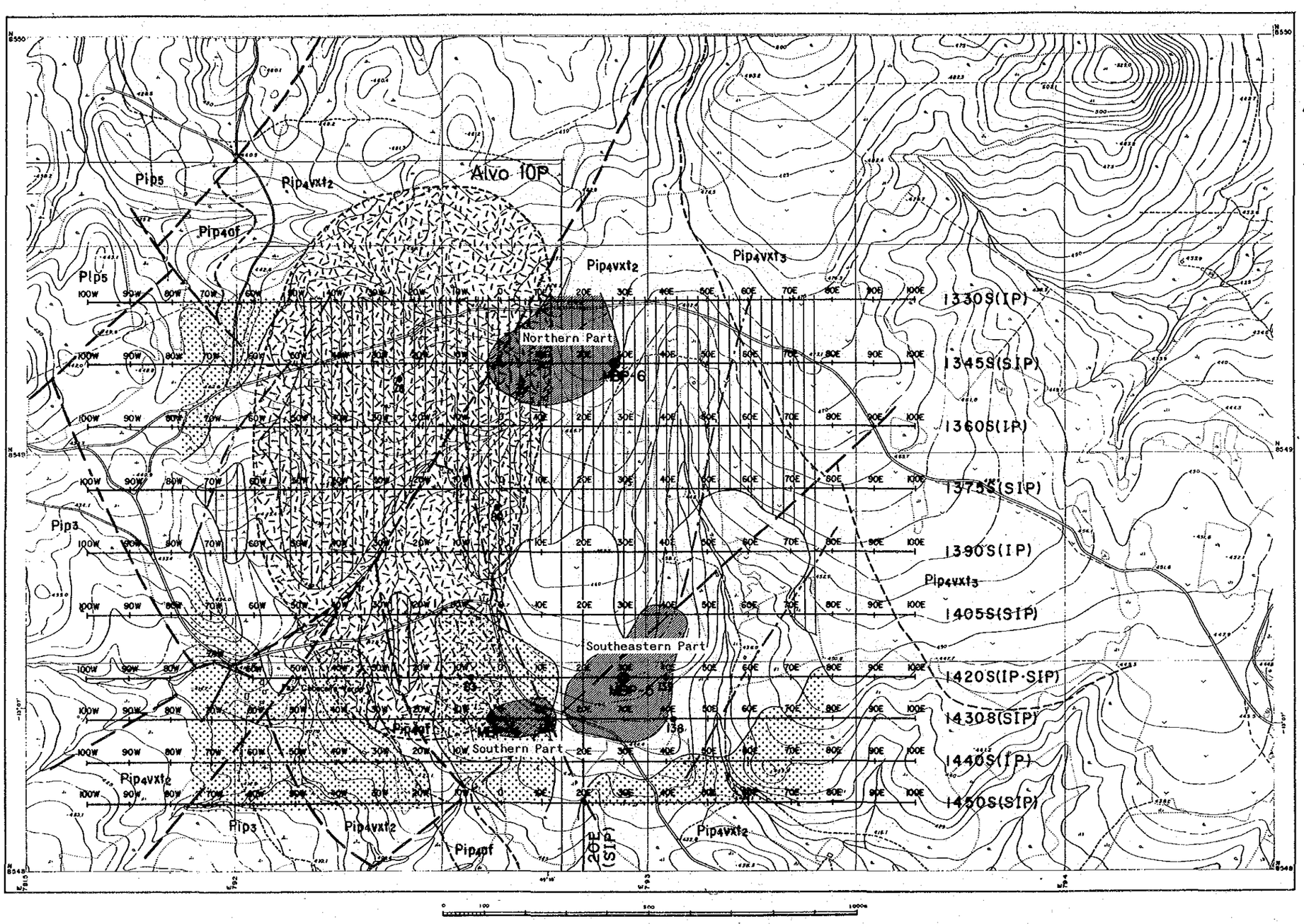

Fig. II-2-31 Geophysical Interpretation Map

2–3–2 Discussion on the Results of Drilling Survey

Three holes were drilled for a total length of 1201.77 meters, taking into consideration the results of the previous surveys and those of the Phase III geophysical exploration.

(1) MBP–4 Hole

Drilling was conducted through the Pip_4 formation down to the bottom of the hole from the ground surface. The final depth was 400 meters. From the distribution of the surface geology, the Pip_4 formation is considered to be divided into $Pip_4 vxt_1$ and $Pip_4 vxt_2$, although their boundary is not clear because of the lack of detailed study on the stratigraphy.

The bed of amphibolite and amphibole schist in 287.65 ~ 350.10 m, which partly intercalate biotite-quartz schist, is regarded as $Pip_4 af$ due to the reason that the bed is thin as shown in the geologic cross section (Fig. II–2–32).

Dipping of the formations is less than 30 degrees in general, but it reaches up to around 50 degrees in some parts. Small foldings with vertical enveloping surfaces are locally observed in the core. Considering the survey results of the surface geology, the strata of the area surrounding the MBP–4 hole are thought to generally dip toward the northeast.

Mineralization detected in this hole is of two types. The first type of mineralization (Type 1) is the one which is accompanied by chalcopyrite, galena and sphalerite in a pyrite-dominated dissemination embedded in Pip_4 formation (muscovite-biotite-quartz schist and biotite-muscovite -quartz schist, etc.) at a depth of approximately between 27 meters and 80 meters below the ground surface. The second type of mineralization (Type 2) is the one consisted mainly of pyrrhotite, which is partly massive, with a small amount of pyrite, and is embedded, inside garnet-plagioclase-biotite-quartz schist of Pip_4, along the boundary between the garnet-plagioclase-biotite-quartz schist of the Pip_4 formation and the amphibolite of $Pip_4 af$, at the depth of between 286.70 meters and 287.65 meters below the ground surface. The second type of mineralization is similar to the C–1 ore deposit in terms of the geological model of occurrence, yet the scale of mineralization is very small. Also, the drilling explorations previously conducted by the CPRM/DNPM and MMAJ in the Alvo 10P area had not detected any mineralization of a similar type. As for the former type of mineralization, assay results indicate contents of Cu, Pb and Zn in the MBP–4 hole higher than in other holes. The highest value for Cu is 1,608 ppm at a core length of 80 centimeters, and that for Pb is 4,294 ppm at a core length of 50 centimeters, while the highest content of Zn is 1.2% at a core length of 80 centimeters.

As for the Pip_4 formation, the values obtained in a whole rock assay generally correspond, except those similar to andesite-basalt, to the average chemical contents of dacite–rhyolite, and thus it has been estimated that its source rocks consist mainly of intermediate to acid rocks with some pelitic and basic rocks intercalated therein (JICA/MMAJ, 1986). Therefore, the Type 1 mineralization is presumably an ore deposit formed along with acidic volcanic activities, and the MBP–4 hole may be located either in its vicinity or in the area to which it was relocated in the proces of the formation of the ore bed. Also, it is most likely that the Type 2 mineralization is located stratigraphically above the C–1 ore deposit from the stratigraphycal evidence of MBP–4.

(2) MBP–5 Hole

Drilling was conducted to the depth of 400.45 meters. Geology of this hole belongs to the Pip_4 formation which, in this hole, is considered to be $Pip_4 vxt_2$ although it may also include $Pip_4 vxt_1$. That was not clarified because of the lack of detailed stratigraphical study. At the depths of between 30–70 meters, between 180–220 meters, and between 303–316 meters, a series of small scale drag folds (or parasitic folds) with generally vertical enveloping surfaces is observed in a continuous form and, therefore, it is presumed that a large scale fold may exist in the vicinity of the MBP–5 hole (Fig. II–2–32). The surface geology of the area indicates that the strata generally strike in the NE to NNE direction with an SE dip, suggesting that the fold axis is in the direction of NE to NNE and that the axial surface of the fold is dipping toward SE. If this fold is an extension of the fold stretching from the C–1 deposit toward the SW direction, this could be an overturned fold with its axial surface dipping toward SE (Fig. II–2–32).

Weak dissemination of pyrite was observed in the entire drilling hole, although the amount of pyrite is slightly more at the depth of between 200 meters and 240 meters below the ground surface than at other depths. At the depths of between 61.65 meters and 61.73 meters, and between 205 meters and 225 meters, pyrite is embedded in muscovite-biotite-quartz schist, in addition to a small amount each of sphalerite and galena. This mineralization is similar, in terms of its mode of occurrence, to the Type 1 mineralization discussed above. In addition, its mineral composition and the depth of mineralization also suggest that this mineralization could be the very source of the anomalies delected in the geophysical exploration. The mineral contents, as discussed previously, are very small, and the highest values for Pb and Zn at the depth of between 222 meters and 233 meters are 444 ppm and 3,540 ppm respectively. The value for Cu is 409 ppm at the depth of between 221 meters and 222 meters. Virtually no gold and silver are contained, and no amount of pyrrhotite is recognized. The same classification of mineralization could be

applied here.

(3) **MBP–6 Hole**

Geology of this hole belongs to the Pip_4 formation which, in this hole, is consdered to be Pip_4vxt_2, but it is not clear whether Pip_4vxt_1 is also included therein. Drilling was conducted to the depth of 401.32 meters.

As in the MBP–5 hole, a series of small-scale drag folds (or parasitic folds) with generally vertical enveloping surfaces is observed in a continuous form, at the depths of between 120–160 meters and between 170–332 meters. Therefore, it is presumed that a large scale fold may also exist in the vicinity of the MBP–6 hole. The surface geology of the area indicates that the strata generally strike in the NNE–SSW direction with an SE dip, suggesting that the fold stretching from the C–1 deposit toward the southwest may extends to the vicinity of the MBP–6 hole. If so, the existence of an overturned fold with an SE-dipping axial surface is presumed (Fig. II–2–32).

Weak and intermittent dissemination of pyrite was detected in the entire drilling hole, accompanied locally by pyrrhotite. At the depth beow 369 meters, a small amount of sphalerite is observed megascopically, in the pyrite dissemination in garnet-muscovite-biotite-quartz schist. Zn content is very small with the highest value being 948 ppm. Pb and Cu contents are also very small with the highest values being 218 ppm and 17 ppm respectively. Virtually no gold and silver are observed. The Cu-Pb-Zn mineralization is similar to the Type 1 mineralization of the MBP–4 hole, and it is most likely that the same classification of mineralization could also be applied here.

As discussed so far, Cu-Pb-An mineralization, although very small in scale, was detected in all the three drilling holes. The drilling of PM–138–GO by CPRM conducted in the IP anomaly zone detected by the Phase III geophysical exploration, also disclosed the existence of a high grade Cu-Pb-Zn mineralization, which partly forms a massive ore deposit, for a core length of 12 meters. Ore minerals of sphalerite, pyrrotite, pyrite, chalcopyrite, galena with massive occurrence were identified in this mineralization by microscopic observation on polished section (Fig. A–3, Phto A–2). In terms of its ore-bearing horizon, mineral components and mode of occurence, this mineralization is similar to the Type 1 mineralization observed in all the three drilling holes discussed above. Considering the fact that the C–1, C–2 and C–3 deposits in the same region are strata-bound deposits, these Type 1 mineralizations, therefore, are also thought to be strata-bound and are likely to consitute a series. The mineralization detected in the PM–138–GO

hole is presumably located near the center of this series in view of its mode of occurrence. The differences in the depth of mineralization may be the results of this series being partly shifted by the faults and folds.

In order to consider the stratigraphic horizons of the mineralization zones in the survey area, they are discussed in comparison with those of the C-1, C-2 and C-3 deposits, as follows:

The second type of mineralization (Type 2) in the MBP–4 hole is similar to the C-1 ore deposit in terms of its mode of occurrence. However, it was located in the horizon above the C-1 ore deposit, because it was emplaced in the Pip_4 formation as described before. And, it is most likely that the Type 1 mineralization is located in the horizon above the C-1 deposit, since all the Type 1 mineralizations are embedded in the Pip_4 formation ($Pip_4\,vxt_1$ and $Pip_4\,vxt_2$). In the meantime, although the C-2 and C-3 deposits were reportedly embedded below the iron formation in the uppermost part of the Pip_4 formation (CPRM), no iron formation was recognized either in the drillings of the MBP–4, MBP-5 and MBP–6 holes or in the drilling conducted in the current survey area by CPRM. Furthermore, the $Pip_4\,vxt_2$ formation, which does not constitute the uppermost part of the Pip_4 formation, is distributed on the ground surface. Therefore, it is that the Type 1 mineralization should be regarded as being comparable to the horizon below the C-1 and C-2 deposits.

Here the effect of the three drilings carried out in Phase III will be discussed. Drillings were vertically conducted the geology of this area slightly dip to NE. As the result of the drilling, the geology was disclosed to dip irregularly or rather steeply due to fold system. Therefore, due to the folding structure, the verticall drilling did not give enough information to further clarify the stratigraphy. Moreover, enough geological data to decide the mineralized horizon were not obtained, because stratigraphicall correlation between drilling holes conducted by MMAJ and CPRM was very difficult. The reason why the structural analysis of fold system was not executed is because the techniques to judge the original situation of beds were not only insufficient, but also key beds above and below the mineralization were not found.

Rock geochemistry could be applied in the future for the judgement of the original state of beds in this folded area. In many biotite-amphibole schist beds grasped by drilling conducted in Phase III, the characteristic mineralogical distribution was observed. That is, biotite is mostly included only at the top and at the bottom of the beds and when the one side, either at the top or at the bottom, is thick, the other side is thin. If the reason why this kind of occurrence took place is elucidated, the technique to reform the original state of the beds would be established, contributing to the structural analysis in this folded area.

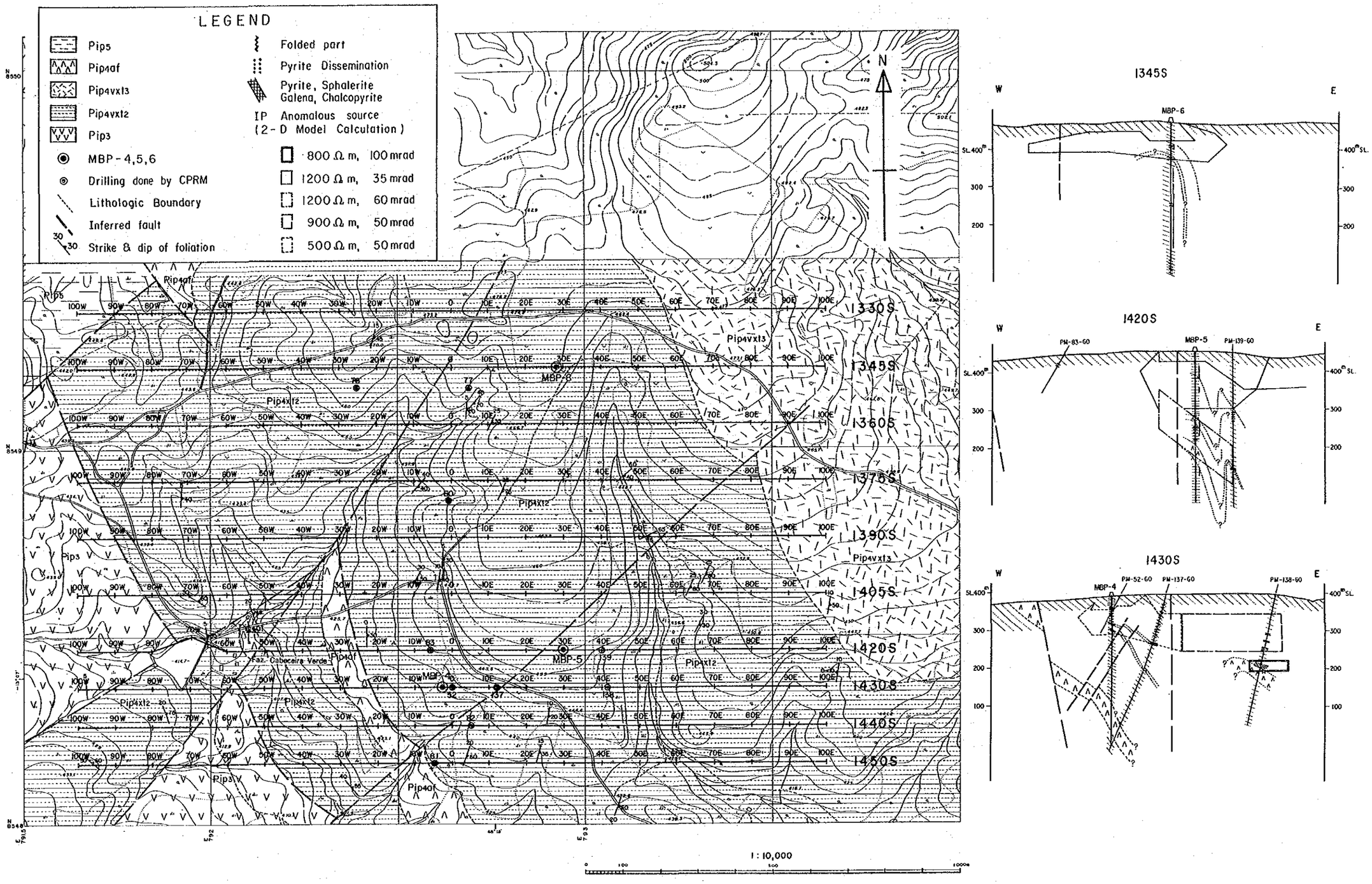

Fig. II-2-32 Geological Profile of MBP-4, MBP-5, and MBP-6

2–3–3 Discussion on the detection of a massive ore

In Phase III, a geophysical survey followed by a drilling detected the mineralization composed mainly of pyrite dissemination. Drilling (PM–138–GO) conducted by CPRM disclosed the massive Cu-Pb-Zn ore deposit in the same IP anomalous area that the pyrite mineralization was detected. However, the location of PM–138–GO was not necessarily decided for the possible massive ore deposit.

It is discussed here why the massive ore deposit could not be targeted at the time when the locations of drill hole were decided.

1) It is thought for the massive ore deposit not to be continuous and to be small in scale, because the SIP spectral pattern of the Cu-Pb-Zn massive ore deposit is not significantly different from the one of the pyrite dissemination.

2) The scale of a mineralization was set fairly large in the model simulation analysis because the IP anomaly was strong and large in scale. Anomalous source could be inferred from the distribution of IP anomalies in the model. However the presence and the location of Cu-Pb-Zn ore deposit on a small scale inside the pyrite dissemination could not be assumed.

3) When the locations of MBP–5 and MBP–6 were decided, the beds of this area had been assumed to dip to the northeast. However this area was disclosed to be a strong folded zone by a drilling. Thus the mineralization zone extends rather vertically than laterally, due to the strata-bound ore deposit. Therefore the form of the mineralization in the model was not properly adjusted to the geological structure. And the distance between the locations of MBP–5 and PM–138–GO is about 150m, and PM–139–GO located about 100m north of PM–138–GO did not detect the massive are body. Thus the possible target is thought to be small.

4) Some IP anomalous sources are thought to be present in the pseudosection of IP anomaly map. MBP–5 targeted the strongest and the largest one of those sources.

5) Geophysical method (IP, SIP methods) is at a present time a very useful technique to detect a mineralization. However, in case that drilling need to detect not only mineralization but also massive ore, the target should be selected through model simulation analysis utilizing the information on a geological structure, the size and the characteristics of the known mineralization. Thus the drilling to disclose a geological structure is needed before the drilling to penetrate an ore deposit.

Considering all of the above, it is desirable to conduct exploration in the areas whose geological structures are similar to that of the Phase III survey area, in the following manner and sequence:

1) detect the resistivity structure in detail by conducting high density resistivity surveys, in order to extract areas of promising mineralization.

2) conduct several drillings at a higher density drilling unit in the promising areas, in order to understand more deeply the geological structure of the possible mineralization.

3) conduct electrical explorations in the most promising areas pinpointed in the resistivity and drilling surveys, in order to confirm the existence, continuity, etc. of the possible mineralization zones, and, at the same time, analyze the spectral patterns of such areas in close reference to the information already available.

4) make a three-dimensional simulation analysis of the conditions of mineralization based on the data collected in the above mentioned surveys, including the anomaly information obtained in the electrical explorations.

5) Conduct grid drillings for the anomaly sources (mineralization zones or ore deposits) indentified in the three-dimensional simulation analysis.

PART III CONCLUSIONS AND RECOMMENDATIONS

CHAPTER 1 CONCLUSIONS

In the Phase III survey, mineralization zones consisted mainly of diseeminated pyrite were detected in three locations with IP anomalies in the southwestern part of the Morro do Acampamento area. The drilling conducted by CPRM also confirmed the presence of a massive Cu-Pb-Zn deposit in one of the three locations. These mineralization zones consisted mainly of disseminated pyrite and massive ore deposit are considered to constitute a series. This large mineralized zone should be surveyed more in detail, because some other massive ore deposits are likely to be found.

Geophysical surveys (SIP, IP methods) are effective to determine the presence of mineralization even in this kind of geological background. However, it is thought that geological structure is a very important factor to analyse the data gained, because the shape of ore deposit is controled by the geological structure. Revealment of the geological structure should be preceded to the geophysical survey to delineate the mineralization.

CHAPTER 2 RECOMMENDATIONS

The areas including IP anomalous zones should be evaluated by the surveys to reveal the geological background of the mineralization and the presence of other massive ore bodies, and to determine the scales of ore body and the reserves intersected by drilling of CPRM.

For this purpose, therefore, the following activities are recommended:

(1) Re-examination of the geological structure of the Alvo 10P area, using the existing drilling data including those obtained in the Phase III Survey. This includes, in particular, a three-dimensional examination of the known ore deposits through the analysis of the fold structure therein. The shape of ore bodies are thought to be controlled by the fold, which are supposed to have northeast trending axes and southeast dipping axial planes in this area. Therefore, the drillings with a northwest inclination should be conducted and the sites should be aranged along a northeast direction.

(2) Stratigraphic analysis of the Alvo 10P area, using the existing drilling data including those obtained in the Phase III Survey. This includes, in particular, the investigation of stratigraphic order and mineralization environment, with close reference to petrology and mineralogy.

(3) Analysis of the genetic and stratigraphic relationship between the mineralization zone in the South Block detected in the Phase II Survey and the anomaly zone detected in the northern part of the Phase III survey area.

(4) A survey program should be sequentially conducted as follows: a) Revealment of geological structure by geophysical techniques b) Revealment of geological structure by drillings c) Determination of mineralization zone by geophysical techniques d) Delineation of mineralization by drillings.

REFERENCES

REFERENCES

(1) Almeida F.F.M., Hasui Y., Brito Neves B.B. and Fuck R.A. – 1981 – Brasilian structural provinces; an introduction, Earth-Sci., Rev., 17: 1-29.

(2) Almeida F.F.M. e Hasui, Y. – 1984 – O Precambriano do Brasil.

(3) CNEN/DNPM/CPRM – 1973 – Levantamento Aerocintilometrico Projecto Serra da Mesa.

(4) CNEN/DNPM/CPRM – 1977 – Projeto Serra da Mesa II-Goias, Relatorio Final.

(5) CPRM – 1984 – Projeto Plameiropolis Informe Tecnico.

(6) DNPM – 1975 – Carta Geologica do Brasil ao Miliodesimo, Folha Goias SD-22.

(7) DNPM/MME – 1981 – Projeto RADAMBRASIL, Vol. 25.

(8) DNPM – 1981 – Geologia e Inventario dos Recursos Minerais do Regiao Central do Estado de Goias – Projeto Brasilia –.

(9) DNPM – 1981 – Os Principais Depositos Minerais do Regäo Centro-Oeste.

(10) DNPM – 1983 – Levantamento Aerogiofisico do Projeto Palmeiropolis-Go.

(12) DNPM – 1983 – Garimpos do Brasil.

(13) DNPM – 1984 – Garimpos do Brasil.

(14) DNPM – 1984 – Geologia do Brasil.

(15) DNPM – Projeto Mapas Metalogeneticos e de Previsão de Recurais Minerais – Porangatu – Folha SD-22-X-D.

(16) DNPM – Projeto Mapas Metalogeneticos e de Previsão de Recurais Minerais – Alvorada – Folha SD-22-X-B.

(17) Whitten, E.H. Timothy – 1966 – Stractural Geology of Folded Rocks, Rand Mc. Nally & Company.

(18) Girardi A.V. and Kurat G. – 1982 – Precambrian Mafic and Ultramafic Rock of the CANA BRAVA Complex, Brasil.

(19) Hasui Y. et al. – 1980 – Datacoes Rb-Sr e K-Ar Centro Norte do Brasil e seu Significado Geologico-Geotectonico, XXXI Congresso Brasileiro de Geologia.

(20) Guilbert, John M. and Park, Charles F. Jr. – 1986 – The Geology of Ore Deposits, W.H. and Company.

(21) Louis L. – 1978 – Aspectos Geotectonicos da Africa Ocidental a Leste do Golfo da Guine com Refrencia as Conexoes Estruturais e Litoloficas Brasil e Africa, XXX Contresso Brasileiro de Geologia.

(22) Meyers, R.E. and MecLean, W.H. – 1983 – The geology of the New Inco copper deposit, Noranda district, Quebec, CAN. J. EARTH SCI., Vol. 20, 1291-1304.

(23) Miyashiro, A., – 1965 – Metamorphic Rocks and Metamorphic Belt, Iwanami Shoten (in Japanese)

(24) MMAJ – 1985 – Report on Morro Agudo and Palmeiropolis Project, Brasil.

(25) MMAJ, JICA – 1986, 1987 – Report on the Cooperative Mineral Exploration in the Palmeiropolis Area, Federative Republic of Brazil.

(26) Sato, Takeo. – 1983 – Kuroko-type Deposits in Earth's History, The Society of Mining Geologists of Japan, Mining Geology Special Issue No. 11.

(27) Severin, P.W.A. – 1982 – Geology of the Sturgeon Lake Copper-Zinc-Lead-Silver-Gold Deposit, CIM. Bull., Vol. 75, 107-123.

(28) Suszczynski E. – 1981 – South America, Structural Framework, Chapter 13 of Precambrian of the Southern Hemisphere.